

# LAYERED MODELS CAN "AUTOMATICALLY" REGULARIZE AND DISCOVER LOW-DIMENSIONAL STRUCTURES VIA FEATURE LEARNING

BY YUNLU CHEN<sup>1,a</sup>, YANG LI<sup>2,c</sup>, KELI LIU<sup>3,d</sup> AND FENG RUAN<sup>1,b</sup>

<sup>1</sup>Department of Statistics and Data Science, Northwestern University, <sup>a</sup>[yunlu.chen2026@u.northwestern.edu](mailto:yunlu.chen2026@u.northwestern.edu);  
<sup>b</sup>[fengruan@northwestern.edu](mailto:fengruan@northwestern.edu)

<sup>2</sup>Department of Mathematics, Massachusetts Institute of Technology, <sup>c</sup>[yangmit@mit.edu](mailto:yangmit@mit.edu)

<sup>3</sup>Company A, <sup>d</sup>[keli.liu25@gmail.com](mailto:keli.liu25@gmail.com)

Layered models like neural networks appear to extract key features from data through empirical risk minimization, yet the theoretical understanding for this process remains unclear. Motivated by these observations, we study a two-layer nonparametric regression model where the input undergoes a linear transformation followed by a nonlinear mapping to predict the output, mirroring the structure of two-layer neural networks. In our model, both layers are optimized jointly through empirical risk minimization, with the nonlinear layer modeled by a reproducing kernel Hilbert space induced by a rotation and translation invariant kernel, regularized by a ridge penalty.

Our main result shows that the two-layer model can “automatically” *induce regularization* and facilitate feature learning. Specifically, the two-layer model promotes dimensionality reduction in the linear layer and identifies a parsimonious subspace of relevant features—even without applying any norm penalty on the linear layer. Notably, this regularization effect arises directly from the model’s layered structure, independent of optimization dynamics.

More precisely, assuming the covariates have nonzero explanatory power for the response only through a low dimensional subspace (central mean subspace), the linear layer consistently estimates both the subspace and its dimension. This demonstrates that layered models can inherently discover low-complexity solutions relevant for prediction, without relying on conventional regularization methods. Real-world data experiments further demonstrate the persistence of this phenomenon in practice.

**1. Introduction.** Layered models, e.g., neural networks, are integral to modern machine learning, appearing to have the capacity to automatically extract meaningful data representations, leading to effective predictions. However, despite their empirical success, theoretical understanding of how these layered structures facilitate feature representation learning remains limited, primarily constrained by the fundamental mathematical challenges arising from nonlinear interactions across layers. Nonetheless, understanding this mechanism is crucial, as it directly impacts the reliability and interpretability of machine learning predictions across numerous applications, from image classification to natural language modeling [11].

Towards this goal, this work examines a two-layer nonparametric regression model within the kernel ridge regression (KRR) framework to advance our understanding of how layered structure facilitates feature extraction. The primary contribution of this work is the discovery that two-layer models can naturally induce sparsity through empirical risk minimization, achieving dimension reduction by identifying a parsimonious subspace of predictive features. Remarkably, this occurs without *calling for any conventional regularization technique*, such

---

*MSC2020 subject classifications:* Primary 62H99; secondary 62J02.

*Keywords and phrases:* layered models, regularization, feature learning, central mean subspace, reproducing kernel Hilbert space, ridge regression, dimension reduction, low-rankness, set identification, sharpness.

as norm penalties or algorithmic adjustments, which are often deemed essential for achieving similar effects in many other models in statistical learning [51].

As a starting point, the traditional kernel ridge regression (KRR) model learns a nonparametric relationship between the input  $X \in \mathbb{R}^d$  and the output  $Y \in \mathbb{R}$  through the following minimization problem [87]:

$$\text{minimize}_{F, \gamma} \frac{1}{2} \mathbb{E}_n [(Y - F(X) - \gamma)^2] + \frac{\lambda}{2} \|F\|_{\mathcal{H}}^2$$

where  $\mathbb{P}_n$  is the empirical distribution of the data  $(X, Y)$  from a population distribution  $\mathbb{P}$ ,  $\mathbb{E}_n$  is the empirical expectation,  $\lambda > 0$  is the ridge regularization parameter,  $\mathcal{H}$  is a reproducing kernel Hilbert space (RKHS) on  $\mathbb{R}^d$ ,  $F : \mathbb{R}^d \mapsto \mathbb{R}$  is the prediction function, and  $\gamma \in \mathbb{R}$ . While the traditional KRR framework provides a powerful nonparametric approach, it relies on a fixed kernel, limiting its capacity to learn features that adapt to the structure of the data.

Building on KRR, we explore a two-layer nonparametric regression model that incorporates feature learning. In this model, we introduce a matrix parameter  $U \in \mathbb{R}^{d \times q}$ , transforming the input  $X \in \mathbb{R}^d$  into  $U^T X \in \mathbb{R}^q$  in the first layer, followed by a nonlinear function  $f : \mathbb{R}^q \rightarrow \mathbb{R}$  in the second layer, where  $f$  resides in an RKHS  $\mathcal{H}_q$  on  $\mathbb{R}^q$ . Unlike traditional KRR, which optimizes only over  $F$  and  $\gamma$ , this two-layer model jointly optimizes over  $f$ ,  $U$ , and  $\gamma$  as follows:

$$(1.1) \quad \text{minimize}_{f, \gamma, U} \frac{1}{2} \mathbb{E}_n [(Y - f(U^T X) - \gamma)^2] + \frac{\lambda}{2} \|f\|_{\mathcal{H}_q}^2.$$

In this two-layer formulation, the first layer  $U^T X$  acts as a learned linear representation of the data, while the prediction takes a compositional structure:  $X \mapsto f(U^T X) + \gamma$ . Such a layered structure draws inspiration from two-layer neural networks and is closely related to them (see Section 1.4.1 and 1.4.2 for related works). For instance, when  $\mathcal{H}_q$  is induced by a linear kernel, it is exactly a two-layer *linear* neural network model<sup>1</sup>. However, much remains to be understood in the nonparametric setting, where the RKHS  $\mathcal{H}_q$  is infinite-dimensional and  $f$  can be *nonlinear*.

This paper is focused on the setting where the RKHS  $\mathcal{H}_q$  is induced by a *rotationally and translation-invariant* kernel,  $k_q(w, w') = \phi(\|w - w'\|_2^2)$ , with the Gaussian kernel  $\phi(z) = \exp(-z)$  as an example. This invariance property ensures that the second-layer function  $f$  bases predictions solely on the relative distances between the first-layer representations  $U^T X$  of the data, rather than their absolute positions or orientations. We require  $q \geq d$ , which is essential to allow the predictive model  $X \mapsto f(U^T X) + \gamma$  to be rich enough to approximate any nonparametric prediction function<sup>2</sup>. We leave the complementary scenario  $q < d$  for future work.

For all such rotationally and translation-invariant kernels, the model (1.1) has an equivalent formulation, when  $q \geq d$  holds:

$$(1.2) \quad \text{minimize}_{F, \gamma, \Sigma} \frac{1}{2} \mathbb{E}_n [(Y - F(X) - \gamma)^2] + \frac{\lambda}{2} \|F\|_{\mathcal{H}_\Sigma}^2 \quad \text{subject to} \quad \Sigma \succeq 0.$$

Here, the choice of the RKHS  $\mathcal{H}_\Sigma$  varies with a positive definite matrix  $\Sigma \succeq 0$  in  $\mathbb{R}^{d \times d}$  and is induced by the kernel  $k_\Sigma(x, x') = \phi(\|x - x'\|_\Sigma^2)$  where  $\|x - x'\|_\Sigma = \sqrt{(x - x')^T \Sigma (x - x')}$ . The two formulations (1.1) (with  $q \geq d$ ) and (1.2) are related through the reparameterization

<sup>1</sup>A two-layer linear neural network has two layers with a linear activation function.

<sup>2</sup>For example,  $F(x) = \|x\|_2^2/2$  can't be written as  $f(U^T x)$  where  $U \in \mathbb{R}^{d \times q}$  with  $q < d$ , since this would imply  $I = \nabla^2 F(x) = U \nabla^2 f(U^T X) U^T$ , which is impossible since the LHS has rank  $d$ , while the RHS has rank at most  $q < d$ .

$\Sigma = UU^T$  and  $F = f \circ U^T$  at their minimizers (Proposition 6). This equivalence shows that the layered formulation (1.1) can be understood as a kernel learning problem, as in (1.2). In this formulation (1.2), the RKHS  $\mathcal{H}_\Sigma$  is learned by optimizing  $\Sigma$ , allowing the model to adapt to the data structure, unlike traditional KRR where the RKHS is fixed in advance.

1.1. *An Illustrative Numerical Experiment.* To provide an intuitive preview of our main theoretical findings, we present a numerical experiment that highlights how the model can identify low-dimensional feature representations without relying on conventional regularization methods, such as norm penalties or early stopping. This empirical evidence highlights the model’s ability to achieve what we refer to as "automatic" regularization, a behavior that underpins the main results of this study.

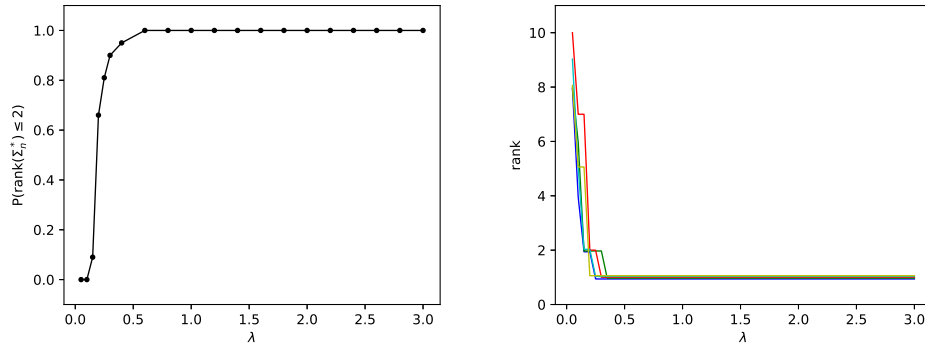


Fig 1: The covariate  $X \sim \mathcal{N}(0, I)$ , and the response  $Y = F(X) + \epsilon$ , where  $F(x) = 0.1(x_1 + x_2 + x_3)^3 + \tanh(x_1 + x_3 + x_5)$  and  $\epsilon \sim \mathcal{N}(0, \sigma^2)$  with  $\sigma = 0.1$ . Here  $n = 300$  and  $d = 50$ . We apply gradient descent to optimize the objective (1.2). For each of 100 repeated samples of the pair  $(X, Y)$ , we record the solution matrix  $\Sigma_n^*$  across a range of  $\lambda$  values from  $(0, 3]$ . On the left panel, we plot the empirical probability of  $\text{rank}(\Sigma_n^*) \leq 2$  against  $\lambda$ . On the right panel, we display how the rank of the solution  $\Sigma_n^*$  changes with different  $\lambda$  values, using 5 examples of  $(X, Y)$ . Both plots suggest a remarkable inclination of the solution matrix  $\Sigma_n^*$  towards low-rankness, even though we don’t apply nuclear norm penalties to  $\Sigma$  in (1.2) and don’t use early stopping techniques.

In the experiment, we generate synthetic data with  $n = 300$  samples, each having a 50-dimensional feature vector  $X$  from an isotropic normal distribution. The response variable,  $Y$ , follows a simple relation with  $X$ :  $Y = 0.1(X_1 + X_2 + X_3)^3 + \tanh(X_1 + X_3 + X_5) + \epsilon$  for some independent noise  $\epsilon \sim \mathcal{N}(0, \sigma^2)$  with  $\sigma = 0.1$ . Here  $(X_1, X_2, \dots, X_{50})$  is the coordinate representation of  $X$ . This setup ensures that  $Y$  depends on  $X$  only through two specific low-dimensional projections:  $X_1 + X_2 + X_3$  and  $X_1 + X_3 + X_5$ , combined through two simple functions: cube and hyperbolic tangent. Ideally, we want  $U$  in the two-layer model (or equivalently  $\Sigma$  in the kernel learning formulation) to capture these two projections.

Using gradient descent, we optimize the kernel learning objective to obtain the solution matrix  $\Sigma_n^* \in \mathbb{R}^{50 \times 50}$  for a wide range of regularization parameter  $\lambda$  (further algorithmic details in Section 9). Strikingly, this  $50 \times 50$  matrix  $\Sigma_n^*$  consistently demonstrates a low rank property— $\text{rank}(\Sigma_n^*) \leq 2$ —for a broad spectrum of the  $\lambda$  values (Figure 1). This finding is particularly intriguing because our experimental setup does not impose any conventional regularization that would encourage low rankness in  $\Sigma$ —no nuclear norm penalties and no early stopping; instead our gradient descent algorithm is carefully tuned towards full convergence.

Yet, despite the absence of these regularization methods, the emerging matrix  $\Sigma_n^*$ , although noisy, hints at a remarkable low-rank inclination:  $\text{rank}(\Sigma_n^*) \leq 2$ , a phenomenon observed across a wide spectrum of  $\lambda$  in over 100 repeated experiments. Further experiments in Section 9 show that this low-rankness phenomenon is neither confined to a specific choice of  $X$  distribution nor to a specific choice of the conditional mean of  $Y$  given  $X$ .

These numerical experiments provide initial evidence that the two-layer model (1.1), or its kernel-learning counterpart (1.2), inherently induces sparse regularization in the finite-sample solution matrices  $U$  and  $\Sigma$  without conventional regularization techniques. Crucially, our main theoretical results will substantiate this observed behavior, demonstrating that these matrices are not only low-rank but also statistically meaningful, identifying the minimal subspace required to capture predictive features. Together, these findings establish that certain layered structures can intrinsically capture low-dimensional structures through feature learning, leading to an "automatic" regularization property formalized in the following sections.

Importantly, this phenomenon extends beyond synthetic experiments and holds practical relevance. In Section 10, we demonstrate that similar low-dimensional structures emerge in two real-world experiments, where the learned bottom-layer weight matrices display remarkable low-rank patterns, even without explicit regularization. On the SVHN dataset—designed to predict house numbers from Google Street View images ( $n = 9993$ ,  $d = 3072$ )—our two-layer kernel ridge regression model performs comparably to two-layer ReLU neural networks in accuracy and *consistently* outperforms classical kernel ridge regression across various tasks and subsampled datasets, with improvement in test accuracy up to almost 10% (with improvement in test accuracy from 80% to 89%). This underscores the importance of feature learning and shows that the model’s ability to extract low-dimensional data representations plays a pivotal role in its success.

While these experiments serve as inspiration and motivation, the primary objective of this paper is not predictive performance but a rigorous understanding of the mechanisms driving this low-rank phenomenon. Our focus lies in the theoretical foundations and the implications for feature learning and automatic regularization in our layered architecture. The implications of these results, e.g., for predictive performance will be touched upon in future work.

**1.2. Main Results.** This paper explores the nature of how two-layer model (1.1) (and its equivalent kernel learning formulation (1.2)) facilitate dimension reduction in feature learning, focusing on the statistical properties of the first-layer weight matrix minimizer.

We investigate the following questions.

- What subspace does the solution matrix  $U$  (or  $\Sigma$  in kernel learning formulation) estimate, and how does this align the model’s learned features with the data structure?
- Why is the finite-sample minimizer  $U$  or  $\Sigma$  low-rank, even without explicit regularization?
- Does this low-rank phenomenon persist with other models, such as when  $\mathcal{H}_q$  is induced by the linear model  $k_q(w, w') = w^T w'$ , i.e., in a two-layer linear neural network?

By addressing these questions, we build a systematic theoretical understanding of the two-layer objective and its equivalent kernel learning formulation, which in turn, enhances our understanding of feature learning in layered architectures.

For technical reasons, our findings below only apply to a variant of the objective given by

$$(1.3) \quad \underset{f, \gamma, U}{\text{minimize}} \quad \frac{1}{2} \mathbb{E}_n [(Y - f(U^T X) - \gamma)^2] + \frac{\lambda}{2} \|f\|_{\mathcal{H}_q}^2 \quad \text{subject to} \quad \|UU^T\| \leq M.$$

or its equivalent formulation

$$(1.4) \quad \underset{F, \gamma, \Sigma}{\text{minimize}} \quad \frac{1}{2} \mathbb{E}_n [(Y - F(X) - \gamma)^2] + \frac{\lambda}{2} \|F\|_{\mathcal{H}_\Sigma}^2 \quad \text{subject to} \quad \Sigma \succeq 0, \quad \|\Sigma\| \leq M.$$

Here, we introduce a constraint,  $\|UU^T\| \leq M$  (resp.  $\|\Sigma\| \leq M$ ), where  $\|\cdot\|$  is a unitarily invariant norm on  $d$ -by- $d$  matrices (e.g., operator norm, Frobenius norm, Schatten norm). The addition of this constraint helps ensure the existence of a minimizer. Nonetheless, our theoretical findings do not depend on the specific choice of  $M$  or the specific norm  $\|\cdot\|$  being added; the constraint is mainly artificial.

**1.2.1. Data Distribution and Regularity Assumptions.** Our main results rely on a few assumptions about the data distributions as well as a mild regularity assumption on the real-valued function  $\phi$ . Throughout this paper, we assume that the data are independently and identically drawn from  $(X, Y) \sim \mathbb{P}$  with  $\mathbb{E}[\|X\|^4] < \infty$  and  $\mathbb{E}[Y^2] < \infty$ .

**Role of Dimension Reduction** Our first assumption is that there is a low-dimension linear projection of  $X$  that captures all information of  $Y$  from the conditional mean  $\mathbb{E}[Y|X]$ . To formalize this idea, we use dimension reduction concepts from statistics [21]. Specifically, a linear subspace  $S$  of the ambient space  $\mathbb{R}^d$  is called a *mean dimension reduction* subspace if  $\mathbb{E}[Y|X] = \mathbb{E}[Y|\Pi_S X]$ , where  $\Pi_S$  denotes the Euclidean projection onto  $S$ . We then introduce the smallest such subspace, termed the *central mean subspace* in the literature [23].

**DEFINITION 1.1 (Central Mean Subspace [23, Definition 2]).** *Let  $S_*$  denote the intersection over all mean dimension-reduction subspaces:*

$$S_* = \cap \{S : \mathbb{E}[Y|X] = \mathbb{E}[Y|\Pi_S X]\}.$$

*If  $S_*$  itself is a mean dimension-reduction subspace, it is termed the central mean subspace.*

**ASSUMPTION 1 (Existence of Central Mean Subspace).** *The central mean subspace  $S_*$  exists.*

Note that the central mean subspace does not always exist, because the intersection of dimension reduction subspaces is not necessarily a dimension reduction subspace. Nonetheless, the central mean subspace does exist under very mild distributional conditions on  $X$ , e.g., when  $X$  is a continuous random variable with convex, open support or has Lebesgue density on  $\mathbb{R}^d$  [23].

**Predictive Power** Our second assumption is mild:  $X$  has predictive power for  $Y$ . Interestingly, this seemingly mild assumption is necessary for the phenomenon to occur.

**ASSUMPTION 2 ( $X$  has predictive power of  $Y$ ).**  $\text{Var}(\mathbb{E}[Y|X]) \neq 0$ .

**Covariate's Dependence Structure** Our third assumption is about the dependence structure of the covariate  $X$ . We'll denote the orthonormal complement of the subspace  $S_*$  with respect to the ambient space  $\mathbb{R}^d$  as  $S_*^\perp$ .

**ASSUMPTION 3 (Dependence Structure of  $X$ ).**

(a)  $\text{Cov}(X)$  has full rank, and (b)  $\Pi_{S_*} X$  is independent of  $\Pi_{S_*^\perp} X$ .

Part (a) is mild. Part (b) is stylized. In fact, our extensive numerical experiments suggest the phenomenon holds in many situations where Part (b) is violated. The independence assumption only reflects the limit of what we are able to prove regarding the observed phenomenon. We shall make further comments on this assumption, and make comparisons to existent results in the literature after we state our main theorems (Section 1.4.3).

**Function  $\phi$ 's Regularity** Finally, our result requires one more regularity condition pertaining to the real-valued function  $\phi$  that defines the kernel  $k$  (resp.  $k_\Sigma$ ).

ASSUMPTION 4 (Regularity of  $\phi$ ). *The representation  $\phi(z) = \int e^{-tz} \mu(dt)$  holds for every  $z \geq 0$  where  $\mu$  is a measure supported on  $[0, \infty)$  not concentrated at zero.*

*Moreover,  $\phi'_+(0) = \lim_{z \rightarrow 0^+} (\phi(z) - \phi(0))/z$  exists.*

The first part of the condition draws inspiration from Schoenberg's fundamental work [77], which characterizes all real-valued functions  $\phi$  ensuring  $k_q(w, w') = \phi(\|w - w'\|_2^2)$  is a *positive definite* kernel in  $\mathbb{R}^q$  for every dimension  $q \in \mathbb{N}$ . Such a function  $\phi$  must conform to  $\phi(z) = \int e^{-tz} \mu(dt)$  with  $\mu$  being a finite, nonnegative measure supported on  $[0, \infty)$  but not concentrated at zero [77]. The second part of the condition implies that  $\phi$  is differentiable on  $(0, \infty)$ , and right differentiable at 0, which will be used to define gradients of the objective to  $U$  (or  $\Sigma$  resp.). Common kernels that meet this criterion include the Gaussian kernel and inverse polynomial kernels.

1.2.2. *Formal Statement.* Our first result (Theorem 1.1) says that at every one of its population minimizers, the model returns a  $U^*$  (or equivalent  $\Sigma^*$ ) whose column space is contained in or *exactly* equal to the central mean subspace  $S_*$ .

For clarity, we write down the corresponding population objectives:

$$(1.5) \quad \underset{f, \gamma, U}{\text{minimize}} \quad \frac{1}{2} \mathbb{E} [(Y - f(U^T X) - \gamma)^2] + \frac{\lambda}{2} \|f\|_{\mathcal{H}_q}^2, \quad \|UU^T\| \leq M,$$

and its equivalent formulation:

$$(1.6) \quad \underset{F, \gamma, \Sigma}{\text{minimize}} \quad \frac{1}{2} \mathbb{E} [(Y - F(X) - \gamma)^2] + \frac{\lambda}{2} \|F\|_{\mathcal{H}_\Sigma}^2 \quad \text{subject to} \quad \Sigma \succeq 0, \quad \|\Sigma\| \leq M.$$

Instead of taking the empirical expectation  $\mathbb{E}_n$  in (1.1) or (1.2), we use population expectation  $\mathbb{E}$ . We'll use  $\text{col}$  to denote the column space of a matrix.

**THEOREM 1.1.** *Let Assumptions 1–4 hold. Fix a unitarily invariant norm  $\|\cdot\|$  and  $M \in (0, \infty)$ . Then any minimizer  $(\Sigma^*, F^*, \gamma^*)$  of the population objective (1.6) obeys:*

- *For every  $\lambda \in (0, \infty)$ ,  $\text{col}(\Sigma^*) \subseteq S_*$ .*
- *For every  $\lambda \in (0, \lambda_0]$ ,  $\text{col}(\Sigma^*) = S_*$ . Here,  $0 < \lambda_0 < \infty$  is dependent on  $\mathbb{P}, \|\cdot\|, M$ .*

*The result also holds verbatim by replacing (1.6) with (1.5) (with  $q \geq d$ ) and  $(\Sigma^*, F^*, \gamma^*)$  with  $(U^*, f^*, \gamma^*)$ , respectively.*

Theorem 1.1 is a foundational result for understanding the kernel learning procedure (1.6) (or equivalently, the layered formulation (1.5)). It demonstrates that the population-level solutions are perfectly aligned with the data's inherent low-dimensional structure. Specifically, when  $\lambda$  is sufficiently small, there are the identities  $\text{col}(\Sigma^*) = S_*$ , and  $\text{rank}(\Sigma^*) = \dim(S_*)$  (and respectively,  $\text{col}(U^*) = S_*$ , and  $\text{rank}(U^*) = \dim(S_*)$ ).

The perhaps surprising result comes when we move from the population to the *finite sample* objective. Our second result, Theorem 1.2, says that in finite samples, the kernel learning objective (1.4) (or its equivalent layered formulation (1.3)) also delivers a solution  $\Sigma_n^*$  (and  $U_n^*$ ) with rank less than or equal to  $\dim(S_*)$  with high probability. Remarkably, the low-rank solution is achieved without explicitly incorporating low-rankness promoting regularizers on  $\Sigma$  in the *finite sample* objective (1.4) (and  $U$  in (1.3) respectively)!

**THEOREM 1.2.** *Let Assumptions 1–4 hold. Fix a unitarily invariant norm  $\|\cdot\|$  and  $M \in (0, \infty)$ . Then,*

- For every  $\lambda \in (0, \infty)$ ,

$$\lim_{n \rightarrow \infty} \mathbb{P}(\text{rank}(\Sigma_n^*) \leq \dim(S_*), \forall (\Sigma_n^*, F_n^*, \gamma_n^*) \text{ minimizing (1.4)}) = 1.$$

- For every  $\lambda \in (0, \lambda_0]$  (with the same  $\lambda_0$  in Theorem 1.1):

$$\lim_{n \rightarrow \infty} \mathbb{P}(\text{rank}(\Sigma_n^*) = \dim(S_*), \forall (\Sigma_n^*, F_n^*, \gamma_n^*) \text{ minimizing (1.4)}) = 1.$$

The result also holds verbatim by replacing (1.4) with (1.3) (with  $q \geq d$ ) and  $(\Sigma_n^*, F_n^*, \gamma_n^*)$  with  $(U_n^*, f_n^*, \gamma_n^*)$ , respectively.

An important statistical consequence of Theorem 1.2 is that the column space of  $\Sigma_n^*$  (resp. the row space of  $U_n^*$ ) can serve as a natural estimator for both the central mean subspace  $S_*$  and its dimension. Indeed,

**THEOREM 1.3.** *Let Assumptions 1–4 hold. Then for every  $\lambda \in (0, \lambda_0]$  (with the same  $\lambda_0$  in Theorem 1.1), there is the convergence in probability as  $n \rightarrow \infty$ :*

$$\sup \{ \|\Pi_{\text{col}(\Sigma_n^*)} - \Pi_{S_*}\| \mid (\Sigma_n^*, F_n^*, \gamma_n^*) \text{ minimizing (1.4)} \} = o_P(1).$$

The result also holds verbatim by replacing (1.4) with (1.3) (with  $q \geq d$ ), and  $(\Sigma_n^*, F_n^*, \gamma_n^*)$  with  $(U_n^*, f_n^*, \gamma_n^*)$ , respectively.

Some remarks of Theorem 1.2 and Theorem 1.3 are in order.

- (Interpretations of Theorem 1.2 and 1.3) Theorem 1.2 and 1.3 provide fundamental guarantees, demonstrating that the solution of our two-layer model can consistently estimate the central mean subspace and its dimensionality under the mild assumption of finite fourth and second moments on  $X$  and  $Y$ . The basic implication is that the two-layer kernel ridge regression models intrinsically favor parsimonious data representations, and have the inherent ability to filter out noise and preserve the relevant features for prediction without external regularizations in finite samples.
- ("Automatic" dimension reduction) Oftentimes, in the literature of statistical learning [51], there is the expectation that explicit regularization techniques, such as nuclear norm penalization, early stopping, or clipping, are essential to achieve low-rank structures in minimization solutions, facilitating dimensionality reduction. Theorem 1.2 shows that such regularization techniques are not necessarily needed for the two-layer model. Theorem 1.3 further clarifies that the linear layer identifies the parsimonious subspace of features relevant for prediction, specifically aligning with the central mean subspace, without conventional regularizations. In Section 1.3, we will delve into the mathematical intuition underpinning these results.
- (Constraint  $\Sigma : \Sigma \succ 0$ ) Some may contend that the semidefinite constraint  $\Sigma \succeq 0$ , which forces the solution  $\Sigma_n^*$  to have non-negative eigenvalues (akin to eigenvalue thresholding), is serving as explicit regularization that induces a low-rank  $\Sigma_n^*$ . Yet our result not only says that  $\Sigma_n^*$  is low-rank, but also that its rank is bounded by  $\dim(S_*)$ . Note the positive semidefinite constraint alone would not lead to this sharper bound: see the next bullet point.
- (Two-layer *linear* neural networks fail) If the RKHS  $\mathcal{H}_q$  in (1.1) is induced by the linear kernel  $(x, x') \mapsto x^T x'$  (or equivalently, if  $\mathcal{H}_\Sigma$  in (1.2) uses the kernel  $(x, x') \mapsto x^T \Sigma x'$ ), then the predictive model  $X \mapsto f(U^T X) + \gamma$  in (1.1) reduces to a two-layer linear neural network model. This switch from a rotationally and translation-invariant kernel to a linear kernel removes the model's ability to achieve dimensionality reduction in the first layer. These findings are documented with empirical evidence in Section 9, with theoretical support in Section 8, showing that kernels of the form  $(x, x') \mapsto \psi(x^T x')$  lack this property.

Section 1.3 will briefly comment on the role of *rotationally and translation invariant* kernel in inducing sparse regularization in the first linear layer.

- (Illustration through real-world data applications) Section 10 presents two real-world data applications illustrating how the two-layer kernel ridge regression model "automatically" regularizes to learn feature subspaces. In the first application, regularization facilitates dimension reduction and helps identify interpretable categorical variables that receive less attention in previous studies. In the second, we show that the two-layer kernel ridge regression model consistently improves prediction accuracy over traditional kernel methods on the SVHN image dataset, including both subsampled datasets and tasks involving different digits, achieving predictive performance comparable to a two-layer ReLU neural network while the bottom-layer weight matrix exhibits a strikingly low-rank structure. These results highlight the role of feature learning in enhancing performance and suggest that such regularization may play a crucial role in both improving predictive accuracy and promoting model interpretability.

1.3. *Technical Insight.* This section elucidates our main technical idea behind proving Theorem 1.2, explaining the mathematical basis for how the low-rank structure is preserved in finite-sample minimizers without using conventional regularization. For space considerations, here we only discuss the case where  $\lambda \in (0, \lambda_0]$  for the  $\lambda_0$  defined in Theorem 1.1.

Given Theorem 1.1, any population minimizer  $\Sigma^*$  must obey  $\text{rank}(\Sigma^*) = \dim(S_*)$ . Our goal is to show that this low rankness property is preserved by the empirical minimizer  $\Sigma_n^*$ :

$$\lim_{n \rightarrow \infty} \mathbb{P}(\text{rank}(\Sigma_n^*) = \dim(S_*), \quad \forall (\Sigma_n^*, F_n^*, \gamma_n^*) \text{ minimizing (1.4)}) = 1.$$

The result for  $U_n^*$  will follow from the equivalence between the formulations (1.3) and (1.4).

To understand this property of  $\Sigma_n^*$ , we first introduce a function that takes partial minimization over the prediction function and the intercept  $\gamma$ :

$$(1.7) \quad J_n(\Sigma) = \min_{F, \gamma} \frac{1}{2} \mathbb{E}_n [(Y - F(X) - \gamma)^2] + \frac{\lambda}{2} \|F\|_{\mathcal{H}_\Sigma}^2.$$

Then the empirical minimizer  $\Sigma_n^*$  corresponds to a minimizer of

$$(1.8) \quad \underset{\Sigma}{\text{minimize}} J_n(\Sigma) \quad \text{subject to} \quad \Sigma \succeq 0, \quad \|\Sigma\| \leq M.$$

Similarly, we define the population objective  $J(\Sigma)$  by replacing  $\mathbb{E}_n$  in (1.7) by  $\mathbb{E}$ . Then the population minimizer  $\Sigma^*$  corresponds to a minimizer of an analogously defined problem:

$$(1.9) \quad \underset{\Sigma}{\text{minimize}} J(\Sigma) \quad \text{subject to} \quad \Sigma \succeq 0, \quad \|\Sigma\| \leq M.$$

Let's denote

$$(1.10) \quad \mathcal{C} = \{\Sigma : \Sigma \succeq 0\} \quad \text{and} \quad \mathcal{M} = \{\Sigma : \Sigma \succeq 0, \text{rank}(\Sigma) = \dim(S_*)\}.$$

We use  $\mathcal{C}_M = \{\Sigma : \Sigma \succeq 0, \|\Sigma\| \leq M\}$  to denote the compact constraint set.

**Main Properties** Our strategy relies on establishing two properties of  $J$  and  $J_n$ .

- (Sharpness) For every minimizer  $\Sigma^*$  of the population objective  $J$ , there is  $\rho > 0$  such that

$$(1.11) \quad \lim_{t \rightarrow 0^+} \frac{1}{t} (J(\Sigma^* + tW) - J(\Sigma^*)) \geq \rho \|W\|$$

holds for every matrix  $W$  in the tangent cone of  $\mathcal{C}$  at  $\Sigma^*$  with  $\text{col}(W) \subseteq \text{col}(\Sigma^*)^\perp$ . Additionally,  $\nabla J$  exists and is continuous on  $\mathcal{C}$  (for gradient definition on  $\mathcal{C}$ , see Definition 2.1).

This property emphasizes the stability of  $\Sigma^*$  as a minimizer: small perturbations in certain directions  $W$  lead to an increase in the objective  $J$  locally at least linear in the size of  $W$ . Note the considered perturbations  $W$  are those in the tangent cone of  $\mathcal{C}$  perpendicular

to the set  $\mathcal{M}^3$ . Technically, this linear increase of  $J$  when deviating away from  $\mathcal{M}$  holds not just at  $\Sigma^*$  but within a neighborhood of  $\Sigma^*$ , thanks to the continuity of  $\nabla J$ .

Statistically, given  $\text{col}(\Sigma^*) = S_*$ , this property says that perturbation of  $\Sigma^*$  in any direction  $W$  whose columns are orthogonal to the central mean subspace  $S_*$  would induce such a linear growth of the population objective  $J$ .

As a comparison, in classical quadratic mean differentiable models where the true parameter is statistically identifiable and lies in the interior of the parameter space, the population objective (expected negative log-likelihood) exhibits local quadratic growth around the minimizer (true parameter), with curvature given by the Fisher information [86]. This quadratic growth is locally slower than the *linear* growth seen in our model (1.11).

- (Uniform Convergence) The function value and gradient of the empirical objective  $J_n$  converge uniformly in probability to those of the population objective  $J$  on the positive semidefinite cone  $\mathcal{C}_M$ , i.e.,

$$(1.12) \quad \sup_{\Sigma \in \mathcal{C}_M} |J_n(\Sigma) - J(\Sigma)| = o_P(1), \quad \sup_{\Sigma \in \mathcal{C}_M} \|\nabla J_n(\Sigma) - \nabla J(\Sigma)\| = o_P(1)$$

as the sample size  $n \rightarrow \infty$ . The  $o_P(1)$  stands for convergence to zero in probability.

**Main Argument** With these properties in mind, our main argument, which is largely inspired by sensitivity analysis of minimizers' set identifiability in the optimization literature [34], is as follows.

- The uniform convergence property of objective values ensures that the empirical minimizers converge (in probability) to their population counterparts as  $n \rightarrow \infty$ . Since all population minimizers fall within  $\mathcal{M}$ , this implies the empirical minimizers converge to  $\mathcal{M}$ .
- To further show the empirical minimizers fall within  $\mathcal{M}$ , the sharpness property becomes crucial. The sharpness property ensures the empirical objective, whose gradient is uniformly close to that of the population objective, is still with high probability sharp, i.e., increasing at least linearly when moving in normal directions away from  $\mathcal{M}$  near the population minimizers.

To summarize, while uniform convergence of objective values implies convergence of minimizers, the sharpness property offers the stability that preserves the minimizers' low rankness property—a special case of set identifiability in optimization—under perturbations.

**Distinction from Two-Layer Linear Neural Networks.** The sharpness property (1.11) at the population level is key to explaining why our two-layer regression model, with a rotationally and translation-invariant kernel, induces sparse regularization in first-layer weight matrix.

In contrast, when the second layer uses a linear kernel, the model reduces to a two-layer linear neural network, lacking both the sharpness property in the objective and the low-rank structure in the minimizer. Consequently, two-layer linear neural networks do not achieve the same dimensionality reduction effect. For details, see Section 8 and Section 9.

1.4. *Summary of Contributions.* We summarize our contributions before discussing our relations to existing work in Section 1.4.1–Section 1.4.5. Specifically, our work is connected to a variety of fields, with the following contributions.

- (Feature Learning in Layered Models) We contribute a new perspective on feature learning, showing that a two-layer model, through optimization over *both layers*, can naturally induce sparse regularization in the first layer, enabling automatic estimation of the central mean subspace and its dimension—all without conventional regularization techniques.

---

<sup>3</sup>Note  $\mathcal{M}$  is a submanifold of the ambient Euclidean space that consists of all symmetric matrices. The normal space at any  $\Sigma' \in \mathcal{M}$  to the ambient space is the set of all symmetric matrices  $\Sigma$  with  $\text{col}(\Sigma) \subseteq \text{col}(\Sigma')^\perp$  [53].

- (Implicit Regularization in Layered Models) This result can be seen as an implicit regularization mechanism that is fundamentally different from existing mechanisms, particularly those in the linear neural network literature.
- (Nonparametric Dimension Reduction) This work provides an inferential tool for estimating the central mean subspace and its dimension, applicable under distributional assumptions no more restrictive than those in the existing literature.
- (Kernel Learning) We can infer the central mean subspace through a kernel learning approach, showing that dimension reduction can be attained without imposing fixed rank constraints, unlike prior methods in the kernel learning literature.
- (Sparse Regularization) Our technical insight emphasizes that the critical factor in determining sparse properties in finite-sample risk minimizers is the sharpness of the population objective near its minimizers, not merely the presence of explicit penalty terms. This perspective links the statistical view of empirical risk as a perturbed form of population risk with optimization insights, revealing that sharpness near population minimizers is crucial for finite-sample solutions to inherit the sparsity of the population minimizer.

Below, we aim to situate our contribution within the context of existing literature.

1.4.1. *Relation to Feature Learning in Two-Layer Models.* Understanding feature learning in layered models is a central problem in modern machine learning, as it raises fundamental questions about how these models process, represent, and utilize data [11]. Despite its importance, the underlying mechanisms of feature learning remain poorly understood. At a fundamental level, these challenges are rooted in the nonlinear compositions of layers, which result in variational problems—defined by minimizing population or empirical risks—that are highly nonlinear in the model parameters.

Recent theoretical efforts in statistical machine learning literature on feature learning focus on two-layer nonparametric models, like two-layer neural networks (see, e.g., [67, Appendix B] for a survey) or two-layer models of the form  $x \mapsto f(U^T x)$  where  $f, U$  are learned and  $f$  is modeled by an RKHS (see, e.g., [14, 39]). These models provide simplified yet powerful frameworks for studying feature learning in layered architectures. In the two-layer model contexts, feature learning aims to understand how, through the minimization of finite sample risk or many iterations of (stochastic) gradient descent, the first layer of the model  $U$  captures key data representations for the second layer’s predictions, ideally aligning with the central mean subspace to better adapt to the data’s low-dimensional structure [67, Appendix B].

Classical statistical and approximation results on layered models, e.g., [32, 9, 48], though abundant, do not explain how these models adapt to and learn the low-dimensional structure of the central mean subspace [67, Appendix B]. Recent results include characterizing how a single gradient step on the empirical risk enhances first-layer alignment toward the central mean subspace [7, 26, 6], how gradient descent and other fine-tuning two phase methods progressively improve alignment within gradient dynamics [1, 28, 2, 14], how explicit penalization on function derivatives helps empirical risk minimizers better align with central mean subspace [38], with some studies further detailing the learning of the second layer prediction function based on first-layer adaptation [15, 12], among others that relax distributional assumptions [16]. At a fundamental level, a key mathematical challenge is understanding the optimization landscape for these *nonlinear* two-layer models (unlike a *linearized* model, e.g., neural tangent kernel or random feature model where the first layer is fixed and does not perform feature learning [55, 67]), particularly on characterizing how the risk function depends on the first-layer weight matrix.

Our work offers a new perspective on feature learning in non-parametric two-layer models, complementing the existing literature. We demonstrate that the model’s layered structure itself can induce *sparse regularization* in the first layer, enabling low-dimensional feature

discovery within finite samples without using conventional regularization techniques. Specifically, by jointly optimizing both layers through minimizing the empirical risk function, our model achieves a statistically meaningful low-rank weight matrix in the first layer that remains consistent in estimating the central mean subspace and its dimension. This built-in regularization of certain two-layer models for feature learning, which enhances model interpretability without external regularizations, is the new perspective that we contribute to the literature.

Technically, our analysis also establishes two nontrivial properties of the population landscape for our two-layer model. First, the global minimizer perfectly aligns with the central mean subspace. Second, perhaps more importantly, we characterize the sharpness property near this minimizer, a local landscape result, which is important to explain why the model induces sparse regularization at the finite sample level. The derivations of either result is far from trivial, as it fundamentally involves nonlinear functional analysis that facilitates characterizing the behavior of population risks with respect to the feature matrix  $U$  (or  $\Sigma$ ).

Finally, while this current work focuses on statics, addressing the role of dynamics, such as characterizing the global optimization landscape and sample complexities for numerical algorithms, are important questions for future investigation.

*1.4.2. Mechanisms Driving Low-Rank Solutions in Layered Models.* A growing body of research suggests that intrinsic aspects of model architectures and optimization algorithms can guide layered models toward low-complexity solutions, such as low-rank weight matrices [31, 3, 46, 85, 84]. We position our findings Theorem 1.2 and Theorem 1.3 into these existing theoretical studies that aim to explain the mechanisms driving this behavior.

One line of prior research ties the emergence of low-rank solutions to specific optimization algorithms e.g., [46, 63, 5, 56, 64, 84]. Unlike this line of work, our main result on solutions' low rankness structure is *algorithm-independent*.

Another line of research demonstrates that the solution's low-rank structure can be inherent to the layered architecture, focusing primarily on *linear* neural networks that require Frobenius or Schatten- $q$  norm regularization on the weight matrices of each layer to ensure low-rank structure in solution [79, 27, 83, 70]. In contrast, our formulation achieves a natural low-rank structure in solutions without imposing such norm penalties on the first layer, within a non-linear, two-layer model. Indeed, had we replaced the RKHS  $\mathcal{H}_q$  in our model (1.1) with a linear kernel, reducing it to a two-layer linear neural network, the solution would fail to exhibit a low-rank structure because there is no norm penalty on the first layer in our formulation (see Section 8 for theory and Section 9 for experiments).

To summarize, unlike prior work, our two-layer regression model achieves an exact low-rank solution in the first linear layer without using explicit norm penalties on the linear layer nor relying on any specific optimization algorithm. To the best of our knowledge, this is the first example of a layered model exhibiting implicit regularization of this kind.

*1.4.3. Relation to Dimension Reduction Literature.* We position Theorem 1.3 within the nonparametric dimension reduction literature. Recall that Theorem 1.3 demonstrates that the minimizers of the two-layer model and (its equivalent kernel learning formulation) can serve as an inferential tool for the central mean subspace. Below we discuss its applicability, and highlight that our assumptions are no more restrictive than existing ones.

In the context of inference, Assumption 1 is necessary. Assumption 2 is mild and can be checked statistically using goodness-of-fit test, e.g., [37]. Assumption 3, which demands independence between  $\Pi_{S_*} X$  and  $\Pi_{S_*^+} X$ , might seem restrictive. Nonetheless, there are scenarios where our findings are directly applicable, including:

- When we can intentionally design  $X$  to follow a specific distribution during data collection, as in computer experiments [74]. Notably, Assumption 3 holds when  $X \sim \mathcal{N}(0, I_d)$ .
- When equipped with prior knowledge regarding the marginal distribution of  $X$  [19]. If  $X$  is continuous with support  $\mathbb{R}^d$ , we can apply the reweighting technique (e.g., [10]) to allocate distinct weights to different data points, reducing the inference problem to the case of  $X \sim \mathcal{N}(0, I_d)$ . In particular, each data point  $X = x$  is given a weight  $w(x) = p_G(x)/p_X(x)$  where  $p_G$  and  $p_X$  denote the densities of  $\mathcal{N}(0, I_d)$  and  $X$ , respectively. In more general cases, the Voronoi weighting method mitigate violations of normality [24].

As a comparison, we note that many well-established methodologies for central mean subspace inference also rely on specific distributional assumptions. Notably:

- Sliced Inverse Regression (SIR) [62]: The inference method based on sliced inverse regression necessitates a coverage condition, see, e.g., [22, 93, 65]. This condition doesn't hold when  $Y$  is categorical with values from a set of  $k$  elements when  $k \leq \dim(S_*)$  [22].
- Minimum Average Variance Estimation (MAVE) [91]: This approach (and related approaches that estimate the derivative of  $\mathbb{E}[Y|X = x]$ , e.g., [73, 54]) relies on  $X$  being continuous and not discrete, see, e.g., [91, 92, 66].
- Fourier method: This approach assumes Gaussianity of  $X$  [95, 94].
- Contour Regression: This method demands that  $X$  follow an elliptically contoured distribution [61].
- Kernel dimension reduction: This approach requires prior knowledge of the dimension of the central mean subspace, imposing a rank constraint based on that dimension [42].

As a result, the distributional assumptions we impose are no more restrictive than those in the existing literature. Specifically, we do not constrain  $X$  to a particular distribution type or make assumptions about the continuity of  $X$  or  $Y$ , nor require prior knowledge of the dimensionality of the central mean subspace.

1.4.4. *Related Work on Kernel Learning.* A large body of research has emphasized the importance of kernel selection in KRR. Recent advances in kernel learning shift the focus from selecting a fixed kernel *a priori* to learning the RKHS itself [44]:

$$\min_{F, \gamma, \theta} \frac{1}{2} \mathbb{E}_n[(Y - F(X) - \gamma)^2] + \frac{\lambda}{2} \|F\|_{\mathcal{H}_\theta}^2$$

where the RKHS  $\mathcal{H}_\theta$ , parameterized by  $\theta$ , is optimization as part of the model. Our formulation (1.2) fits into this framework, with kernel parameterization  $\phi(\|x - x'\|_\Sigma^2)$ .

This section highlights our contribution to the theoretical understanding of the solution matrix  $\Sigma$ , an area with abundant empirical studies but relatively sparse theoretical results. To set the stage, we first provide a quick survey of key developments in this field.

Learning kernels parameterized by  $k_\Sigma(x, x') = \phi(\|x - x'\|_\Sigma^2)$  with a matrix  $\Sigma$  is well noted in the literature. Early work by Vapnik and colleagues [89, 20, 47], introduced a method equivalent for learning a diagonal matrix  $\Sigma$  in  $k_\Sigma$  to perform raw feature selection by removing redundant coordinates in  $x$ . Fukumizu, Bach, and Jordan [41, 42] extended this to learn an orthogonal projection matrix  $\Sigma$  for subspace dimension reduction. While the approach of learning the full matrix  $\Sigma$  may offer less interpretability compared to learning a diagonal  $\Sigma$ , which aligns with raw feature selection, it demonstrates strong predictive performance across fields such as bioinformatics [75], and sensing and imaging [82]. Recent empirical work further supports this direction, with numerical results suggesting that learning a full matrix  $\Sigma$  in kernel ridge regressions achieves state-of-the-art predictive performance on a collection of tabular benchmark datasets [71]. Despite these advances, theoretical studies on the statistical properties of  $\Sigma$  are limited, which is the focus of our contribution.

A notable work related to us is the work by Fukumizu, Bach, and Jordan [42], which addresses sufficient dimension reduction. Their approach relies on a critical assumption: the dimension  $r$  of the central dimension reduction subspace is known. Using this knowledge, their objective enforces an explicit rank constraint  $\Sigma \in \Lambda_r$ , where  $\Lambda_r = \{\Pi_S \mid \dim(S) = r\}$  represents the set of all orthogonal projection matrices of rank  $r$ . In their kernel learning objective (which has this rank constraint), they showed that the column space of  $\Sigma$  converges to the target central dimension reduction subspace.

In contrast, our approach does not require prior knowledge of the dimension of the central mean subspace. We do not impose a rank constraint  $\Sigma \in \Lambda_r$  in the objective. Our main result shows, under appropriate statistical assumptions and choice of  $\lambda$ , the empirical minimizer  $\Sigma$  adapts to the problem's low dimensional structure, with  $\text{rank}(\Sigma) = \dim(S_*)$  holding with high probability. We then leverage the result  $\text{rank}(\Sigma) = \dim(S_*)$  to show the consistency of the column space of  $\Sigma$  for the central mean subspace  $S_*$ .

In recent work, Jordan and a subset of authors focused on learning a diagonal matrix  $\Sigma$  [57], relying on exact zero *initialization* and the projected gradient descent *algorithm* to produce sparse diagonal matrices. However, there are two fundamental distinctions:

- The statistical properties of these matrices remain unclear in the existing work, particularly whether they consistently capture all relevant features for prediction [57]. In contrast, our findings show that the minimizer of our kernel learning objective consistently estimates the central mean subspace, thus capturing all relevant features.
- Prior work shows gradient descent with *exact zero initialization* produces exact sparse solutions [57]. In contrast, our findings show that the minimizer's low-rank structure arises inherently from the model, independent of optimization dynamics or initialization entirely.

These distinctions are critical to the establishment of the central message of this work: two-layer models can inherently perform dimension reduction—by consistently estimating both the central mean subspace and its dimension—in an unconventional way that does not rely on traditional sparse regularization techniques.

Technically, achieving these results relies on a solid statistical foundation of the variational problem (1.6) which we systematically develop in this paper (mainly, Section 2–5). Importantly, our analysis reveals non-trivial insights at the population level: (i) the identification of the global minimizer of the central mean subspace (Section 3) and (ii) the sharpness of the objective's local landscape near this minimizer (Section 4). These results, combined with the uniform convergence of the empirical objective's values and gradients to their population counterparts (Section 5), they collectively explain why the finite sample minimizer is low-rank and consistent in estimating the central mean subspace.

**1.4.5. Sparse Regularization: this Paper's Perspective.** In statistics and machine learning, sparse regularization typically refers to techniques that promote "simplicity" in solutions, often implemented by adding penalty terms to the loss function to deter solution complexity [51]. To achieve solutions "simple" in structure, common penalty terms such as the  $\ell_1$  norm encourage vector sparsity, while the nuclear norm targets matrices of low-rank structure [52]. Ideas supporting the importance of penalty terms are based on "intuitions" that sparsity of vectors and low rankness of matrices are unstable under perturbations.

This paper, however, shows that assessing solution sparsity or low rankness based merely on the presence or absence of penalty terms does not capture the full picture. The perspective we offer is grounded in the sensitivity analysis techniques of minimizers' set identifiability in the optimization literature [90, 60, 50, 33, 34, 36]. This domain tackles a key problem: given that a solution  $\theta^*$  to a minimizing objective aligns with the set inclusion  $\theta^* \in S$ , under what conditions will a smooth perturbation of the objective ensure that the minimizers of the perturbed problems align with the set inclusion  $\theta_n^* \in S$ ?

The crux of the answer often lies in the original minimizing objective obeying a "sharpness" property near its minimizers, meaning that the objective grows at least linearly when moving away from the set  $S$  (the term "sharpness" is borrowed from [60, 34] among many in the field). Specifically, in nonlinear constrained optimization when  $S$  forms a smooth subset of *convex* constraint set boundary (called an "identifiable surface"), sharpness aligns with the notion of strict complementary slackness at  $\theta^*$  [90]. For a submanifold  $S$  embedded in a Euclidean space, sharpness requires the objective's directional derivative at  $\theta^*$  to be bounded away from zero along the normal directions near  $\theta^*$  with respect to  $S$ , which is formalized in the concept of *partial smoothness* [60]. Defining a "sharpness" condition for general sets  $S$  remain case-specific (as we analyze for a set of low-rank matrices in Section 6), where only the notion of *identifiable set* offers the broad framework [33, 34].

Building on this insight, we argue that an empirical minimizer would maintain the "simple" structure of the population solution if the population objective possesses a form of sharpness property in relation to the set of "simple" solutions, and if the gradient and value of the empirical objective converge uniformly to the population counterparts. This perspective is useful as it explains why, despite our objective lacking explicit nuclear norm regularization (or other low-rank-promoting penalties), we still observe exact low-rank solutions in finite samples. Specifically, in our case, the set  $S$  corresponds to the set of low-rank matrices. Since in our case the population objective  $J$  displays "sharpness" with respect to  $S$ , by establishing identifiability with respect to the set of low-rank matrices, we demonstrate the low-rankness of minimizers of the empirical objective.

**1.5. Basic Definition and Notation.** Throughout this paper, we use several standard notation in the literature. The inner product in  $\mathbb{R}^d$  is represented as  $\langle v_1, v_2 \rangle = v_1^T v_2$ .  $I$  denotes the  $d$ -by- $d$  identity matrix and  $\text{col}$ ,  $\text{tr}$  and  $\text{det}$  denote the column space, trace and determinant of a matrix, respectively.  $\text{Sym}_d$  denotes the space of  $d$ -by- $d$  symmetric matrices with inner product  $\langle \Sigma_1, \Sigma_2 \rangle = \text{tr}(\Sigma_1^T \Sigma_2)$ . A norm  $\|\cdot\|$  on  $d$ -by- $d$  matrices is called a unitarily invariant norm if  $\|\Sigma\| = \|O_1 \Sigma O_2^T\|$  holds for every square matrix  $\Sigma$  and orthonormal matrix  $O_1, O_2$ . We write  $A \succeq B$  (resp.  $A \succ B$ ) for  $A, B \in \text{Sym}_d$  if  $A - B$  is positive semidefinite (resp. positive definite). For a differentiable function  $f : \mathbb{R} \rightarrow \mathbb{R}$ , we use  $f'$  to denote its gradient.

**Probability and Measure:** The notation  $X_n = o_P(1)$  means that  $X_n$  converges to zero in probability as  $n \rightarrow \infty$ , and  $X_n = O_P(1)$  means that for every  $\epsilon > 0$ , there exist finite  $M, N$  such that  $\mathbb{P}(|X_n| > M) < \epsilon$  for every  $n \geq N$ . The  $L_r$  norm of a random variable  $X$  under a probability measure  $\mathbb{Q}$  is denoted as  $\|X\|_{L_r(\mathbb{Q})}$ . The support of a measure  $\mu$  is  $\text{supp}(\mu)$ .

**Convex Analysis:** For a convex set  $\mathcal{C}$ , the tangent cone at  $x \in \mathcal{C}$ ,  $\mathcal{T}_{\mathcal{C}}(x)$ , is the set of limits  $v = \lim_{n \rightarrow \infty} t_n(x_n - x)$  for some sequence  $x_n \in \mathcal{C}$  and  $t_n \rightarrow \infty$ . The normal cone at  $x \in \mathcal{C}$ ,  $\mathcal{N}_{\mathcal{C}}(x)$ , assuming  $\mathcal{C}$  is embedded in a Euclidean space with inner product  $\langle \cdot, \cdot \rangle$ , is the set of  $w$  such that  $\langle w, v \rangle \leq 0$  for every  $v \in \mathcal{T}_{\mathcal{C}}(x)$ .

**Variational Analysis:** Let  $f : \mathbb{R}^d \mapsto \mathbb{R} \cup \{+\infty\}$  with a point  $x \in \mathbb{R}^d$  such that  $f(x)$  is finite. The subdifferential of  $f$  at  $x$ , denoted by  $\partial f(x)$ , consists of all vectors  $v$  such that  $f(\tilde{x}) \geq f(x) + \langle v, \tilde{x} - x \rangle + o(\|\tilde{x} - x\|_2)$  as  $\tilde{x} \rightarrow x$ .

**Function Spaces and Norms:** The Lebesgue space  $\mathcal{L}_r(\mathbb{R}^d)$  consists of all real-valued functions  $f : \mathbb{R}^d \rightarrow \mathbb{R}$  such that  $\|f\|_{L_r(\mathbb{R}^d)} < \infty$  where  $r \in [1, \infty]$ . The space  $\mathcal{C}_b(\mathbb{R}^d)$  consists of all bounded, continuous functions  $f : \mathbb{R}^d \rightarrow \mathbb{R}$  and is endowed with  $L_\infty(\mathbb{R}^d)$  norm. For ease of notation, we also use  $\|f\|_\infty$  to represent  $\|f\|_{L_\infty(\mathbb{R}^d)}$ .

**Kernel:** A symmetric function  $k : \mathbb{R}^d \times \mathbb{R}^d \rightarrow \mathbb{R}$  is called a positive semidefinite kernel if  $\sum_{i,j=1}^m \alpha_i \alpha_j k(x_i, x_j) \geq 0$  holds for all  $m$ ,  $\alpha_1, \alpha_2, \dots, \alpha_m \in \mathbb{R}$ , and  $x_1, x_2, \dots, x_m \in \mathbb{R}^d$ . It is called a positive definite kernel if it is positive semidefinite, and moreover, for all mutually distinct  $x_1, x_2, \dots, x_m \in \mathbb{R}^d$ ,  $\sum_{i,j=1}^m \alpha_i \alpha_j k(x_i, x_j) = 0$  holds if and only if  $\alpha_1 = \alpha_2 = \dots = \alpha_m = 0$ . It is called an integrally positive definite kernel if  $\int_{\mathbb{R}^d} \int_{\mathbb{R}^d} k(x, x') d\nu(x) d\nu(x') > 0$  holds for every nonzero signed measure  $\nu$  on  $\mathbb{R}^d$  with finite total variation.

1.6. *Paper Organization.* The rest of the paper is organized as follows.

Section 2 prepares the mathematical foundations for the analysis, connecting compositional and kernel learning formulations, outlining key properties of the RKHS spaces  $\mathcal{H}_q$  and  $\mathcal{H}_\Sigma$ , and addressing the continuity of the KRR minimizer and objective differentiability.

Section 3 provides the proof of Theorem 1.1, showing that every minimizer of the population objective aligns closely with the central mean subspace, with its rank bounded by the dimension of the central mean subspace.

Section 4 further characterizes the population objective by establishing the sharpness property of  $J$  near the population minimizers.

Section 5 establishes uniformly, the value and the gradient of the empirical objective  $J_n$  converge to those of the population objective  $J$  on any given compact set.

Section 6 provides the proof of Theorem 1.2, demonstrating that every minimizer of the empirical objective  $J_n$  is low-rank with high probability. The proof builds upon Theorem 1.1, the sharpness property of  $J$  (Section 4), and the uniform convergence (Section 5).

Section 7 proves Theorem 1.3, showing that the column space of  $U$  (and  $\Sigma$ ) consistently infers the central mean subspace and its dimension, capturing the data's low-dimensional structure. The proof directly builds upon Theorem 1.1 and 1.2 established earlier.

Section 8 shows that the observed phenomenon does not occur if the kernel in the formulation (1.2) is replaced by the kernel of the form  $(x, x') \mapsto \psi(x^T \Sigma x')$  as the new population objective no longer satisfies the sharpness property. In particular, this failure applies to two-layer linear neural network models.

Section 9 presents additional simulations exploring how the observed low-rank structure of the minimizer varies across different data distributions and different kernels.

Section 10 presents two real-data applications to illustrate the two-layer kernel ridge regression models. Our illustration demonstrates how the model "automatically" regularizes to facilitate dimension reduction for enhanced interpretability and to improve prediction accuracy through feature learning.

Section 11 concludes the paper with future work discussions.

1.7. *Reproducibility.* The codes for all experiments and figures are available online:

<https://github.com/tinachentc/kernel-learning-in-ridge-regression>

**2. Preliminaries and Background.** This section sets up the mathematical foundations necessary for our later analysis. It begins with a review of standard kernel ridge regression (KRR) in Section 2.1. It then outlines key properties of the RKHS  $\mathcal{H}_q$  and  $\mathcal{H}_\Sigma$  in Section 2.2 and Section 2.3, respectively. It then formalizes the equivalence between layered modeling and kernel learning formulations in Section 2.4. It also addresses the continuity of the KRR minimizer with respect to model parameter  $\Sigma$  in Section 2.5, while focusing on the differentiability of the objective function  $J$  to  $\Sigma$  in Section 2.6. These results form the foundation, as the core of kernel learning lies in understanding how the problem varies with  $\Sigma$ . Importantly, all results in this section are basic, and built only upon minimal assumptions on the underlying probability measure: a finite fourth-moment condition on  $X$ ,  $\mathbb{E}[\|X\|^4] < \infty$  and a finite second moment condition on  $Y$ ,  $\mathbb{E}[Y^2] < \infty$ .

Notably, the equivalence results and the continuity/differentiability analysis are new contributions to the literature. The KRR review is essential for developing these results, and some RKHS properties discussed are relatively standard but not always covered in the literature.

2.1. *A Review of Standard Kernel Ridge Regression.* Consider the standard KRR:

$$(2.1) \quad \underset{F, \gamma}{\text{minimize}} \quad \frac{1}{2} \mathbb{E}[(Y - F(X) - \gamma)^2] + \frac{\lambda}{2} \|F\|_{\mathcal{H}}^2$$

where  $\mathcal{H}$  is an RKHS with a kernel  $k$  on  $\mathbb{R}^d$ , and  $\mathbb{E}[Y^2] < \infty$ . A foundation result is:

LEMMA 2.1 (Existence and Uniqueness of the Minimizer [25]). *There exists one unique minimizer  $(F^*, \gamma^*)$  to problem (2.1).*

By taking the first variation, we deduce the following characterization of the minimizer.

LEMMA 2.2 (Euler-Lagrange). *The unique minimizer  $(F^*, \gamma^*)$  to problem (2.1) satisfies*

$$(2.2) \quad \mathbb{E}[(Y - F^*(X) - \gamma^*)h(X)] = \lambda \langle F^*, h \rangle_{\mathcal{H}} \text{ for every } h \in \mathcal{H}.$$

Additionally,  $\gamma^* = \mathbb{E}[Y - F^*(X)]$ .

LEMMA 2.3 (Trivial Upper Bound). *The minimum value of (2.1) is at most  $\text{Var}(Y)/2$ . If  $\text{Cov}(Y, h(X)) \neq 0$  for some  $h \in \mathcal{H}$ , then this bound is strict.*

PROOF. The first part follows by plugging in the test function  $F \equiv 0$  and  $\gamma = \mathbb{E}[Y]$  in the cost function of (2.1). The equality is achieved only when  $F \equiv 0$  and  $\gamma = \mathbb{E}[Y]$  is the minimizer, which then implies  $\text{Cov}(Y, h(X)) = 0$  for every  $h \in \mathcal{H}$  by Lemma 2.2.  $\square$

LEMMA 2.4. *The unique minimizer  $(F^*, \gamma^*)$  to (2.1) obeys  $\|F^*\|_{\mathcal{H}}^2 \leq \text{Var}(Y)/\lambda$ .*

PROOF. This follows directly from Lemma 2.3 and the minimizing property of  $F^*$ .  $\square$

As a consequence of the Euler-Lagrangian characterization, we deduce the following version of the representer theorem [58].

LEMMA 2.5 (Representer Theorem). *Let  $X'$  be independent of  $(X, Y)$  and have the same distribution as  $X$ . The unique minimizer  $(F^*, \gamma^*)$  to (2.1) can be expressed as*

$$F^*(x) = \mathbb{E}[a(X)k(X, x)] \text{ for some } a : \mathbb{R}^d \rightarrow \mathbb{R} \text{ with } a(X) \in \mathcal{L}_2(\mathbb{P})$$

where the identity holds pointwise for  $x$  in  $\mathbb{R}^d$ . Consequentially, the minimum value (2.1) is:

$$\min_{a, \gamma} \frac{1}{2} \mathbb{E}[(Y - \mathbb{E}[a(X')k(X, X')|X] - \gamma)^2] + \frac{\lambda}{2} \mathbb{E}[a(X)a(X')k(X, X')]$$

where the minimization is over functions  $a : \mathbb{R}^d \rightarrow \mathbb{R}$  and scalars  $\gamma \in \mathbb{R}$  with  $a(X) \in \mathcal{L}_2(\mathbb{P})$ .

PROOF. Let  $a^*(X) = (\mathbb{E}[Y|X] - F^*(X) - \gamma^*)/\lambda$ . Note  $a^*(X) \in \mathcal{L}_2(\mathbb{P})$  since  $\mathbb{E}[Y^2] < \infty$ . Using the reproducing property and the Euler-Lagrange equation (2.2), we obtain:

$$\lambda \langle \mathbb{E}[a^*(X')k(X', \cdot)], h \rangle_{\mathcal{H}} = \lambda \mathbb{E}[a^*(X')h(X')] = \lambda \langle F^*, h \rangle_{\mathcal{H}}$$

holding for every  $h \in \mathcal{H}$ . Thus  $F^*(\cdot) = \mathbb{E}[a^*(X')k(X', \cdot)]$  in  $\mathcal{H}$  by Riesz's representation theorem. Applying the reproducing property again, this identity also holds pointwise.

For the second part, when  $F(\cdot) = \mathbb{E}[a(X)k(X, \cdot)]$  in  $\mathcal{H}$ , we have:

$$\|F\|_{\mathcal{H}}^2 = \langle F, F \rangle_{\mathcal{H}} = \langle \mathbb{E}[a(X)k(X, \cdot)], \mathbb{E}[a(X')k(X', \cdot)] \rangle_{\mathcal{H}} = \mathbb{E}[a(X)a(X')k(X, X')],$$

where the last identity uses the reproducing property of  $\mathcal{H}$ . The second part of the result then follows directly from the representation of the minimizer  $F^*$  in the first part.  $\square$

2.2. *Properties of the RKHS  $\mathcal{H}_\Sigma$ .* We are interested in kernels  $k_\Sigma$  of the form:

$$(2.3) \quad k_\Sigma(x, x') = \phi(\|x - x'\|_\Sigma^2) = \int_0^\infty e^{-t\|x-x'\|_\Sigma^2} \mu(dt)$$

where  $\mu$ , following Assumption 4, is a nonnegative finite measure with support on  $[0, \infty)$  not concentrated at zero. Clearly,  $k_\Sigma$  is a positive semidefinite kernel on  $\mathbb{R}^d$  for every  $\Sigma \succeq 0$ , and positive definite for every  $\Sigma \succ 0$ . By the foundational result in RKHS theory, there is a unique RKHS  $\mathcal{H}_\Sigma$  on  $\mathbb{R}^d$  which is associated with  $k_\Sigma$  [4, 88]. We denote the norm and the inner product on  $\mathcal{H}_\Sigma$  by  $\|\cdot\|_{\mathcal{H}_\Sigma}$  and  $\langle \cdot, \cdot \rangle_{\mathcal{H}_\Sigma}$  respectively throughout this paper.

Our analysis requires three basic properties of the RKHS  $\mathcal{H}_\Sigma$  whose proofs are relatively standard. The first concerns the embedding of the RKHS  $\mathcal{H}_\Sigma$  into  $\mathcal{C}_b(\mathbb{R}^d)$ .

PROPOSITION 1 (Continuous Embedding of  $\mathcal{H}_\Sigma$  into  $\mathcal{C}_b(\mathbb{R}^d)$ ). *For every  $\Sigma \succeq 0$ , we have*

$$\|F\|_{L^\infty(\mathbb{R}^d)} \leq \sqrt{\phi(0)} \|F\|_{\mathcal{H}_\Sigma} \text{ for every } F \in \mathcal{H}_\Sigma.$$

PROOF.  $|F(x)| = |\langle F, k_\Sigma(x, \cdot) \rangle_{\mathcal{H}_\Sigma}| \leq \|F\|_{\mathcal{H}_\Sigma} \|k_\Sigma(x, \cdot)\|_{\mathcal{H}_\Sigma} = \sqrt{\phi(0)} \|F\|_{\mathcal{H}_\Sigma}$  for every  $F \in \mathcal{H}_\Sigma$  and  $x$ . Both identities use the reproducing property of  $k_\Sigma$  with respect to  $\mathcal{H}_\Sigma$ .  $\square$

The second is about the relations between different RKHS  $\mathcal{H}_\Sigma$  over the matrix parameter  $\Sigma \succeq 0$ . Let  $\mathcal{H}_I$  denote the RKHS corresponding to  $k_I$ , which is the kernel  $k_I(x, x') = \phi(\|x - x'\|_2^2)$  for the identity matrix  $I \in \mathbb{R}^{d \times d}$ . We then have the following proposition.

PROPOSITION 2 (Connections between  $\mathcal{H}_\Sigma$  and  $\mathcal{H}_I$ ). *Let  $\Sigma = UU^T \succeq 0$  where  $\Sigma$  and  $U$  are both  $d \times d$  matrices. Then we have the following equality in the sense of sets:*

$$\mathcal{H}_\Sigma = \{F : \mathbb{R}^d \mapsto \mathbb{R} \mid \text{there exists } f : \mathbb{R}^d \mapsto \mathbb{R} \text{ such that } F(x) = f(U^T x) \text{ for } f \in \mathcal{H}_I\}.$$

Moreover, when  $\Sigma \succ 0$ , there exists a unique map  $\iota_U : \mathcal{H}_\Sigma \rightarrow \mathcal{H}_I$  that assigns each  $F \in \mathcal{H}_\Sigma$  to the unique  $f \in \mathcal{H}_I$  such that  $F(x) = f(U^T x)$  for all  $x \in \mathbb{R}^d$ . This mapping  $\iota_U$  is further an isometry between the two Hilbert spaces:

$$\langle F_1, F_2 \rangle_{\mathcal{H}_\Sigma} = \langle \iota_U F_1, \iota_U F_2 \rangle_{\mathcal{H}_I} \text{ for every } F_1, F_2 \in \mathcal{H}_\Sigma.$$

PROOF. We note for  $\Sigma = UU^T$ , the associated kernel  $k_\Sigma$  obeys  $k_\Sigma(x, x') = k_I(U^T x, U^T x')$  for every  $x, x'$ . Proposition 2 then follows from the standard construction of a general RKHS, e.g., [88, Theorem 12.11]. This result is also noted in the literature, e.g., [42].  $\square$

The last is on the expressive power of  $\mathcal{H}_\Sigma$ . Let us denote the vector space:

$$\mathcal{H}_\Sigma + \mathbb{R} = \left\{ u : \mathbb{R}^d \rightarrow \mathbb{R} \mid u(x) = F(x) + \gamma \text{ for some } F \in \mathcal{H}_\Sigma \text{ and } \gamma \in \mathbb{R} \right\}.$$

PROPOSITION 3 (Denseness of  $\mathcal{H}_\Sigma + \mathbb{R}$  in  $\mathcal{L}_2(\mathbb{Q})$ ). *Let Assumption 4 hold and  $\Sigma \succ 0$ . For any probability measure  $\mathbb{Q}$  on  $\mathbb{R}^d$ , the space  $\mathcal{H}_\Sigma + \mathbb{R}$  is dense in  $\mathcal{L}_2(\mathbb{Q})$ . Specifically, for any  $u \in \mathcal{L}_2(\mathbb{Q})$  and any  $\epsilon > 0$ , there exists  $u_\epsilon \in \mathcal{H}_\Sigma + \mathbb{R}$  such that  $\|u - u_\epsilon\|_{\mathcal{L}_2(\mathbb{Q})} < \epsilon$ .*

PROOF. We leverage a result in [42, Proposition 5], which says, for an RKHS  $\mathcal{H}$ ,  $\mathcal{H} + \mathbb{R}$  is dense in  $\mathcal{L}_2(\mathbb{Q})$  for every probability measure  $\mathbb{Q}$  if and only if  $\mathcal{H}$  is characteristic, meaning that if two probability measures  $\mathbb{Q}_1$  and  $\mathbb{Q}_2$  are such that  $\int F d\mathbb{Q}_1 = \int F d\mathbb{Q}_2$  holds for every  $F \in \mathcal{H}$ , then  $\mathbb{Q}_1 = \mathbb{Q}_2$ . Using this result, it suffices to show that  $\mathcal{H}_\Sigma$  is a characteristic RKHS for every  $\Sigma \succ 0$ .

That  $\mathcal{H}_I$  being characteristic is implied by a known result on radial kernels [80, Proposition 5], which states that an RKHS with kernel  $(x, x') \mapsto \int_0^\infty e^{-t\|x-x'\|_2^2} \nu(dt)$  is characteristic if the finite measure  $\nu$  is not a point mass at zero. The case for general  $\mathcal{H}_\Sigma$  is implied by the fact that  $\mathcal{H}_I$  is a characteristic RKHS thanks to Proposition 2.  $\square$

2.3. *An Invariance Property of  $\mathcal{H}_q$ .* We establish the translation and rotation invariance of the RKHS norm of  $\mathcal{H}_q$ . Recall that the RKHS  $\mathcal{H}_q$  is induced by a translation- and rotation-invariant kernel of the form  $k_q(w, w') = \phi(\|w - w'\|_2^2)$ , where  $w, w' \in \mathbb{R}^q$ .

Let  $O \in \mathbb{R}^{q \times q}$  be an orthonormal matrix, and  $t \in \mathbb{R}$ . Define the operator  $\mathcal{T}_{O,t}$ , which maps a function  $f : \mathbb{R}^q \rightarrow \mathbb{R}$  to another function  $\mathcal{T}_{O,t}(f) : \mathbb{R}^q \rightarrow \mathbb{R}$ , given by

$$\mathcal{T}_{O,t}(f)(w) = f(Ow + t), \quad \forall w \in \mathbb{R}^q.$$

PROPOSITION 4. *For every orthonormal matrix  $O \in \mathbb{R}^{q \times q}$ ,  $t \in \mathbb{R}$ , and  $f \in \mathcal{H}_q$ :*

$$\|\mathcal{T}_{O,t}(f)\|_{\mathcal{H}_q} = \|f\|_{\mathcal{H}_q}.$$

PROOF. We exploit the translation- and rotation-invariance property of the kernel  $k_q$ :

$$k_q(Ow + t, Ow' + t) = k_q(w, w'), \quad \forall w, w' \in \mathbb{R}^q.$$

Consider the vector space  $\tilde{\mathcal{H}}_q \subseteq \mathcal{H}_q$ , consisting of functions of the form:  $f(\cdot) = \sum_{i=1}^N \alpha_i k_q(w_i, \cdot)$  for some  $N < \infty$ ,  $w_i \in \mathbb{R}^q$  and  $\alpha_i \in \mathbb{R}$ . By the reproducing property, for such  $f \in \tilde{\mathcal{H}}_q$ ,

$$\|f\|_{\mathcal{H}_q}^2 = \sum_{i,j} \alpha_i \alpha_j k_q(w_i, w_j) = \sum_{i,j} \alpha_i \alpha_j k_q(Ow_i + t, Ow_j + t) = \|\mathcal{T}_{O,t}(f)\|_{\mathcal{H}_q}^2.$$

The second equality follows from the invariance of the kernel  $k_q$ .

To extend this to all  $f \in \mathcal{H}_q$ , we apply a standard density argument. We use the standard construction process of an RKHS, e.g., [88, Theorem 12.11] to conclude that any  $f \in \mathcal{H}_q$  is the limit of a sequence  $f_m \in \tilde{\mathcal{H}}_q$  with  $f_m \rightarrow f$  in the  $\mathcal{H}_q$ -norm. Hence,  $f_m$  forms a Cauchy sequence in  $\mathcal{H}_q$ , and by the reproducing property, this convergence  $f_m \rightarrow f$  also holds pointwise. As a result,  $\mathcal{T}_{O,t}(f_m)$  also forms a Cauchy sequence in  $\mathcal{H}_q$ , and converges pointwise to  $\mathcal{T}_{O,t}(f)$ . This further implies convergence  $\mathcal{T}_{O,t}(f_m) \rightarrow \mathcal{T}_{O,t}(f)$  in the  $\mathcal{H}_q$ -norm. Therefore,

$$\|f\|_{\mathcal{H}_q} = \lim_m \|f_m\|_{\mathcal{H}_q} = \lim_m \|\mathcal{T}_{O,t}(f_m)\|_{\mathcal{H}_q} = \|\mathcal{T}_{O,t}(f)\|_{\mathcal{H}_q}.$$

This result, valid for all  $f \in \mathcal{H}_q$ , completes the proof of Proposition 4.  $\square$

2.4. *Equivalence between layered formulation and kernel learning formulation.* Consider the minimum values of the following two kernel ridge regressions problems:

$$(2.4) \quad \begin{aligned} J(\Sigma, \lambda) &= \min_{F, \gamma} \frac{1}{2} \mathbb{E}[(Y - F(X) - \gamma)^2] + \frac{\lambda}{2} \|F\|_{\mathcal{H}_\Sigma}^2 \\ H(U, \lambda) &= \min_{f, \gamma} \frac{1}{2} \mathbb{E}[(Y - f(U^T X) - \gamma)^2] + \frac{\lambda}{2} \|f\|_{\mathcal{H}_q}^2 \end{aligned}$$

where  $\Sigma \in \mathbb{R}^{d \times d}$  and  $U \in \mathbb{R}^{d \times q}$ , respectively. We frequently drop the notational dependence of  $H, J$  on  $\lambda$  when the context is clear. Assume  $\mathbb{E}[Y^2] < \infty$ .

PROPOSITION 5. *For every  $q, d \in \mathbb{N}$ ,  $J(\Sigma) = H(U)$  if  $\Sigma = UU^T$ .*

PROOF. If  $\Sigma = UU^T$ , then the values of the kernels match at the corresponding covariates:

$$k_q(U^T X', U^T X) = \phi(\|U^T(X - X')\|_2^2) = \phi(\|X - X'\|_\Sigma^2) = k_\Sigma(X, X').$$

By the representer theorem (Lemma 2.5), the minimizers  $F^*$  and  $f^*$  of (2.4) satisfy, pointwise

$$F^*(\cdot) = \mathbb{E}[a_F(X')k(X', \cdot)], \quad f^*(\cdot) = \mathbb{E}[a_f(X')k(U^T X', \cdot)]$$

where  $a_F : \mathbb{R}^d \rightarrow \mathbb{R}$  and  $a_f : \mathbb{R}^d \rightarrow \mathbb{R}$  are some functions such that  $a_F(X), a_f(X) \in \mathcal{L}_2(\mathbb{P})$ . Therefore, we deduce

$$\begin{aligned} J(\Sigma) &= \min_{a, \gamma} \frac{1}{2} \mathbb{E}[(Y - \mathbb{E}[a(X')k_\Sigma(X', X) | X] - \gamma)^2] + \frac{\lambda}{2} \mathbb{E}[a(X)a(X')k_\Sigma(X, X')] \\ &= \min_{a, \gamma} \frac{1}{2} \mathbb{E}[(Y - \mathbb{E}[a(X')k_q(U^T X', U^T X) | X] - \gamma)^2] + \frac{\lambda}{2} \mathbb{E}[a(X)a(X')k_q(U^T X, U^T X')] \\ &= H(U), \end{aligned}$$

where the first and the last identities follow the same calculations in Lemma 2.5.  $\square$

With Proposition 5, we establish the central result of the section: an equivalence between all the layered and kernel learning formulations mentioned in the introduction. Essentially, these equivalences amount to changes of variables.

**PROPOSITION 6.** *The minimum value of (1.1) where  $q \geq d$  (resp. (1.3) and (1.5)) is the same as the minimum value of (1.2) (resp. (1.4) and (1.6)). The minimizers are connected by:*

$$(2.5) \quad F = f \circ U^T, \quad \Sigma = UU^T.$$

*In other words, suppose  $f, U, \Sigma, F$  satisfying (2.5), then  $(f, U, \gamma)$  minimizes (1.1) where  $q \geq d$  (resp. (1.3) and (1.5)) if and only if  $(F, \Sigma, \gamma)$  minimizes (1.2) (resp. (1.4) and (1.6)).*

**PROOF.** The result follows from Proposition 5 and a reparameterization of the parameters. Consider (1.5) and (1.6), first. The minimum value of (1.5) is the same as

$$\underset{U}{\text{minimize}} H(U) \quad \text{subject to} \quad \|\|UU^T\|\| \leq M$$

while the minimum value of (1.6) is the same as

$$\underset{\Sigma}{\text{minimize}} J(\Sigma) \quad \text{subject to} \quad \|\|\Sigma\|\| \leq M, \quad \Sigma \succeq 0.$$

By Proposition 5, there is the correspondence of the cost function  $H(U) = J(\Sigma)$  whenever  $\Sigma = UU^T$  holds. Additionally, if  $q \geq d$ , the following sets are equal:

$$\{UU^T \in \mathbb{R}^{d \times d} \mid U \in \mathbb{R}^{d \times q}, \|\|UU^T\|\| \leq M\} = \{\Sigma \in \mathbb{R}^{d \times d} \mid \Sigma \succeq 0, \|\|\Sigma\|\| \leq M\}.$$

These results imply the minimum values of (1.5) and (1.6) are identical. Consequently, it follows that the minimizers are related through the formula (2.5).

Applying the same argument to the empirical measure one gets the other correspondence between (1.1) (resp. (1.3)) and (1.2) (resp. (1.4)).  $\square$

**2.5. Uniform Bound and Lipschitz Continuity of Prediction Function in Parameter.** Let  $(F_\Sigma, \gamma_\Sigma)$  denote the unique minimizer of the cost function in the definition of  $J(\Sigma)$  in (2.4). Lemma 2.6 gives an  $L_\infty$  upper bound on the prediction function  $x \mapsto F_\Sigma(x) + \gamma_\Sigma$  that holds uniform in  $\Sigma$ .

**LEMMA 2.6 (Uniform Bound of Prediction Function in Parameter).** *For all  $\Sigma$ ,*

$$\|F_\Sigma(\cdot) + \gamma_\Sigma\|_{L_\infty(\mathbb{R}^d)} \leq 2\sqrt{\phi(0)\text{Var}(Y)/\lambda} + \mathbb{E}[|Y|].$$

**PROOF.** This follows from Lemma 2.2 and Lemma 2.4.  $\square$

Our future analysis relies on a basic Lipschitz continuity property regarding the prediction function  $x \mapsto F_\Sigma(x) + \gamma_\Sigma$  with respect to the matrix parameter  $\Sigma$ , as stated in Lemma 2.7.

LEMMA 2.7 (Lipschitz Continuity of Prediction Function in Parameter). *Let  $\mathbb{E}[Y^2] < \infty$  and  $\mathbb{E}[\|X\|^4] < \infty$ . Assume Assumption 4 holds. Then*

$$\lim_{\Sigma' \rightarrow \Sigma} \|(F_{\Sigma'}(X) + \gamma_{\Sigma'}) - (F_{\Sigma}(X) + \gamma_{\Sigma})\|_{L_2(\mathbb{P})} = 0.$$

Moreover, for any matrices  $\Sigma, \Sigma'$ , there is the quantitative estimate: for  $c = 16(\phi'_+(0))^2/\lambda^2$ ,

$$\|(F_{\Sigma'}(X) + \gamma_{\Sigma'}) - (F_{\Sigma}(X) + \gamma_{\Sigma})\|_{L_2(\mathbb{P})}^2 \leq c\mathbb{E}[\|X\|_2^4]\mathbb{E}[Y^2] \|\Sigma' - \Sigma\|_{\text{op}}^2.$$

PROOF. Applying Riesz representation theorem to the Euler-Lagrange equation (Lemma 2.2), the minimizer  $(F_{\Sigma}, \gamma_{\Sigma})$  satisfies the following integral equation for every  $x \in \mathbb{R}^d$ :

$$\mathbb{E}[(Y - F_{\Sigma}(X) - \gamma_{\Sigma})k_{\Sigma}(X, x)] = \lambda F_{\Sigma}(x).$$

A similar equation holds for  $F_{\Sigma'}$ . Thereby, the difference  $g(x) = (F_{\Sigma}(x) + \gamma_{\Sigma}) - (F_{\Sigma'}(x) + \gamma_{\Sigma'})$  satisfies the following integral equation for every  $x \in \mathbb{R}^d$ :

$$(2.6) \quad \mathbb{E}[r_{\Sigma}(X, Y)(k_{\Sigma} - k_{\Sigma'})(X, x)] = \mathbb{E}[g(X)k_{\Sigma}(X, x)] + \lambda(g(x) - (\gamma_{\Sigma} - \gamma_{\Sigma'}))$$

where  $r_{\Sigma}(x, y) = y - F_{\Sigma}(x) - \gamma_{\Sigma}$  denotes the residual at  $\Sigma$ .

Let  $X'$  be an independent copy of  $X$ . We substitute  $x$  with  $X'$  in equation (2.6), multiply both sides by  $g(X')$  and take expectation. Given  $\mathbb{E}[g(X)] = 0$  (by Lemma 2.2), this yields:

$$(2.7) \quad \begin{aligned} & \mathbb{E}[r_{\Sigma}(X, Y)((k_{\Sigma} - k_{\Sigma'})(X, X'))g(X')] \\ & = \mathbb{E}[g(X)k_{\Sigma}(X, X')g(X')] + \lambda\mathbb{E}[g(X)^2]. \end{aligned}$$

Let  $\Sigma = UU^T$  with  $U \in \mathbb{R}^{d \times d}$ , and define  $Z = U^T X$ . Note that  $k_{\Sigma}(X, X') = k_I(Z, Z')$ . By Proposition 2,  $g$  can be expressed as  $g(X) = h(Z)$  for some  $h$ . Thereby,

$$\mathbb{E}[g(X)k_{\Sigma}(X, X')g(X')] = \mathbb{E}[h(Z)k_I(Z, Z')h(Z')].$$

We show this quantity is nonnegative. Define  $\zeta_t(\omega) = \frac{1}{(4\pi t)^{d/2}} e^{-\|\omega\|_2^2/(4t)}$  and observe:

$$\begin{aligned} \mathbb{E}[h(Z)k_I(Z, Z')h(Z')] &= \int \mathbb{E}[h(Z)h(Z')e^{-t\|Z-Z'\|_2^2}] \mu(dt) \\ &= \int \mathbb{E}[h(Z)h(Z') \int e^{-it\langle \omega, Z-Z' \rangle} \zeta_t(\omega) d\omega] \mu(dt) \\ &= \iint \left| \mathbb{E}[h(Z)e^{-it\langle \omega, Z \rangle}] \right|^2 \zeta_t(\omega) d\omega \mu(dt) \geq 0. \end{aligned}$$

The identities follow from the definition of  $k_I$ , the fact that Fourier transform of a Gaussian is Gaussian, and Fubini's theorem. Thus, the RHS of (2.7) is bounded below by  $\lambda\mathbb{E}[g(X)^2]$ .

Substituting this estimate into (2.7), we deduce:

$$\lambda\mathbb{E}[g(X)^2] \leq \mathbb{E}[r_{\Sigma}(X, Y)((k_{\Sigma} - k_{\Sigma'})(X, X'))g(X')].$$

Applying Cauchy Schwarz's inequality to the RHS gives the estimate:

$$\mathbb{E}[g(X)^2] \leq \frac{1}{\lambda^2} \mathbb{E}[r_{\Sigma}(X, Y)^2] \mathbb{E}[(k_{\Sigma} - k_{\Sigma'})(X, X')^2].$$

By Lemma 2.3,  $\mathbb{E}[r_{\Sigma}(X, Y)^2] \leq \text{Var}(Y) < \infty$ . Additionally, we have

$$\mathbb{E}[(k_{\Sigma} - k_{\Sigma'})(X, X')^2] \leq (\phi'_+(0))^2 \|\Sigma - \Sigma'\|_{\text{op}}^2 \mathbb{E}[\|X - X'\|_2^4].$$

Lemma 2.7 follows.  $\square$

2.6. *Continuous Differentiability of  $J$  and Gradient Formula.* Our analysis requires a basic smoothness property of the function  $J$ , which is crucial for defining and proving *sharpness* described in the introduction. Recall our definition of  $J$  in (2.4).

The function  $J$  is defined on the semidefinite cone  $\mathcal{C} = \{\Sigma \mid \Sigma \succeq 0\}$ . To deal with matrices  $\Sigma$  that lie on the boundaries of  $\mathcal{C}$ , we introduce the following notion of gradient. Essentially, the gradient is defined through a first-order Taylor expansion of  $h$  within the set  $\mathcal{C}$ .

**DEFINITION 2.1 (Gradient on  $\mathcal{C}$ ).** *Let  $h : \mathcal{C} \rightarrow \mathbb{R}$ . The function  $h$  has a gradient  $\nabla h(\Sigma)$  at  $\Sigma \in \mathcal{C}$  if  $\nabla h(\Sigma)$  is a symmetric matrix, and for every converging sequence  $\Sigma_n \in \mathcal{C}$  to  $\Sigma$ :*

$$h(\Sigma_n) = h(\Sigma) + \langle \nabla h(\Sigma), \Sigma_n - \Sigma \rangle + o(\|\Sigma_n - \Sigma\|_F).$$

We say  $h$  is differentiable on  $\mathcal{C}$  if  $\nabla h$  is everywhere well-defined on  $\mathcal{C}$ .

**REMARK.** *The gradient of  $h$  at  $\Sigma$ , if exists, is unique because the tangent cone  $\mathcal{T}_{\mathcal{C}}(\Sigma)$  contains an open ball. Moreover, this gradient agrees with the standard definition of the gradient when  $\Sigma$  is in the interior of  $\mathcal{C}$  (i.e., when  $\Sigma \succ 0$ ).*

The following foundational result establishes the continuous differentiability of  $J$  on the semidefinite cone  $\mathcal{C}$ , assuming only moments conditions on  $X$  and  $Y$ . Additionally, it provides an explicit gradient formula in (2.9), which is crucial for proving *sharpness* property of  $J$  near its minimizer later. The notation  $\partial_{\Sigma} k_{\Sigma}(x, x')$  denotes the partial derivative of the kernel  $k_{\Sigma}(x, x')$  with respect to  $\Sigma$ . More explicitly, it is the matrix

$$(2.8) \quad \partial_{\Sigma} k_{\Sigma}(x, x') = \phi'(\|x - x'\|_{\Sigma}^2)(x - x')(x - x')^T.$$

In the above,  $\phi'$  is the derivative of  $\phi$ , and its value at 0 is understood as  $\phi'_+(0)$ .

**LEMMA 2.8 (Gradient Formula).** *Assume  $\mathbb{E}[\|X\|^4] < \infty$ ,  $\mathbb{E}[Y^2] < \infty$  and Assumption 4. Then,  $\nabla J(\Sigma)$  exists for every  $\Sigma \in \mathcal{C}$  as defined in Definition 2.1. It has the expression:*

$$(2.9) \quad \nabla J(\Sigma) = -\frac{1}{2\lambda} \mathbb{E}[r_{\Sigma}(X, Y)r_{\Sigma}(X', Y')\partial_{\Sigma} k_{\Sigma}(X, X')],$$

where  $(X', Y')$  denotes an independent copy of  $(X, Y)$  and  $r_{\Sigma}(X, Y) = Y - F_{\Sigma}(X) - \gamma_{\Sigma}$ , with  $(F_{\Sigma}, \gamma_{\Sigma})$  the unique minimizer of the cost function in the definition of  $J(\Sigma)$  in (2.4).

**PROOF.** Let

$$V(\Sigma, a, \gamma) = \frac{1}{2} \mathbb{E}[(Y - \mathbb{E}[a(X')k_{\Sigma}(X, X')|X] - \gamma)^2] + \frac{\lambda}{2} \mathbb{E}[a(X)a(X')k_{\Sigma}(X, X')].$$

By the representer theorem (Lemma 2.5)

$$J(\Sigma) = \min_{a, \gamma} V(\Sigma, a, \gamma) = V(\Sigma, a_{\Sigma}, \gamma_{\Sigma})$$

where the minimization is over functions  $a : \mathbb{R}^d \rightarrow \mathbb{R}$  with  $a(X) \in L_2(\mathbb{P})$  and scalars  $\gamma \in \mathbb{R}$ . The same theorem also shows the unique minimizer  $(a_{\Sigma}, \gamma_{\Sigma})$  satisfies

$$a_{\Sigma}(X) = \frac{1}{\lambda} (\mathbb{E}[Y|X] - F_{\Sigma}(X) - \gamma_{\Sigma}) = \frac{1}{\lambda} \mathbb{E}[r_{\Sigma}(X, Y) | X].$$

Let

$$\begin{aligned} b(\Sigma, a, \gamma) &= \partial_{\Sigma} V(\Sigma, a, \gamma) \\ R_{\Sigma, a, \gamma}(X, Y) &= Y - \mathbb{E}[a(X')k_{\Sigma}(X, X')|X] - \gamma \end{aligned}$$

When evaluating  $b$ , we apply Lebesgue's dominated convergence theorem to justify exchanging the order of expectation and partial derivative in  $\Sigma$ . Using the fact that:

$$\mathbb{E}[\sup_{\Sigma \in \mathcal{N}} \|\partial_{\Sigma} k_{\Sigma}(X, X')\|^2] < \infty, \quad \mathbb{E}[\sup_{\Sigma \in \mathcal{N}} R_{\Sigma, a, \gamma}(X, Y)^2] < \infty$$

for any compact set  $\mathcal{N}$ , which follows from the assumption  $\mathbb{E}[\|X\|^4] < \infty$ , we obtain the following expression for  $b$  that holds for all  $a$  with  $a(X) \in L_2(\mathbb{P})$  and  $\gamma \in \mathbb{R}$ :

$$b(\Sigma, a, \gamma) = -\mathbb{E}[a(X')R_{\Sigma, a, \gamma}(X, Y)\partial_{\Sigma}k_{\Sigma}(X, X')] + \frac{\lambda}{2}\mathbb{E}[a(X)a(X')\partial_{\Sigma}k_{\Sigma}(X, X')].$$

Let  $\partial_{\Sigma}k_{\Sigma}|_{\Sigma=\Sigma'}$  denote the partial derivative of  $k_{\Sigma}$  with respect to  $\Sigma$  evaluated at a matrix  $\Sigma'$ . It follows that

$$\begin{aligned} b(\Sigma_1, a_{\Sigma_2}, \gamma_{\Sigma_2}) &= -\frac{1}{\lambda}\mathbb{E}[r_{\Sigma_2}(X', Y')R_{\Sigma_1, a_{\Sigma_2}, \gamma_{\Sigma_2}}(X, Y)\partial_{\Sigma}k_{\Sigma}|_{\Sigma=\Sigma_1}(X, X')] \\ &\quad + \frac{1}{2\lambda}\mathbb{E}[r_{\Sigma_2}(X, Y)r_{\Sigma_2}(X', Y')\partial_{\Sigma}k_{\Sigma}|_{\Sigma=\Sigma_1}(X, X')]. \end{aligned}$$

In particular, when specializing  $\Sigma_1 = \Sigma_2 = \Sigma_0$ , we obtain that

$$b(\Sigma_0, a_{\Sigma_0}, \gamma_{\Sigma_0}) = -\frac{1}{2\lambda}\mathbb{E}[r_{\Sigma_0}(X, Y)r_{\Sigma_0}(X', Y')\partial_{\Sigma}k_{\Sigma}|_{\Sigma=\Sigma_0}(X, X')].$$

Using Lemma 2.7 which implies convergence  $a_{\Sigma'} \rightarrow a_{\Sigma}$ ,  $r_{\Sigma'} \rightarrow r_{\Sigma}$  as  $\Sigma' \rightarrow \Sigma$  in  $\mathcal{L}_2(\mathbb{P})$ , and applying Lebesgue's dominated convergence theorem, we get at any matrix  $\Sigma_0$ :

$$\lim_{\Sigma_1 \rightarrow \Sigma_0, \Sigma_2 \rightarrow \Sigma_0} b(\Sigma_1, a_{\Sigma_2}, \gamma_{\Sigma_2}) = b(\Sigma_0, a_{\Sigma_0}, \gamma_{\Sigma_0}).$$

Moreover, the same lemma ensures that  $(\Sigma_1, \Sigma_2) \mapsto b(\Sigma_1, a_{\Sigma_2}, \gamma_{\Sigma_2})$  is uniformly continuous in a neighborhood of  $\Sigma_0$ . Verifying these conditions involves applying the triangle inequality and the Cauchy-Schwarz inequality.

Back to the proof of Lemma 2.8. Fix  $\Sigma_0$ . By Taylor's intermediate theorem, for every  $\Sigma$ , there is a matrix  $\Sigma'$  on the segment of  $\Sigma$  and  $\Sigma_0$  such that

$$J(\Sigma) = V(\Sigma, a_{\Sigma}, \gamma_{\Sigma}) = V(\Sigma_0, a_{\Sigma}, \gamma_{\Sigma}) + \langle b_{\Sigma}(\Sigma', a_{\Sigma}, \gamma_{\Sigma}), \Sigma - \Sigma_0 \rangle.$$

Given  $V(\Sigma_0, a_{\Sigma}, \gamma_{\Sigma}) \geq J(\Sigma_0)$  by the minimizing property of  $J$ , we deduce

$$J(\Sigma) \geq J(\Sigma_0) + \langle b_{\Sigma}(\Sigma_0, a_{\Sigma_0}, \gamma_{\Sigma_0}), \Sigma - \Sigma_0 \rangle + o(\|\Sigma - \Sigma_0\|).$$

Reversing the role of  $\Sigma$  and  $\Sigma_0$ , and using the uniform continuity of  $(\Sigma_1, \Sigma_2) \mapsto b(\Sigma_1, a_{\Sigma_2}, \gamma_{\Sigma_2})$  in a neighborhood of  $\Sigma_0$ , we obtain the reverse estimate

$$J(\Sigma) \leq J(\Sigma_0) + \langle b_{\Sigma}(\Sigma_0, a_{\Sigma_0}, \gamma_{\Sigma_0}), \Sigma - \Sigma_0 \rangle + o(\|\Sigma - \Sigma_0\|).$$

This proves that  $J$  is differentiable in the sense of Definition 2.4, with

$$\nabla J(\Sigma_0) = b(\Sigma_0, a_{\Sigma_0}, \gamma_{\Sigma_0}) = -\frac{1}{2\lambda}\mathbb{E}[r_{\Sigma_0}(X)r_{\Sigma_0}(X')\partial_{\Sigma}k_{\Sigma}|_{\Sigma=\Sigma_0}(X, X')].$$

□

As an almost immediate consequence, we obtain:

**LEMMA 2.9 (Continuous Differentiability of  $J$ ).** *Assume the condition of Lemma 2.8. Then the gradient  $\Sigma \mapsto \nabla J(\Sigma)$  is continuous everywhere on  $\mathcal{C}$ .*

**PROOF.** This follows from Lemma 2.6, 2.7, and 2.8, by applying the dominated convergence theorem and noting the continuity and boundedness of  $\phi'$  in the definition of  $\partial_{\Sigma}k_{\Sigma}$ . □

**3. Properties of the Population Minimizer.** In this section, we investigate the statistical properties of the population minimizers  $U^*$  of (1.5), and  $\Sigma^*$  of (1.6), under the distributional assumptions 1–4. Our analysis demonstrates that the column spaces of  $U^*$  and  $\Sigma^*$  align with the central mean subspace  $S_*$ , culminating in the proof of Theorem 1.1 at the end of Section 3.

For reader's convenience, we recall

$$(3.1) \quad H(U, \lambda) = \min_{f, \gamma} \frac{1}{2} \mathbb{E}[(Y - f(U^T X) - \gamma)^2] + \frac{\lambda}{2} \|f\|_{\mathcal{H}_q}^2.$$

We consider the minimization problem:

$$(3.2) \quad \underset{U}{\text{minimize}} H(U, \lambda) \quad \text{subject to} \quad \|UU^T\| \leq M.$$

By definition, any minimizer  $U^*$  of (1.5) minimizes (3.2), and vice versa.

This section is organized as follows. First, we analyze the minimizer  $U^*$  under two different regimes of  $\lambda$ : (i) the general case, where we establish  $\text{col}(U_*) \subseteq S_*$ , and (ii) the small  $\lambda$  case, where we show  $\text{col}(U_*) = S_*$ . These results are detailed in Sections 3.1 and 3.2, respectively. Next, we extend these findings to  $\text{col}(\Sigma^*)$  and conclude with the proof of Theorem 1.1 in Section 3.3.

**3.1. Column Space Containment for General  $\lambda$ .** Throughout this subsection 3.1, we fix  $\lambda \in (0, \infty)$  and establish the result  $\text{col}(U^*) \subseteq S_*$  in Lemma 3.3. To achieve this, we first prove two key properties of the objective function  $H$ , stated in Lemma 3.1 and Lemma 3.2.

**LEMMA 3.1 (Reduction of  $H$  via Projection Onto  $S_*$ ).** *Let Assumptions 1, 3, 4 hold. For every  $U \in \mathbb{R}^{d \times q}$ , we have:*

$$H(U) \geq H(\Pi_{S_*} U).$$

*The inequality is strict if both  $H(U) < H(0)$  and  $U \neq \Pi_{S_*} U$  hold.*

**PROOF.** Let us denote  $Y(X) = \mathbb{E}[Y|X]$ , and  $c = \mathbb{E}[\text{Var}(Y|X)]$ . We recall the definition of  $H$ , and deduce the following identity:

$$(3.3) \quad \begin{aligned} 2H(U) &= \min_{f, \gamma} \mathbb{E}[(Y - f(U^T X) - \gamma)^2] + \lambda \|f\|_{\mathcal{H}_q}^2 \\ &= \min_{f, \gamma} \mathbb{E}[(Y(X) - f(U^T X) - \gamma)^2] + \lambda \|f\|_{\mathcal{H}_q}^2 + c. \end{aligned}$$

We then decompose  $X = X_{\parallel} + X_{\perp}$  where  $X_{\parallel} = \Pi_{S_*} X$  and  $X_{\perp} = \Pi_{S_*^\perp} X$ . Applying the law of iterated expectation we deduce:

$$(3.4) \quad \begin{aligned} 2H(U) &= \min_{f, \gamma} \left\{ \mathbb{E} \left[ \mathbb{E}[(Y(X) - f(U^T X_{\parallel} + U^T X_{\perp}) - \gamma)^2 \mid X_{\perp}] + \lambda \|f\|_{\mathcal{H}_q}^2 + c \right] \right\} \\ &\geq \mathbb{E} \left[ \min_{f, \gamma} \left\{ \mathbb{E}[(Y(X) - f(U^T X_{\parallel} + U^T X_{\perp}) - \gamma)^2 \mid X_{\perp}] + \lambda \|f\|_{\mathcal{H}_q}^2 + c \right\} \right]. \end{aligned}$$

Let us define

$$V(z; f, \gamma) = \mathbb{E}[(Y(X) - f(U^T X_{\parallel} + z) - \gamma)^2] + \lambda \|f\|_{\mathcal{H}_q}^2 + c,$$

which depends on  $z$ , and

$$(3.5) \quad \iota(z) = \min_{f, \gamma} V(z; f, \gamma).$$

Given that  $Y(X) = \mathbb{E}[Y|X] = \mathbb{E}[Y|X_{\parallel}]$  is a function of  $X_{\parallel}$ , which is independent from  $X_{\perp}$  by Assumption 3, the RHS of (3.4) is equal to  $\mathbb{E}[\iota(U^T X_{\perp})]$  by Fubini's theorem. Thus, the inequality (3.4) is the same as

$$(3.6) \quad 2H(U) \geq \mathbb{E}[\iota(U^T X_{\perp})].$$

We now argue that  $\iota$  is constant. Let us denote  $(f_z, \gamma_z)$  to be the unique minimizer of the partial minimization (3.5). Because the norm  $\|\cdot\|_{\mathcal{H}_q}$  is translation-invariant by Proposition 4, these minimizers must satisfy

$$(3.7) \quad f_z(\cdot + z) = f_0(\cdot) \quad \text{and} \quad \gamma_z = \gamma_0.$$

Consequentially, we deduce

$$\iota(z) = V(z; f_z, \gamma_z) = V(0; f_0, \gamma_0) = \iota(0).$$

Thus,  $\iota$  is constant. Following the bound (3.6), we get

$$(3.8) \quad \begin{aligned} 2H(U) &\geq \mathbb{E}[\iota(U^T X_{\perp})] = \iota(0) \\ &= \min_{f, \gamma} \mathbb{E}[(Y(X) - f(U^T X_{\parallel}) - \gamma)^2] + \lambda \|f\|_{\mathcal{H}_q}^2 + c = 2H(\Pi_{S^*} U). \end{aligned}$$

The last identity follows by plugging  $\Pi_{S^*} U$  into  $U$  in (3.3). To summarize, we have established the desired inequality  $H(U) \geq H(\Pi_{S^*} U)$  holding for every  $U$ .

Now we examine the case of equality  $H(U) = H(\Pi_{S^*} U)$ . From our earlier derivation, equality holds if and only if the inequality in (3.4) is tight, which occurs if and only if

$$fZ = fZ'$$

holds almost surely under  $\mathbb{P}$  over independent copies  $Z = U^T X_{\perp}$  and  $Z' = U^T X'_{\perp}$ . Now we suppose that  $U \neq \Pi_{S^*} U$  or  $\Pi_{S^*} U \neq 0$ . Under Assumption 3, where  $\text{Cov}(X)$  is full rank, it follows that  $\text{supp}(U^T X_{\perp})$  is not a singleton. Consequently, by (3.7),  $f_0(\cdot + c) = f_0(\cdot)$  must hold pointwise for some constant  $c \neq 0$ . Applying the representer theorem (Lemma 2.5), we have  $f_0(w) = \mathbb{E}[a_0(W)k_q(W, w)]$  for some  $a_0$  such that  $\mathbb{E}[a_0(W)^2] < \infty$  where  $W = U^T X_{\parallel}$ . Given that  $k_q(w, w') = \phi(\|w - w'\|_2^2)$  and  $\lim_{z \rightarrow \infty} \phi(z) = 0$ , we deduce that

$$\lim_{w \rightarrow \infty} f_0(w) = \mathbb{E}[\lim_{w \rightarrow \infty} a_0(W)\phi(\|W - w\|_2^2)] = 0$$

using Lebesgue's dominated convergence theorem. Thus,  $f_0(w) = \lim_{k \rightarrow \infty} f_0(w + kc) = 0$  for all  $w$ . Note this occurs only when  $\gamma_0 = \mathbb{E}[Y]$ , and  $H(U) = H(0) = \frac{1}{2}\text{Var}(Y)$ .

Thus, if both conditions  $H(U) < H(0)$  and  $U \neq \Pi_{S^*} U$  hold, then the inequality must be strict:  $H(U) > H(\Pi_{S^*} U)$ . This proves Lemma 3.1. □

By Lemma 2.3,  $H(U)$  is trivially upper bounded by  $\text{Var}(Y)/2$  for every  $U$ . However, the following lemma shows that the minimum value of (3.2) is strictly less than this upper bound.

LEMMA 3.2. *Let Assumption 2 hold. Then*

$$H(U^*) < H(0) = \text{Var}(Y)/2.$$

PROOF. We first see the identity:

$$H(0) = \min_{f, \gamma} \frac{1}{2} \mathbb{E}[(Y - f(0) - \gamma)^2] + \frac{\lambda}{2} \|f\|_{\mathcal{H}_q}^2 = \frac{1}{2} \min_{\gamma} \mathbb{E}[(Y - \gamma)^2] = \frac{1}{2} \text{Var}(Y).$$

Next, we fix a matrix  $U \in \mathbb{R}^{d \times q}$  with  $\text{rank}(U) = d$ . We show  $H(U) < H(0)$ . By Proposition 5,  $H(U) = J(\Sigma)$  where  $\Sigma = UU^T \succ 0$ . Suppose, for the sake of contradiction, that  $J(\Sigma) = \text{Var}(Y)/2$  holds. By Lemma 2.3, such an equality implies that  $\text{Cov}(Y, h(X)) = 0$  holds for every  $h \in \mathcal{H}_\Sigma$ , which then further implies that

$$\mathbb{E}[(\mathbb{E}[Y|X] - \mathbb{E}[Y])(h(X) + \gamma)] = 0 \text{ for every } h \in \mathcal{H}_\Sigma \text{ and } \gamma \in \mathbb{R}.$$

By Proposition 3, the set of all random variables of the form  $h(X) + \gamma$  where  $h \in \mathcal{H}_\Sigma$  and  $\gamma \in \mathbb{R}$  is dense in  $\mathcal{L}_2(\mathbb{P})$ . This would then imply that  $\mathbb{E}[Y|X] = \mathbb{E}[Y]$ , leading to  $\text{Var}(\mathbb{E}[Y|X]) = 0$ , which contradicts Assumption 2! This proves that  $H(U) = J(\Sigma) < \text{Var}(Y)/2$ . Given that  $H(U^*)$  is the minimum value of (3.2), this implies that  $H(U^*) \leq H(U) < \text{Var}(Y)/2$ .  $\square$

We build on the results of Lemma 3.1 and Lemma 3.2 to establish that  $\text{col}(U^*) \subseteq S_*$ . This key result represents the main conclusion of this subsection 3.1.

**LEMMA 3.3 (Column Space Contained in  $S_*$ ).** *Let Assumptions 1–4 hold. For every  $\lambda > 0$ , every minimizer  $U^*$  of (1.5) satisfies  $\text{col}(U^*) \subseteq S_*$ .*

**PROOF.** Consider a minimizer  $U^*$  of (1.5). By definition, it is also a minimizer of (3.2). Applying Lemma 3.1 to  $U = U^*$ , and using Lemma 3.2, it follows that  $U^* = \Pi_{S_*} U^*$ . Thus,  $\text{col}(U^*) = \text{col}(\Pi_{S_*} U^*) \subseteq S_*$  must hold for the minimizer  $U^*$ .  $\square$

**3.2. Exact Identification in the Small  $\lambda$  Regime.** We then prove the existence of  $\lambda_0 \in (0, \infty)$  such that for every  $\lambda \in (0, \lambda_0]$ , every minimizer  $U^*$  of (1.5) satisfies  $\text{col}(U^*) = S_*$ .

A fundamental fact of the central mean subspace  $S_*$  is that any subspace  $S$  with  $\dim(S) < \dim(S_*)$  satisfies

$$\epsilon(S) := \mathbb{E}[\text{Var}(Y|\Pi_S X)] - \mathbb{E}[\text{Var}(Y|X)] > 0.$$

Lemma 3.4 further shows that this bound can be made uniform in the subspaces  $S$ . The proof of Lemma 3.4 is given in Appendix A.1.

**LEMMA 3.4 (Property of Central Mean Subspace  $S_*$ ).**

$$\inf \{ \mathbb{E}[\text{Var}(Y|\Pi_S X)] : \dim(S) < \dim(S_*) \} > \mathbb{E}[\text{Var}(Y|X)].$$

With Lemma 3.4 at hand, we deduce a uniform lower bound of  $H(U, \lambda)$  over all matrix  $U$  with  $\text{rank}(U) < \dim(S_*)$  in Lemma 3.5.

**LEMMA 3.5 (A Strict Uniform Lower Bound on  $H$  with  $\text{rank}(U) < \dim(S_*)$ ).**

$$\inf \{ H(U, \lambda) \mid \text{rank}(U) < \dim(S_*) \} > \frac{1}{2} \mathbb{E}[\text{Var}(Y|X)].$$

**PROOF.** We start with a basic lower bound that holds for every  $U$ :

$$H(U, \lambda) \geq \frac{1}{2} \mathbb{E}[\text{Var}(Y|\Pi_{\text{col}(U)} X)].$$

By taking the infimum we obtain that

$$\inf \{ H(U, \lambda) \mid \text{rank}(U) < \dim(S_*) \} \geq \frac{1}{2} \cdot \inf \{ \mathbb{E}[\text{Var}(Y|\Pi_S X)] \mid \dim(S) < \dim(S_*) \}.$$

Lemma 3.5 follows from Lemma 3.4.  $\square$

Let us denote the minimum value of (3.2) to be  $H^*(\lambda)$ , which depends on the regularization parameter  $\lambda$ . Lemma 3.6 characterizes its limit as  $\lambda \rightarrow 0^+$ .

LEMMA 3.6. *Let Assumption 4 hold. Then*

$$\lim_{\lambda \rightarrow 0^+} H^*(\lambda) = \frac{1}{2} \mathbb{E}[\text{Var}(Y|X)].$$

PROOF. Fix a matrix  $U \in \mathbb{R}^{d \times q}$  with  $\text{rank}(U) = d$ , and define  $\Sigma = UU^T \succ 0$ . Note

$$H^*(\lambda) \leq H(U, \lambda) = J(\Sigma, \lambda).$$

Proposition 3 shows that  $\mathbb{E}[Y|X]$  can be arbitrarily approximated by  $F(X) + \gamma$  where  $F \in \mathcal{H}_\Sigma$  and  $\gamma \in \mathbb{R}$  under  $\mathcal{L}_2(\mathbb{P})$ . This implies  $\limsup_{\lambda \rightarrow 0^+} H^*(\lambda) \leq \frac{1}{2} \mathbb{E}[\text{Var}(Y|X)]$ .

Conversely,  $H^*(\lambda) \geq \frac{1}{2} \mathbb{E}[\text{Var}(Y|X)]$  for all  $\lambda$ . Thus,  $\liminf_{\lambda \rightarrow 0^+} H^*(\lambda) \geq \frac{1}{2} \mathbb{E}[\text{Var}(Y|X)]$ . This completes the proof of Lemma 3.6.  $\square$

We build on the results of Lemma 3.5 and Lemma 3.6 to establish that  $\text{col}(U^*) = S_*$  for all small enough  $\lambda > 0$ . This key result represents the main conclusion of this subsection 3.2.

LEMMA 3.7 (Exact Column Space Identification). *Let Assumptions 1–4 hold.*

*There exists  $\lambda_0 > 0$ , which depends only on  $\mathbb{P}, M, \|\cdot\|$ , such that for every  $\lambda \in (0, \lambda_0]$ , every minimizer  $U^*$  of (1.5) satisfies  $\text{col}(U^*) = S_*$ .*

PROOF. By definition, every minimizer  $U^*$  of (1.5) must also minimize (3.2), and vice versa. By Lemma 3.5 and Lemma 3.6, we can find  $0 < \lambda_0 < \infty$  such that for every  $\lambda \in (0, \lambda_0]$ :

$$\inf \{H(U, \lambda) \mid \text{rank}(U) < \dim(S_*)\} > H^*(\lambda).$$

Therefore, with  $\lambda \in (0, \lambda_0]$ , any minimizer  $U^*$  of (3.2) must satisfy  $\text{rank}(U^*) \geq \dim(S_*)$  as  $H^*(\lambda)$  represents the minimum value of (3.2). On the other hand, any minimizer  $U^*$  of (3.2) must also satisfy  $\text{col}(U^*) \subseteq S_*$ , as established in Lemma 3.3 earlier.

Consequently, we must have both  $\text{rank}(U^*) = \dim(S_*)$  and  $\text{col}(U^*) = S_*$  whenever  $\lambda \in (0, \lambda_0]$  holds. This completes the proof.  $\square$

3.3. *Proof of Theorem 1.1.* We now explain how Lemma 3.3 and Lemma 3.7 lead to the proof of Theorem 1.1. By Propositions 5 and 6, the minimizers  $U^*$  of (1.5) are related to the minimizers  $\Sigma^*$  of (1.6) through the reparameterization  $\Sigma^* = U^*(U^*)^T$ . Since  $\text{col}(\Sigma^*) = \text{col}(U^*)$  whenever  $\Sigma^* = U^*(U^*)^T$  holds, Lemma 3.3 and Lemma 3.7 about  $\text{col}(U^*)$  directly translate to  $\text{col}(\Sigma^*)$ . This completes the proof of Theorem 1.1.

**4. Sharpness of the Population Objective near its Minimizer.** In this section, we establish the sharpness property of the *population* objective near its minimizer. Let us recall:

$$J(\Sigma) = \underset{F, \gamma}{\text{minimize}} \frac{1}{2} \mathbb{E}[(Y - F(X) - \gamma)^2] + \frac{\lambda}{2} \|F\|_{\mathcal{H}_\Sigma}^2$$

We are interested in the minimization problem:

$$(4.1) \quad \underset{\Sigma}{\text{minimize}} J(\Sigma) \quad \text{subject to} \quad \|\Sigma\| \leq M.$$

By definition, any minimizer  $\Sigma^*$  of (1.6) must be a minimizer of (4.1), and vice versa.

The key finding in Section 4 is that the population objective  $J$  exhibits a "sharp" growth near its minimizer. Specifically, we prove that for every minimizer  $\Sigma^*$  of (4.1), there exists a  $\rho > 0$  such that for every perturbation matrix  $W \in \mathcal{T}_C(\Sigma^*)$  with  $\text{col}(W) \subseteq S_*^\perp$ :

$$(4.2) \quad \lim_{t \rightarrow 0^+} \frac{1}{t} (J(\Sigma^* + tW) - J(\Sigma^*)) \geq \rho \|W\|.$$

Our proof of the sharpness property (4.2) starts with showing a form of non-degeneracy condition at every minimizer  $\Sigma^*$ , as stated in Theorem 4.1. We then show this non-degeneracy condition directly implies the sharpness property (4.2) as stated in Corollary 4.1.

To gain some intuition, we note this non-degeneracy condition—expressed in (4.3)—is the same as the notion of *strict complementary slackness condition* (see, e.g., [13, Section 3.3.3]) for the minimization problem (4.1) when the minimizer  $\Sigma^*$  does not activate the artificial constraint  $\|\cdot\| \leq M$  and when the minimizer  $\Sigma^*$  satisfies  $\text{col}(\Sigma^*) = S_*$ .

**THEOREM 4.1 (Non-degeneracy Condition at  $\Sigma^*$ ).** *Let Assumptions 1–4 hold. Fix  $\lambda, M \in (0, \infty)$  and the unitarily invariant norm  $\|\cdot\|$ .*

*For any minimizer  $\Sigma^*$  of (4.1), there exists a  $\rho > 0$  such that*

$$(4.3) \quad \Pi_{S_*^\perp} \nabla J(\Sigma^*) \Pi_{S_*^\perp} \succeq \rho \Pi_{S_*^\perp}.$$

**PROOF.** Recall  $\phi(z) = \int_0^\infty \exp(-tz) \mu(dt)$ . Let us introduce  $\tilde{\phi}(z) = \int_0^\infty \exp(-tz) \tilde{\mu}(dt)$  where  $\tilde{\mu}(dt) = t\mu(dt)$ . Under Assumption 4, we can express the matrix  $\partial_\Sigma k_\Sigma(x, x')$  as

$$\partial_\Sigma k_\Sigma(x, x') = -\tilde{k}_\Sigma(x, x') \cdot (x - x')(x - x')^T$$

where  $\tilde{k}_\Sigma(x, x') = \tilde{\phi}(\|x - x'\|_\Sigma^2)$ . Substituting this formula into (2.9) results in

$$(4.4) \quad \nabla J(\Sigma) = \frac{1}{2\lambda} \mathbb{E} \left[ r_\Sigma(X, Y) r_\Sigma(X', Y') \tilde{k}_\Sigma(X, X') \cdot (X - X')(X - X')^T \right].$$

Let  $\Sigma^*$  denote a minimizer. By substituting  $\Sigma^*$  into  $\Sigma$  in (4.4), we obtain the identity:

$$(4.5) \quad \begin{aligned} & \Pi_{S_*^\perp} \nabla J(\Sigma^*) \Pi_{S_*^\perp} \\ &= \frac{1}{2\lambda} \mathbb{E} \left[ r_{\Sigma^*}(X, Y) r_{\Sigma^*}(X', Y') \tilde{k}_{\Sigma^*}(X, X') \cdot \Pi_{S_*^\perp} (X - X')(X - X')^T \Pi_{S_*^\perp} \right]. \end{aligned}$$

Theorem 1.1 shows that  $\text{col}(\Sigma^*) \subseteq S_*$ . Thus  $\mathbb{E}[r_{\Sigma^*}(X, Y)|X] = \mathbb{E}[r_{\Sigma^*}(X, Y)|\Pi_{S_*} X]$  since  $\mathbb{E}[Y|X] = \mathbb{E}[Y|\Pi_{S_*} X]$  by the definition of  $S_*$ , and  $\mathbb{E}[F_{\Sigma^*}(X)|X] = \mathbb{E}[F_{\Sigma^*}(X)|\Pi_{S_*} X]$  by Proposition 2. Similarly,  $\tilde{k}_{\Sigma^*}(X, X') = \mathbb{E}[\tilde{k}_{\Sigma^*}(X, X')|\Pi_{S_*} X, \Pi_{S_*} X']$  because  $\text{col}(\Sigma^*) \subseteq S_*$ . Given that  $\Pi_{S_*} X$  and  $\Pi_{S_*^\perp} X$  are independent by Assumption 3, it follows that

$$\mathbb{E}[r_{\Sigma^*}(X, Y) r_{\Sigma^*}(X', Y') \tilde{k}_{\Sigma^*}(X, X') | X, X'] \quad \text{and} \quad \Pi_{S_*^\perp} (X - X')(X - X')^T \Pi_{S_*^\perp}$$

are also independent. This allows us to split the expectation of their product into the product of their expectations, leading to the expression that follows (4.5):

$$(4.6) \quad \begin{aligned} & \Pi_{S_*^\perp} \nabla J(\Sigma^*) \Pi_{S_*^\perp} \\ &= \frac{1}{2\lambda} \mathbb{E}[r_{\Sigma^*}(X, Y) r_{\Sigma^*}(X', Y') \tilde{k}_{\Sigma^*}(X, X')] \cdot \mathbb{E}[\Pi_{S_*^\perp} (X - X')(X - X')^T \Pi_{S_*^\perp}]. \end{aligned}$$

To complete the proof of Theorem 4.1, we further lower bound the RHS of (4.6). First, let  $\gamma$  denote the minimum eigenvalue of  $\text{Cov}(X)$ , with  $\gamma > 0$  by Assumption 3. Then:

$$(4.7) \quad \mathbb{E}[\Pi_{S_*^\perp} (X - X')(X - X')^T \Pi_{S_*^\perp}] \succeq 2\gamma \Pi_{S_*^\perp}.$$

Next, we claim that the quadratic form is strictly positive:

$$(4.8) \quad \mathbb{E}[r_{\Sigma^*}(X, Y)r_{\Sigma^*}(X', Y')\tilde{k}_{\Sigma^*}(X, X')] > 0.$$

With (4.6), (4.7), and the claim (4.8), we can immediately see the existence of  $\rho > 0$  such that the nondegeneracy condition (4.3) holds. The rest of the proof will substantiate (4.8).

To prove the claim (4.8), our key observation is that  $(x, x') \mapsto \tilde{k}_I(x, x')$  is an integrally positive definite kernel, which means that for any nonzero signed measure  $\nu$  with finite total variation,  $\int_{\mathbb{R}^d} \int_{\mathbb{R}^d} \tilde{k}_I(x, x')\nu(dx)\nu(dx') > 0$ . This property can be deduced by Proposition 5 of [80], given the fact that  $\tilde{k}_I$  is a radial kernel with  $\tilde{\mu}$  not a zero measure. For a more transparent argument, we introduce the notation  $\zeta_t(\omega) = \frac{1}{(4\pi t)^{d/2}} e^{-\|\omega\|_2^2/(4t)}$  and note the identities:

$$(4.9) \quad \begin{aligned} \iint \tilde{k}_I(x, x')\nu(dx)\nu(dx') &\stackrel{(a)}{=} \iint \left( \int e^{-t\|x-x'\|_2^2} \tilde{\mu}(dt) \right) \nu(dx)\nu(dx') \\ &\stackrel{(b)}{=} \iint \left( \iint e^{-i\langle x-x', \omega \rangle} \zeta_t(\omega) d\omega \tilde{\mu}(dt) \right) \nu(dx)\nu(dx') \\ &\stackrel{(c)}{=} \iint \left( \iint e^{-i\langle x-x', \omega \rangle} \nu(dx)\nu(dx') \right) \zeta_t(\omega) d\omega \tilde{\mu}(dt) \\ &= \iint \left| \int e^{-i\langle x, \omega \rangle} \nu(dx) \right|^2 \zeta_t(\omega) d\omega \tilde{\mu}(dt). \end{aligned}$$

In the above, step (a) is due to the definition of  $\tilde{k}_I$ , step (b) is due to the known fact that Fourier transform of Gaussian is Gaussian and step (c) is due to Fubini's theorem. Given that  $\zeta_t(\omega) > 0$  for all  $t, \omega$ , the integral is nonnegative, and since  $\tilde{\mu}$  is not a zero measure, it is zero only if  $\omega \mapsto \int e^{-i\langle x, \omega \rangle} \nu(dx)$  is a zero constant, which happens only if  $\nu$  is a zero measure. This proves that  $\iint \tilde{k}_I(x, x')\nu(dx)\nu(dx') > 0$  for all nonzero finite signed measure  $\nu$ .

Now we write  $\Sigma^* = (U^*)(U^*)^T$  for a matrix  $U^* \in \mathbb{R}^{d \times d}$ . Using  $\tilde{k}_{\Sigma^*}(X, X') = \tilde{k}_I(Z, Z')$  where  $Z = (U^*)^T X$  and the tower property we can rewrite the LHS of (4.8) into:

$$(4.10) \quad \begin{aligned} &\mathbb{E}[r_{\Sigma^*}(X, Y)r_{\Sigma^*}(X', Y')\tilde{k}_{\Sigma^*}(X, X')] \\ &= \mathbb{E}[\mathbb{E}[r_{\Sigma^*}(X, Y)|Z] \cdot \mathbb{E}[r_{\Sigma^*}(X', Y')|Z'] \cdot \tilde{k}_I(Z, Z')]. \end{aligned}$$

Since  $(x, x') \mapsto \tilde{k}_I(x, x')$  is an integrally positive definite kernel by (4.9), proving the claim (4.8) reduces to verifying that  $\mathbb{E}[r_{\Sigma^*}(X, Y)|Z]$  is not almost surely equal to zero.

To verify this, we apply the Euler-Lagrange equation in Lemma 2.2 and note first that:

$$(4.11) \quad \lambda \langle f_{\Sigma^*}, h \rangle_{\mathcal{H}_{\Sigma^*}} = \mathbb{E}[r_{\Sigma^*}(X, Y)h(X)] \quad \text{for every } h \in \mathcal{H}_{\Sigma^*}.$$

Assume, for contradiction, that  $\mathbb{E}[r_{\Sigma^*}(X, Y)|Z] = 0$ . Since, for  $h \in \mathcal{H}_{\Sigma^*}$ ,  $h(x)$  is a function of  $(U^*)^T x$  by Proposition 2, applying the tower property to the RHS of (4.11) gives:

$$(4.12) \quad \begin{aligned} \lambda \langle f_{\Sigma^*}, h \rangle_{\mathcal{H}_{\Sigma^*}} &= \mathbb{E}[\mathbb{E}[r_{\Sigma^*}(X, Y) \cdot h(X)|Z]] \\ &= \mathbb{E}[\mathbb{E}[r_{\Sigma^*}(X, Y)|Z] \cdot h(X)] = 0 \quad \text{for every } h \in \mathcal{H}_{\Sigma^*}. \end{aligned}$$

This implies that  $\langle f_{\Sigma^*}, h \rangle_{\mathcal{H}_{\Sigma^*}} = 0$  for every  $h \in \mathcal{H}_{\Sigma^*}$ , which forces  $f_{\Sigma^*} \equiv 0$ , meaning that  $f_{\Sigma^*}$  must be the zero function. As a result,  $\gamma_{\Sigma^*} = \mathbb{E}[Y]$  and  $r_{\Sigma^*}(X, Y) = Y - \mathbb{E}[Y]$ , resulting in  $J(\Sigma^*) = \frac{1}{2} \text{Var}(Y) = J(0)$ . This, however, contradicts Lemma 3.2, which shows that the minimum value of (4.1),  $J(\Sigma^*)$ , must be strictly smaller than  $J(0)$ ! Thus,  $\mathbb{E}[r_{\Sigma^*}(X, Y)|Z]$  cannot be almost surely zero under  $\mathbb{P}$ . This finishes the proof of the claim (4.8).  $\square$

Theorem 4.1 implies the sharpness property (4.2) as we will detail in Corollary 4.1. Before stating and proving Corollary 4.1, we need one lemma that characterizes the set of all possible perturbation matrices  $W$ . For every matrix  $\Sigma^*$  that minimizes (4.1), we denote:

$$\mathcal{W}(\Sigma^*) = \{W : W \in \mathcal{T}_{\mathcal{C}}(\Sigma^*), \text{col}(W) \subseteq S_*^\perp\}.$$

LEMMA 4.1.  $\mathcal{W}(\Sigma^*) = \{W : W = \Pi_{S_*^\perp} W \Pi_{S_*^\perp} \succeq 0\}$ .

PROOF. Suppose  $W \in \mathcal{W}$ . Since  $W \in \mathcal{T}_{\mathcal{C}}(\Sigma^*)$ , we have  $W = \lim_m t_m(\Sigma_m - \Sigma^*)$  for some sequence  $\Sigma_m \in \mathcal{C}$  and  $t_m > 0$ . By Theorem 1.1,  $\text{col}(\Sigma^*) \subseteq \text{col}(S_*)$ , so:  $\Pi_{S_*^\perp}(\Sigma_m - \Sigma^*)\Pi_{S_*^\perp} = \Pi_{S_*^\perp}\Sigma_m\Pi_{S_*^\perp} \succeq 0$ . Taking the limit, we get  $\Pi_{S_*^\perp}W\Pi_{S_*^\perp} \succeq 0$ . Since  $W = W^T$  and  $\text{col}(W) \subseteq S_*^\perp$ , we conclude  $W = \Pi_{S_*^\perp}W\Pi_{S_*^\perp} \succeq 0$ . For the other direction, any matrix  $W \succeq 0$  must belong to  $\mathcal{T}_{\mathcal{C}}(\Sigma^*)$ , and any matrix  $W = \Pi_{S_*^\perp}W\Pi_{S_*^\perp}$  must satisfy  $\text{col}(W) \subseteq S_*^\perp$ .  $\square$

Corollary 4.1 is a formal restatement of the sharpness property (4.2).

COROLLARY 4.1 (Sharpness Property). *Let Assumptions 1–4 hold. Fix  $\lambda, M \in (0, \infty)$  and the unitarily invariant norm  $\|\cdot\|$ . For any minimizer  $\Sigma^*$  of (4.1), there is a  $\rho > 0$  so that*

$$(4.13) \quad \langle \nabla J(\Sigma^*), W \rangle \geq \rho \|W\|$$

holds for every matrix  $W \in \mathcal{T}_{\mathcal{C}}(\Sigma^*)$  with  $\text{col}(W) \subseteq S_*^\perp$ .

PROOF. Take any matrix  $W \in \mathcal{T}_{\mathcal{C}}(\Sigma^*)$  with  $\text{col}(W) \subseteq S_*^\perp$ . Then  $W = \Pi_{S_*^\perp}W\Pi_{S_*^\perp} \succeq 0$  by Lemma 4.1. Thereby,

$$\langle \nabla J(\Sigma^*), W \rangle = \langle \Pi_{S_*^\perp} \nabla J(\Sigma^*) \Pi_{S_*^\perp}, W \rangle.$$

Using Theorem 4.1, we can lower bound the RHS quantity by  $\rho \text{tr}(W)$  where  $\rho > 0$  satisfies the non-degeneracy condition (4.3) in Theorem 4.1. The proof is complete since  $\text{tr}(W)$  is uniformly lower bounded by  $\|W\|$  up to a positive constant over  $W \in \mathcal{C}$ .  $\square$

**5. Uniform Convergence of Objective Values and Gradients.** In this section, we show that there is, on any given compact set, with probability tending to one, the uniform convergence of the empirical objective  $J_n$  to its population counterpart  $J$ . Furthermore, we show that there is a parallel result for the gradient where  $\nabla J_n$  converges uniformly to  $\nabla J$ .

THEOREM 5.1 (Uniform Convergence of Objectives and Gradients). *Let  $\mathbb{E}[Y^2] < \infty$  and  $\mathbb{E}[\|X\|^4] < \infty$ . Assume Assumption 4 holds.*

*For any compact set  $\Sigma$  within the semidefinite cone  $\{\Sigma : \Sigma \succeq 0\}$ , we have the following convergence as the sample size  $n \rightarrow \infty$*

$$(5.1) \quad \sup_{\Sigma \in \Sigma} |J_n(\Sigma) - J(\Sigma)| = o_P(1),$$

$$(5.2) \quad \sup_{\Sigma \in \Sigma} \|\nabla J_n(\Sigma) - \nabla J(\Sigma)\| = o_P(1).$$

REMARK. *The convergence is established under moment conditions  $\mathbb{E}[\|X\|^4] < \infty$  and  $\mathbb{E}[Y^2] < \infty$ . Refined convergence rates (e.g., high probability bounds) can be obtained by imposing stronger tail conditions on  $(X, Y)$ .*

The main challenge to establish uniform convergence comes from the appearance of the prediction function  $f$ , which is *infinite-dimensional* in its nature, in the definition of  $J$ .

Note, however, the uniform convergence of the objective value (equation (5.1)), for a specific set  $\Sigma$ , appeared in the statistics literature [42], where  $\Sigma$  collects all projection matrices of a given rank. Here, we show uniform convergence holds for a general compact set  $\Sigma$ .

The main contribution here, thereby, is to show the uniform convergence of the gradient (equation (5.2)). For our proof, we repackage key elements in Fukumizu et. al. [42]’s proof of the convergence of objective values, namely, tools from the empirical process theory in the RKHS setting. More precisely, Fukumizu et. al. [42]’s arguments construct a suitable family of covariance operators in the RKHS, and by showing their uniform convergence, infer the same for the objective value, as the objective is a continuous functional of the operators. Our arguments show that the uniform convergence of operators also leads to that of the gradient, utilizing the connections between the gradient and covariance operator we build below based on the gradient formula in Lemma 2.8.

Section 5.1 elaborates on these ideas and concludes with a proof outline. Sections 5.2–5.5 provide a detailed substantiation of these ideas and establish Theorem 5.1.

*5.1. Analysis Framework: Representation Using Covariance Operators.* In our convergence analysis, we shall study our objective function  $J$  and its gradient  $\nabla J$ . Here we introduce a notation that emphasizes its dependence on the underlying probability measure  $\mathbb{Q}$ :

$$(5.3) \quad J(\Sigma; \mathbb{Q}) = \min_{F, \gamma} \frac{1}{2} \mathbb{E}_{\mathbb{Q}} [(Y - F(X) - \gamma)^2] + \frac{\lambda}{2} \|F\|_{\mathcal{H}_{\Sigma}}^2.$$

This notation unifies the population and empirical objectives:

$$J(\Sigma) = J(\Sigma; \mathbb{P}) \quad \text{and} \quad J_n(\Sigma) = J(\Sigma; \mathbb{P}_n).$$

We are interested in how  $J(\Sigma; \mathbb{Q})$  and  $\nabla J(\Sigma; \mathbb{Q})$  change when  $\mathbb{Q}$  is switched from  $\mathbb{P}$  to  $\mathbb{P}_n$ .

Similarly, we define, for every probability measure  $\mathbb{Q}$  and matrix parameter  $U \in \mathbb{R}^{d \times q}$ :

$$(5.4) \quad H(U; \mathbb{Q}) = \min_{f, \gamma} \frac{1}{2} \mathbb{E}_{\mathbb{Q}} [(Y - f(U^T X) - \gamma)^2] + \frac{\lambda}{2} \|f\|_{\mathcal{H}_q}^2.$$

By Lemma 5, the following identity holds whenever  $\Sigma = UU^T$  holds:

$$(5.5) \quad J(\Sigma; \mathbb{Q}) = H(U; \mathbb{Q}).$$

Let  $(f_{U; \mathbb{Q}}, \gamma_{U; \mathbb{Q}})$  be the unique minimizer of the objective in equation (5.4). By Lemma 2.2, at the minimizer the intercept obeys  $\gamma_{U; \mathbb{Q}} = \mathbb{E}_{\mathbb{Q}}[Y] - \mathbb{E}_{\mathbb{Q}}[f_{U; \mathbb{Q}}(X)]$ .

A central tool in our convergence analysis is the *cross-covariance operator*, introduced in [8]. Essentially, the cross-covariance operator, as a generalization of the covariance matrix, captures covariance relations between random variables under a collection of test functions. Below, for a given matrix  $U$ , we construct covariance operators  $C_{U; \mathbb{Q}}, V_{U; \mathbb{Q}}$  in the same way as in [42]. Later, we shall see how these operators connect to  $J(\Sigma; \mathbb{Q})$  and  $\nabla J(\Sigma; \mathbb{Q})$ .

Given the RKHS  $\mathcal{H}_q$ , and a matrix  $U$ , we use  $C_{U; \mathbb{Q}} : \mathcal{H}_q \rightarrow \mathcal{H}_q$  to denote the unique linear operator such that for every pair of test functions  $h_1, h_2 \in \mathcal{H}_q$ :

$$(5.6) \quad \langle h_1, C_{U; \mathbb{Q}} h_2 \rangle_{\mathcal{H}_q} = \text{Cov}_{\mathbb{Q}}(h_1(U^T X), h_2(U^T X)).$$

Similarly,  $V_{U; \mathbb{Q}} : \mathcal{H}_q \rightarrow \mathbb{R}$  denotes the unique linear operator such that for every  $h \in \mathcal{H}_q$

$$(5.7) \quad V_{U; \mathbb{Q}} h = \text{Cov}_{\mathbb{Q}}(h(U^T X), Y).$$

The existence of such cross-covariance operators  $C_{U; \mathbb{Q}}$  and  $V_{U; \mathbb{Q}}$  is discussed in [42, Section 2]. The operator  $C_{U; \mathbb{Q}}$  is always a bounded, self-adjoint, non-negative operator, for every  $U$

and measure  $\mathbb{Q}$ . The operator  $V_{U;\mathbb{Q}}$  is bounded whenever  $\mathbb{E}_{\mathbb{Q}}[Y^2] < \infty$ , in which case the Riesz representation theorem says there is  $v_{U;\mathbb{Q}} \in \mathcal{H}_I$  for which  $V_{U;\mathbb{Q}}h = \langle v_{U;\mathbb{Q}}, h \rangle_{\mathcal{H}_q}$  holds for every  $h \in \mathcal{H}_q$ . Furthermore, there is the isometry  $\|V_{U;\mathbb{Q}}\|_{\text{op}} = \|v_{U;\mathbb{Q}}\|_{\mathcal{H}_q}$ , where  $\|\cdot\|_{\text{op}}$  denotes the operator norm.

Covariance operators aid our analysis through their connections to the objective  $J(\Sigma; \mathbb{Q})$  and its gradient  $\nabla J(\Sigma; \mathbb{Q})$ . Their connection to  $J(\Sigma; \mathbb{Q})$  is known in the literature (e.g., [41, 42]), for which we review. At every  $\Sigma = UU^T$ , the objective  $J(\Sigma; \mathbb{Q})$  obeys

$$\begin{aligned}
 (5.8) \quad J(\Sigma; \mathbb{Q}) &= H(U; \mathbb{Q}) = \min_{f, \gamma} \frac{1}{2} \mathbb{E}_{\mathbb{Q}} [(Y - f(U^T X) - \gamma)^2] + \frac{\lambda}{2} \|f\|_{\mathcal{H}_q}^2 \\
 &= \min_f \left\{ \frac{1}{2} \text{Var}_{\mathbb{Q}}(Y - f(U^T X)) + \frac{\lambda}{2} \|f\|_{\mathcal{H}_q}^2 \right\} \\
 &= \min_f \left\{ \frac{1}{2} \text{Var}_{\mathbb{Q}}(Y) + \frac{1}{2} \langle f, (C_{U;\mathbb{Q}} + \lambda I) f \rangle_{\mathcal{H}_q} - \langle v_{U;\mathbb{Q}}, f \rangle_{\mathcal{H}_q} \right\}.
 \end{aligned}$$

where in the last line,  $I: \mathcal{H}_q \rightarrow \mathcal{H}_q$  denotes the identity map. Since the objective inside the last curly brackets is quadratic in  $f$ , we can complete the square and find the minimizer  $f_{U;\mathbb{Q}}$

$$(5.9) \quad f_{U;\mathbb{Q}} = (C_{U;\mathbb{Q}} + \lambda I)^{-1} v_{U;\mathbb{Q}}.$$

Note the operator  $C_{U;\mathbb{Q}} + \lambda I: \mathcal{H}_q \rightarrow \mathcal{H}_q$  is invertible as it is a positive, self-adjoint operator whose eigenvalue is bounded away from zero. Therefore, as long as  $\Sigma = UU^T$  holds, then

$$(5.10) \quad J(\Sigma; \mathbb{Q}) = \frac{1}{2} \text{Var}_{\mathbb{Q}}(Y) - \frac{1}{2} \left\| (C_{U;\mathbb{Q}} + \lambda I)^{-1/2} v_{U;\mathbb{Q}} \right\|_{\mathcal{H}_q}^2.$$

This builds the connection between the covariance operators and the objective value  $J$ .

To build the connection between the covariance operators and the gradient  $\nabla J$ , we exploit the gradient formula (equation (2.9)) in Lemma 2.8. Lemma 2.8 shows that

$$(5.11) \quad \nabla J(\Sigma; \mathbb{Q}) = -\frac{1}{2\lambda} \mathbb{E}_{\mathbb{Q}} [r_{\Sigma;\mathbb{Q}}(X; Y) r_{\Sigma;\mathbb{Q}}(X'; Y') \partial_{\Sigma} k_{\Sigma}(X, X')],$$

where  $(X, Y), (X', Y')$  are independent copies from  $\mathbb{Q}$ , and the term  $r_{\Sigma;\mathbb{Q}}(x, y)$  represents the residual at  $\Sigma$ , i.e.,  $r_{\Sigma;\mathbb{Q}}(x, y) = y - F_{\Sigma;\mathbb{Q}}(x) - \gamma_{\Sigma;\mathbb{Q}}$  with  $(F_{\Sigma;\mathbb{Q}}, \gamma_{\Sigma;\mathbb{Q}})$  the unique minimizer of the cost function in (5.3). When  $\Sigma = UU^T$  holds, by Lemma 5, the term  $r_{\Sigma;\mathbb{Q}}(x, y)$  can be expressed by:

$$\begin{aligned}
 (5.12) \quad r_{\Sigma;\mathbb{Q}}(x, y) &= y - f_{U;\mathbb{Q}}(U^T x) - \gamma_{U;\mathbb{Q}} \\
 &= y - f_{U;\mathbb{Q}}(U^T x) - (\mathbb{E}_{\mathbb{Q}}[Y] - \mathbb{E}_{\mathbb{Q}}[f_{U;\mathbb{Q}}(U^T X)]),
 \end{aligned}$$

where we recall that  $f_{U;\mathbb{Q}}$  can be represented by the covariance operators through (5.9). As a result, equations (5.11), (5.12), and (5.9) together form the needed connection in our proof between the gradient  $\nabla J(\Sigma)$  and the cross-covariance operators  $C_U$  and  $v_U$  where  $\Sigma = UU^T$ .

Here's the roadmap for the rest of the proofs. In Section 5.2, we establish the uniform convergence of the empirical covariance operators to the population counterparts. Section 5.3 shows how this convergence of operators translates to that of the objectives  $J$ . Section 5.4 shows how this convergence of operators translates to that of the residual function in (5.12), which is then used in Section 5.5 to show the convergence of the gradients  $\nabla J$ .

5.2. *Uniform Convergence of Covariance Operators.* It is widely known in the literature that there is the pointwise convergence of the empirical cross-covariance operators to the population counterpart under the operator norm, e.g., [59, 43, 45]. Indeed, given a matrix  $U$  and a measure  $\mathbb{P}$ , there is the convergence in probability as the sample size  $n \rightarrow \infty$ :

$$(5.13) \quad \|\mathbb{C}_{U;\mathbb{P}_n} - \mathbb{C}_{U;\mathbb{P}}\|_{\text{op}} = o_P(1), \quad \|\mathbb{V}_{U;\mathbb{P}_n} - \mathbb{V}_{U;\mathbb{P}}\|_{\text{op}} = o_P(1).$$

Here, we need to refine pointwise convergence by showing that such convergence could be made uniform over a collection of matrices  $U \in \mathcal{U}$ . While uniform convergence of such operators has been shown for specific sets that comprise projection matrices of a given rank [42], the same result indeed holds for every compact set  $\mathcal{U}$ . The proof is standard, and is deferred to Appendix A.2.

LEMMA 5.1 (Uniform Convergence of Covariance Operators). *For any compact set  $\mathcal{U}$ , we have the convergence as the sample size  $n \rightarrow \infty$ :*

$$(5.14) \quad \sup_{U \in \mathcal{U}} \|\mathbb{C}_{U;\mathbb{P}_n} - \mathbb{C}_{U;\mathbb{P}}\|_{\text{op}} = o_P(1), \quad \sup_{U \in \mathcal{U}} \|\mathbb{V}_{U;\mathbb{P}_n} - \mathbb{V}_{U;\mathbb{P}}\|_{\text{op}} = o_P(1).$$

5.3. *Uniform Convergence of Objectives.* We prove Part I of Theorem 5.1, which asserts the uniform convergence of objective values described in (5.1). The proof relies on the uniform convergence of covariance operators in Lemma 5.1 and the connection between the objective value and these operators given in equation (5.10).

Recall equation (5.10). For a measure  $\mathbb{Q}$ , there is the identity at every  $\Sigma = UU^T$ :

$$(5.15) \quad J(\Sigma; \mathbb{Q}) = \frac{1}{2} \text{Var}_{\mathbb{Q}}(Y) - \frac{1}{2} T(\mathbb{C}_{U;\mathbb{Q}}, v_{U;\mathbb{Q}})$$

where the notation  $T$  denotes the functional  $\mathcal{P}(\mathcal{H}_q) \times \mathcal{H}_q \rightarrow \mathbb{R}$ :

$$(5.16) \quad T : (C, v) \mapsto \left\| (C + \lambda I)^{-1/2} v \right\|_{\mathcal{H}_q}^2.$$

Here,  $\mathcal{P}(\mathcal{H}_q)$  represents the set of non-negative, self-adjoint, bounded operators on the Hilbert space  $\mathcal{H}_q$ , equipped with the subspace topology from  $\mathcal{B}(\mathcal{H}_q)$ , the Banach space consisting of all self-adjoint and bounded operators on  $\mathcal{H}_q$ , endowed with the operator norm topology. The product space  $\mathcal{P}(\mathcal{H}_I) \times \mathcal{H}_I$  is then endowed with the product topology.

Note then, for  $\lambda > 0$ , the functional  $T$  is continuous on its domain  $\mathcal{P}(\mathcal{H}_I) \times \mathcal{H}_I$ . The uniform convergence of covariance operators on every compact set  $\mathcal{U}$  (Lemma 5.1) translates to that of the objective values. Indeed, for every compact set  $\mathcal{U}$ , we must have as  $n \rightarrow \infty$ :

$$\sup_{U \in \mathcal{U}} |T(\mathbb{C}_{U;\mathbb{P}_n}, v_{U;\mathbb{P}_n}) - T(\mathbb{C}_{U;\mathbb{P}}, v_{U;\mathbb{P}})| = o_P(1).$$

Consequently, using (5.15), this leads to the convergence

$$\sup_{\Sigma \in \Sigma} |J(\Sigma; \mathbb{Q}_n) - J(\Sigma; \mathbb{Q})| = o_P(1)$$

that holds on any given compact set  $\Sigma$  as  $n \rightarrow \infty$ . This completes the proof.

5.4. *Uniform Convergence of Residuals.* In this section, we prove the uniform convergence of the residual function  $r_\Sigma$ , whose expression can be recalled from (5.12).

LEMMA 5.2. *For any compact set  $\Sigma$ , there is the convergence as  $n \rightarrow \infty$ :*

$$(5.17) \quad \sup_{\Sigma \in \Sigma} \|r_{\Sigma;\mathbb{P}_n} - r_{\Sigma;\mathbb{P}}\|_{\infty} = o_P(1).$$

PROOF. We initiate our proof with an inequality that holds at every  $\Sigma = UU^T$ :

$$(5.18) \quad \|r_{\Sigma; \mathbb{P}_n} - r_{\Sigma; \mathbb{P}}\|_{\infty} \leq 2 \|f_{U; \mathbb{P}} - f_{U; \mathbb{P}_n}\|_{\infty} \leq 2\sqrt{\phi(0)} \|f_{U; \mathbb{P}} - f_{U; \mathbb{P}_n}\|_{\mathcal{H}_q}.$$

The first inequality follows from (5.12) and the triangle inequality, while the second inequality is based on the continuous embedding of the RKHS  $\mathcal{H}_q$  into the space  $\mathcal{C}_b$ .

To complete the proof, we need to show that for any compact set  $U$  of  $\mathbb{R}^{d \times q}$ , the following convergence holds as  $n \rightarrow \infty$ :

$$(5.19) \quad \sup_{U \in \mathcal{U}} \|f_{U; \mathbb{P}} - f_{U; \mathbb{P}_n}\|_{\mathcal{H}_q} = o_P(1).$$

This uniform convergence of  $f$  is a consequence of the uniform convergence of the cross-covariance operators stated in Lemma 5.1. Specifically, from equation (5.9), we have

$$f_{U; \mathbb{P}} = W(C_{U; \mathbb{P}}, v_{U; \mathbb{P}}) \text{ and } f_{U; \mathbb{P}_n} = W(C_{U; \mathbb{P}_n}, v_{U; \mathbb{P}_n}),$$

where  $W : \mathcal{P}(\mathcal{H}_q) \times \mathcal{H}_q \rightarrow \mathcal{H}_q$  is defined as:

$$(5.20) \quad W : (C, v) \mapsto (C + \lambda I)^{-1}v.$$

This map is continuous for  $\lambda > 0$  when  $\mathcal{H}_q$  has the norm topology, and  $\mathcal{P}(\mathcal{H}_q) \times \mathcal{H}_q$  is equipped with the product topology. Consequently, the uniform convergence of the covariance operators in Lemma 5.1 ensures the uniform convergence of  $f$  as stated in (5.19).  $\square$

**5.5. Uniform Convergence of Gradients.** Here we prove Part II of Theorem 5.1, namely, the uniform convergence of gradients described in (5.2). We start with the gradient formula for  $J$  from Lemma 2.8:

$$(5.21) \quad \begin{aligned} \nabla J(\Sigma; \mathbb{P}) &= -\frac{1}{2\lambda} \mathbb{E}_{\mathbb{P}}[r_{\Sigma; \mathbb{P}}(X; Y)r_{\Sigma; \mathbb{P}}(X'; Y')\partial_{\Sigma}k_{\Sigma}(X, X')] \\ \nabla J(\Sigma; \mathbb{P}_n) &= -\frac{1}{2\lambda} \mathbb{E}_{\mathbb{P}_n}[r_{\Sigma; \mathbb{P}_n}(X; Y)r_{\Sigma; \mathbb{P}_n}(X'; Y')\partial_{\Sigma}k_{\Sigma}(X, X')] \end{aligned}$$

Our proof introduces an intermediate quantity  $\psi_n(\Sigma)$ , which serves as a proof device that interpolates between the population gradient  $\nabla J(\Sigma; \mathbb{P})$  and the empirical gradient  $\nabla J(\Sigma; \mathbb{P}_n)$ :

$$(5.22) \quad \psi_n(\Sigma) = -\frac{1}{2\lambda} \mathbb{E}_{\mathbb{P}_n}[r_{\Sigma; \mathbb{P}}(X; Y)r_{\Sigma; \mathbb{P}}(X'; Y')\partial_{\Sigma}k_{\Sigma}(X, X')].$$

The convergence of gradients follow from two lemmas, which state that  $\psi_n(\Sigma)$  is uniformly close to both the empirical gradient  $\nabla J(\Sigma; \mathbb{P}_n)$  and the population gradient  $\nabla J(\Sigma; \mathbb{P})$  over  $\Sigma \in \Sigma$ . Together, these results establish the uniform convergence of the gradients.

**LEMMA 5.3 (Uniform Closeness between  $\psi_n(\Sigma)$  and  $\nabla J(\Sigma; \mathbb{P}_n)$ ).** *For any compact set  $\Sigma$ , there is the convergence as the sample size  $n \rightarrow \infty$ :*

$$(5.23) \quad \sup_{\Sigma \in \Sigma} \|\nabla J(\Sigma; \mathbb{P}_n) - \psi_n(\Sigma)\| = o_P(1).$$

**LEMMA 5.4 (Uniform Closeness between  $\psi_n(\Sigma)$  and  $\nabla J(\Sigma; \mathbb{P})$ ).** *For any compact set  $\Sigma$ , there is the convergence as the sample size  $n \rightarrow \infty$ :*

$$(5.24) \quad \sup_{\Sigma \in \Sigma} \|\nabla J(\Sigma; \mathbb{P}) - \psi_n(\Sigma)\| = o_P(1).$$

5.5.1. *Proof of Lemma 5.3.* Let  $e_1, e_2, \dots, e_p$  be a standard basis of  $\mathbb{R}^d$ . To prove Lemma 5.3, it suffices to prove that entrywise there is the uniform convergence

$$(5.25) \quad \sup_{\Sigma \in \Sigma} |e_i^T (\nabla J(\Sigma; \mathbb{P}_n) - \psi_n(\Sigma)) e_j| = o_P(1).$$

for every pair  $(i, j)$ . Below we establish this.

Fix some index  $(i, j)$ . We compute and bound the difference

$$(5.26) \quad \begin{aligned} & |e_i^T (\nabla J(\Sigma; \mathbb{P}_n) - \psi_n(\Sigma)) e_j| \\ &= \frac{1}{2\lambda} \times |\mathbb{E}_{P_n} [(r_{\Sigma; \mathbb{P}_n}(X, Y) - r_{\Sigma; \mathbb{P}}(X, Y))(r_{\Sigma; \mathbb{P}_n}(X', Y') + r_{\Sigma; \mathbb{P}}(X', Y')) \partial_{\Sigma_{ij}} k_{\Sigma}(X, X')]| \\ &\leq \frac{1}{2\lambda} \times \|(r_{\Sigma; \mathbb{P}_n} - r_{\Sigma; \mathbb{P}})(X, Y)\|_{L_{\infty}(\mathbb{P}_n)} \times \|\partial_{\Sigma_{ij}} k_{\Sigma}(X, X')\|_{L_2(\mathbb{P}_n)} \times \|(r_{\Sigma; \mathbb{P}_n} + r_{\Sigma; \mathbb{P}})(X, Y)\|_{L_2(\mathbb{P}_n)}. \end{aligned}$$

The last line above follows from Hölder's inequality. Next, we bound each term on the RHS of (5.26) uniformly over matrices  $\Sigma \in \Sigma$ .

For the first term, it converges uniformly to zero in probability thanks to Lemma 5.2:

$$(5.27) \quad \sup_{\Sigma \in \Sigma} \|(r_{\Sigma; \mathbb{P}_n} - r_{\Sigma; \mathbb{P}})(X, Y)\|_{L_{\infty}(\mathbb{P}_n)} = o_P(1).$$

For the second term, note that  $\partial_{\Sigma_{ij}} k_{\Sigma}(x, x') = \phi'(\|x - x'\|_{\Sigma}^2) e_i^T (x - x')(x - x')^T e_j$ . By Hölder's inequality we have the uniform estimate

$$\sup_{\Sigma \in \Sigma} \|\partial_{\Sigma_{ij}} k_{\Sigma}(X, X')\|_{L_2(\mathbb{P}_n)} \leq 4 \|\phi'\|_{\infty} \cdot \|e_i^T X\|_{L_4(\mathbb{P}_n)} \cdot \|e_j^T X\|_{L_4(\mathbb{P}_n)} = O_P(1).$$

The last equality holds because  $\|\phi'\|_{\infty} \leq |\phi'_+(0)| < \infty$  and the assumption  $\mathbb{E}_{\mathbb{P}}[\|X\|^4] < \infty$ .

For the last term, by Lemma 2.3 we know the estimate  $\|r_{\Sigma; \mathbb{Q}}(X, Y)\|_{L_2(\mathbb{Q})} \leq \|Y\|_{L_2(\mathbb{Q})}$  holds for every matrix  $\Sigma$  and every measure  $\mathbb{Q}$ . By triangle inequality, we obtain

$$(5.28) \quad \sup_{\Sigma \in \Sigma} \|(r_{\Sigma; \mathbb{P}_n} + r_{\Sigma; \mathbb{P}})(X, Y)\|_{L_2(\mathbb{P}_n)} \leq \sup_{\Sigma \in \Sigma} \|(r_{\Sigma; \mathbb{P}_n} - r_{\Sigma; \mathbb{P}})(X, Y)\|_{L_{\infty}(\mathbb{P}_n)} + 2\|Y\|_{L_2(\mathbb{P}_n)} = O_P(1)$$

where the last identity is due to Lemma 5.2 and the moment assumption  $\mathbb{E}_{\mathbb{P}}[Y^2] < \infty$ .

Substituting all the above three uniform estimates, namely, equations from (5.27) to (5.28), into equation (5.26) yields the desired Lemma 5.3.

5.5.2. *Proof of Lemma 5.4.* Let  $e_1, e_2, \dots, e_p$  be a standard basis of  $\mathbb{R}^d$ . It suffices to prove that entrywise there is the uniform convergence in probability for every pair of indices  $(i, j)$

$$(5.29) \quad \sup_{\Sigma \in \Sigma} |e_i^T (\nabla J(\Sigma; \mathbb{P}) - \psi_n(\Sigma)) e_j| = o_P(1).$$

Fix  $(i, j)$ . To prove it, we apply a fundamental result due to [69, Theorem 2.1]. Given any compact set  $\Sigma$ , uniform convergence in probability holds (equation (5.29)) if and only if

(i) pointwise convergence holds, i.e., for every given matrix  $\Sigma$ , there is the convergence as  $n \rightarrow \infty$

$$e_i^T \psi_n(\Sigma) e_j - e_i^T \nabla J(\Sigma; \mathbb{P}_n) e_j = o_P(1).$$

(ii) stochastic equicontinuity is enjoyed by the random map  $\Sigma \mapsto e_i^T \psi_n(\Sigma) e_j$ , i.e., for every  $\epsilon, \eta > 0$ , there exists  $\delta > 0$  such that

$$\limsup_{n \rightarrow \infty} \mathbb{P} \left( \sup_{\|\Sigma - \Sigma'\|_{\text{op}} < \delta} |e_i^T \psi_n(\Sigma) e_j - e_i^T \psi_n(\Sigma') e_j| > \epsilon \right) < \eta.$$

Below we shall verify these two conditions, which imply Lemma 5.4.

(Pointwise Convergence). The individual convergence in probability follows from the law of large numbers applied to the V-statistics

$$e_i^T \psi_n(\Sigma) e_j = \mathbb{E}_{P_n} [r_{\Sigma; \mathbb{P}}(X, Y) r_{\Sigma; \mathbb{P}}(X', Y') \partial_{\Sigma_{ij}} k_{\Sigma}(X, X')],$$

which converges almost surely to  $\mathbb{E}_{\mathbb{P}} [r_{\Sigma; \mathbb{P}}(X, Y) r_{\Sigma; \mathbb{P}}(X', Y') \partial_{\Sigma_{ij}} k_{\Sigma}(X, X')] = e_i^T \nabla J(\Sigma; \mathbb{P}) e_j$ .

(Stochastic Equicontinuity). The stochastic equicontinuity is implied by the following condition ([69, Corollary 2.2]): there is a sequence of random variables  $B_n = O_P(1)$ ,  $\delta_n = o_P(1)$  such that

$$(5.30) \quad |e_i^T \psi_n(\Sigma) e_j - e_i^T \psi_n(\Sigma') e_j| \leq B_n \cdot \|\Sigma - \Sigma'\| + \delta_n$$

holds for every  $\Sigma, \Sigma' \in \Sigma$ . Below we construct  $B_n$  and  $\delta_n$  that satisfy this desirable property.

We compute and bound for every  $\Sigma, \Sigma' \in \Sigma$

$$\begin{aligned} & |e_i^T \psi_n(\Sigma) e_j - e_i^T \psi_n(\Sigma') e_j| \\ &= \frac{1}{2\lambda} \times \mathbb{E}_{P_n} [(r_{\Sigma; \mathbb{P}}(X, Y) - r_{\Sigma'; \mathbb{P}}(X, Y))(r_{\Sigma; \mathbb{P}}(X', Y') + r_{\Sigma'; \mathbb{P}}(X', Y')) \partial_{\Sigma_{ij}} k_{\Sigma}(X, X')] \\ &\leq \frac{1}{2\lambda} \times \|(r_{\Sigma; \mathbb{P}} - r_{\Sigma'; \mathbb{P}})(X, Y)\|_{L_2(\mathbb{P}_n)} \times \|(r_{\Sigma; \mathbb{P}} + r_{\Sigma'; \mathbb{P}})(X, Y)\|_{L_2(\mathbb{P}_n)} \times \|\partial_{\Sigma_{ij}} k_{\Sigma}(X, X')\|_{L_2(\mathbb{P}_n)} \end{aligned}$$

where the last inequality follows from Cauchy's inequality, using the independence between  $(X, Y)$  and  $(X', Y')$  under the measure  $\mathbb{P}_n$ . We then have

$$\begin{aligned} \|(r_{\Sigma; \mathbb{P}} - r_{\Sigma'; \mathbb{P}})(X, Y)\|_{L_2(\mathbb{P}_n)} &\leq \|(r_{\Sigma; \mathbb{P}_n} - r_{\Sigma'; \mathbb{P}_n})(X, Y)\|_{L_2(\mathbb{P}_n)} + 2 \sup_{\Sigma \in \Sigma} \|(r_{\Sigma; \mathbb{P}} - r_{\Sigma; \mathbb{P}_n})(X, Y)\|_{L_2(\mathbb{P}_n)} \\ &\leq c \cdot \|X\|_2 \|Y\|_{L_2(P_n)} \|\Sigma' - \Sigma\| + 2 \sup_{\Sigma \in \Sigma} \|(r_{\Sigma; \mathbb{P}} - r_{\Sigma; \mathbb{P}_n})(X, Y)\|_{L_2(\mathbb{P}_n)} \end{aligned}$$

where the second inequality follow from Lemma 2.7, and the constant  $c < \infty$  depends only on  $\phi, \lambda, \|\cdot\|$ . Using these bounds, we have:

$$|e_i^T \psi_n(\Sigma) e_j - e_i^T \psi_n(\Sigma') e_j| \leq B_n \cdot \|\Sigma - \Sigma'\| + \delta_n$$

where  $B_n = \Gamma_n C_n$  and  $\delta_n = \Gamma_n h_n$  with:

$$\begin{aligned} \Gamma_n &= \frac{1}{\lambda} \times \sup_{\Sigma \in \Sigma} \|r_{\Sigma; \mathbb{P}}(X, Y)\|_{L_2(\mathbb{P}_n)} \times \sup_{\Sigma \in \Sigma} \|\partial_{\Sigma_{ij}} k_{\Sigma}(X, X')\|_{L_2(\mathbb{P}_n)}, \\ C_n &= c \|X\|_2 \|Y\|_{L_2(P_n)}, \quad h_n = 2 \sup_{\Sigma \in \Sigma} \|(r_{\Sigma; \mathbb{P}} - r_{\Sigma; \mathbb{P}_n})(X, Y)\|. \end{aligned}$$

Clearly,  $C_n = O_P(1)$ , By Lemma 5.2,  $h_n = o_P(1)$ . We now show that  $\Gamma_n = O_P(1)$  by bounding each term in its definition. For the first term:

$$\begin{aligned} \sup_{\Sigma \in \Sigma} \|r_{\Sigma; \mathbb{P}}(X, Y)\|_{L_2(\mathbb{P}_n)} &\leq \sup_{\Sigma \in \Sigma} \|r_{\Sigma; \mathbb{P}_n}(X, Y)\|_{L_2(\mathbb{P}_n)} + \sup_{\Sigma \in \Sigma} \|(r_{\Sigma; \mathbb{P}} - r_{\Sigma; \mathbb{P}_n})(X, Y)\|_{L_2(\mathbb{P}_n)} \\ &\leq \|Y\|_{L_2(\mathbb{P}_n)} + \sup_{\Sigma \in \Sigma} \|(r_{\Sigma; \mathbb{P}} - r_{\Sigma; \mathbb{P}_n})(X, Y)\|_{L_2(\mathbb{P}_n)} = O_P(1) \end{aligned}$$

where the second inequality follows from Lemma 2.3, and the last identity uses Lemma 5.2. For the second term, we note that  $\partial_{\Sigma_{ij}} k_{\Sigma}(x, x') = \phi'(\|x - x'\|_{\Sigma}^2) e_i^T (x - x')(x - x')^T e_j$ . By Hölder's inequality we deduce

$$\sup_{\Sigma \in \Sigma} \|\partial_{\Sigma_{ij}} k_{\Sigma}(X, X')\|_{L_2(\mathbb{P}_n)} \leq 4 \|\phi'\|_{\infty} \cdot \|e_i^T X\|_{L_4(\mathbb{P}_n)} \cdot \|e_j^T X\|_{L_4(\mathbb{P}_n)} = O_P(1)$$

where the last equality uses  $\|\phi'\|_{\infty} \leq |\phi'_+(0)| < \infty$  and the assumption  $\mathbb{E}_P[\|X\|^4] < \infty$ .

This establishes stochastic equicontinuity as desired.

**6. Preserving Low Rankness in Finite Samples.** This section proves Theorem 1.2. As described in the introduction (Section 1.3), our proof technique is largely based on the idea of set identifiability in the optimization literature.

Let us denote the set of low-rank matrices of interest to be:

$$(6.1) \quad \begin{aligned} \mathcal{M}_0 &= \{\Sigma : \Sigma \succeq 0, \text{rank}(\Sigma) \leq \dim(S_*)\} \\ \mathcal{M} &= \{\Sigma : \Sigma \succeq 0, \text{rank}(\Sigma) = \dim(S_*)\}. \end{aligned}$$

The theorem is divided into two cases based on the value of the parameter  $\lambda$ . In the first case, where  $\lambda \in (0, \infty)$ , the goal is to demonstrate that with high probability every empirical minimizer  $\Sigma_n^* \in \mathcal{M}_0$  holds. The proof strategy for this case comprises two main parts:

- (Identifiability) We shall first prove that  $\mathcal{M}_0$  is the *identifiable set* with respect to the population objective (4.1) at every its minimizer  $\Sigma^*$  (see Definition 6.1). Roughly speaking, it says that any deterministic converging sequence  $\Sigma_i \rightarrow \Sigma^*$  nearly stationary to the population objective (4.1) must obey  $\Sigma_i \in \mathcal{M}_0$  for all large enough indices  $i$ .

This result completely deterministic in its nature is elaborated in Section 6.1.

- (Convergence of Minimizers) We next prove the sequence of empirical minimizer  $\Sigma_n^*$  converges in probability to the population counterparts as  $n \rightarrow \infty$ , and  $\Sigma_n^*$  is nearly stationary with respect to the *population* objective (4.1) with probability tending to one.

This part probabilistic in its nature is elaborated in detail in Section 6.2.

With these two results, we conclude  $\Sigma_n^* \in \mathcal{M}_0$  holds with probability tending to one as  $n \rightarrow \infty$ . This holds for every given  $\lambda \in (0, \infty)$ . It is worth mentioning that the same technique works for the second case where  $\lambda \in (0, \lambda_0]$ .

The key element that underpins identifiability is the sharpness property of the population objective near its minimizers, which we established in Section 4. The key element that underpins convergence of minimizers is the uniform convergence of values and gradients of the empirical objective to the population counterparts, which we established in Section 5.

In the existing literature, a well-documented relationship exists between sharpness and set identifiability, see, e.g., [35, 18, 90, 60, 49, 34]. Notably, a large body of work in this area delineates this relation in scenarios where the identifiable set is characterized as a smooth submanifold within an ambient Euclidean space (e.g., [60, 34]). In the context of our research, while the set  $\mathcal{M}$  conforms to this smooth structure, the set  $\mathcal{M}_0$  is not a smooth submanifold of the ambient space of symmetric matrices. Consequently, ascertaining the identifiability of  $\mathcal{M}_0$  presents a greater challenge compared to the set  $\mathcal{M}$ . A notable element of our proof delves into highlighting how the sharpness property (Corollary 4.1) connects with the identifiability of  $\mathcal{M}_0$ , as detailed in Theorem 6.1 in Section 6.1.

**6.1. Identifiability of Set of Low-rank Matrices.** Here we formally introduce the notion of identifiable sets, following the thesis work [33, Definition 7.2.1] (or its published version [29, Definition 3.12]).

**DEFINITION 6.1 (Identifiable Sets).** Consider an  $f : \mathbb{R}^m \mapsto \mathbb{R} \cup \{+\infty\}$  and a critical point  $x \in \mathbb{R}^m$  where  $0 \in \partial f(x)$ . A set  $S$  is identifiable with respect to  $f$  at  $x$  if for any sequence  $(x_i, f(x_i), v_i) \rightarrow (x, f(x), 0)$ , with  $v_i \in \partial f(x_i)$ , the points  $x_i$  must lie in  $S$  for all sufficiently large indices  $i$  (i.e.,  $\exists N_0 < \infty$  such that  $x_i \in S$  for every  $i \geq N_0$ ).

Theorem 6.1 below presents the main result of the section. Recall the population objective

$$\underset{\Sigma}{\text{minimize}} J(\Sigma) \quad \text{subject to} \quad \Sigma \in \mathcal{C}_M$$

where  $\mathcal{C}_M = \{\Sigma : \Sigma \succeq 0, \|\Sigma\| \leq M\}$ . Following the standard ideas in optimization, we can convert a constrained minimization problem into an unconstrained minimization:

$$\underset{\Sigma}{\text{minimize}} \quad \tilde{J}(\Sigma)$$

where  $\tilde{J}(\Sigma) = J(\Sigma) + \mathbf{1}_{\mathcal{C}_M}(\Sigma)$  where  $\mathbf{1}_{\mathcal{C}_M}(\Sigma) = 0$  if  $\Sigma \in \mathcal{C}_M$  and  $\mathbf{1}_{\mathcal{C}_M}(\Sigma) = +\infty$  if  $\Sigma \notin \mathcal{C}_M$ . The subgradient calculus yields the following basic formula that holds for every  $\Sigma \in \mathcal{C}_M$ :

$$(6.2) \quad \partial\tilde{J}(\Sigma) = \nabla J(\Sigma) + \mathbf{N}_{\mathcal{C}_M}(\Sigma).$$

In the above,  $\partial\tilde{J}(\Sigma)$  is the subdifferential of  $\tilde{J}$  at  $\Sigma$ , and  $\nabla J(\Sigma)$  is interpreted as the gradient of  $J$  at  $\Sigma$  in terms of Definition 2.1, and  $\mathbf{N}_{\mathcal{C}_M}(\Sigma)$  is the normal cone at  $\Sigma$  relative to the constraint  $\mathcal{C}_M$ . It is clear that  $0 \in \partial\tilde{J}(\Sigma^*)$  since  $\Sigma^*$  is a global minimizer of  $\tilde{J}$ .

By converting to an equivalent unconstrained minimization, we can state our main result on low rank set identifiability for the population objective using the terms from Definition 6.1.

**THEOREM 6.1** (Identifiability of  $\mathcal{M}_0, \mathcal{M}$  with respect to  $\tilde{J}$ ). *Let Assumptions 1–4 hold.*

- For every  $\lambda \in (0, \infty)$ ,  $\mathcal{M}_0$  is identifiable with respect to  $\tilde{J}$  at every its minimizer  $\Sigma^*$ .
- For every  $\lambda \in (0, \lambda_0]$ ,  $\mathcal{M}$  is identifiable with respect to  $\tilde{J}$  at every its minimizer  $\Sigma^*$ .

In the above,  $0 < \lambda_0 < \infty$  is identical to  $\lambda_0$  in Theorem 1.1.

Our proof of Theorem 6.1 relies on a characterization of the normal cone  $\mathbf{N}_{\mathcal{C}_M}$ .

**LEMMA 6.1.** *Let  $\Sigma \in \mathcal{C}_M$  and  $Z \in \mathbf{N}_{\mathcal{C}_M}(\Sigma)$ . Then  $\Pi_{\text{col}(\Sigma)} Z \Pi_{\text{col}(\Sigma)} \succeq 0$ .*

**PROOF.** Let  $v \in \text{col}(\Sigma)$ . Then  $\Sigma - \epsilon vv^T \in \mathcal{C}_M$  for all small  $\epsilon > 0$ . Since  $Z \in \mathbf{N}_{\mathcal{C}_M}(\Sigma)$ ,  $\langle \Sigma' - \Sigma, Z \rangle \leq 0$  for any  $\Sigma' \in \mathcal{C}_M$ . Taking  $\Sigma' = \Sigma - \epsilon vv^T$  yields  $\langle Z, vv^T \rangle \geq 0$ , or  $v^T Z v \geq 0$ . The result follows as  $v \in \text{col}(\Sigma)$  is arbitrary.  $\square$

**PROOF OF THEOREM 6.1.** Let  $\Sigma^*$  denote a minimizer.

Consider the first case where  $\lambda \in (0, \infty)$ . Then  $\Sigma^* \in \mathcal{M}_0$  by Theorem 1.1. Consider a sequence of matrices  $\Sigma_i$  for which  $(\Sigma_i, \tilde{J}(\Sigma_i), V_i) \rightarrow (\Sigma^*, \tilde{J}(\Sigma^*), 0)$  where  $V_i \in \partial\tilde{J}(\Sigma_i)$ . Our goal is to show that  $\Sigma_i \in \mathcal{M}_0$  for large enough indices  $i$ .

Clearly,  $\Sigma_i \in \mathcal{C}_M$  for all large enough  $i$ , since  $\tilde{J}(\Sigma_i) \rightarrow \tilde{J}(\Sigma^*) < \infty$ . This means that for all large enough  $i$ , the subgradient  $V_i$  takes the form of  $V_i = \nabla J(\Sigma_i) + Z_i$  where  $Z_i \in \mathbf{N}_{\mathcal{C}_M}(\Sigma_i)$ . We shall use the fact that  $V_i \rightarrow 0$  to conclude that  $\Sigma_i \in \mathcal{M}_0$  eventually.

The key to our analysis is the sharpness property of  $J$  at  $\Sigma^*$  in Corollary 4.1. By Corollary 4.1, and Lemma 4.1, there is  $\rho > 0$  such that for every vector  $w \in S_*^\perp$ :

$$(6.3) \quad w^T \nabla J(\Sigma^*) w = \langle \nabla J(\Sigma^*), w w^T \rangle \geq \rho \|w\|_2^2.$$

Since  $\Sigma_i \rightarrow \Sigma^*$ ,  $\nabla J(\Sigma_i) \rightarrow \nabla J(\Sigma^*)$  by Lemma 2.9. Therefore, there is an  $N < \infty$  such that every  $i \geq N$  obeys the property

$$(6.4) \quad w^T \nabla J(\Sigma_i) w \geq \frac{\rho}{2} \|w\|_2^2 \quad \text{holds for every } w \in S_*^\perp.$$

Applying Lemma 6.1 to the sequence  $\Sigma_i$ , we obtain

$$(6.5) \quad \Pi_{\text{col}(\Sigma_i)} Z_i \Pi_{\text{col}(\Sigma_i)} \succeq 0.$$

Suppose, for the sake of contradiction, that there is a subsequence  $i_k$  for which  $\Sigma_{i_k} \notin \mathcal{M}_0$ , meaning that  $\text{rank}(\Sigma_{i_k}) > \dim(S_*)$ . Then,  $\dim(\text{col}(\Sigma_{i_k})) + \dim(S_*^\perp) > \dim(S_*) +$

$\dim(S_*^\perp) = d$ , the ambient dimension. Hence  $\text{col}(\Sigma_{i_k}) \cap S_*^\perp \neq \emptyset$ , meaning that we can find a vector  $w_{i_k} \in \text{col}(\Sigma_{i_k}) \cap S_*^\perp$  with  $\|w_{i_k}\|_2 = 1$ . For this vector, we have for every index  $i_k \geq N$ :

$$w_{i_k}^T V_{i_k} w_{i_k} = w_{i_k}^T \nabla J(\Sigma_{i_k}) w_{i_k} + w_{i_k}^T Z_{i_k} w_{i_k} \geq w_{i_k}^T \nabla J(\Sigma_{i_k}) w_{i_k} \geq \frac{\rho}{2}$$

where the inequality follows from (6.4) and (6.5), and our choice of  $w_{i_k} \in \text{col}(\Sigma_{i_k}) \cap S_*^\perp$ . This leads to the contraction with  $V_{i_k} \rightarrow 0$  assumed at the beginning!

Therefore, it must hold that  $\Sigma_i \in \mathcal{M}_0$  for every large enough index  $i$ , meaning that  $\mathcal{M}_0$  is an identifiable set with respect to  $\tilde{J}$  at every its minimizer  $\Sigma^*$ .

Consider the second case where  $\lambda \in (0, \lambda_0]$ . In this case,  $\Sigma^* \in \mathcal{M}$ , and thus  $\text{rank}(\Sigma^*) = \dim(S_*)$ . Since  $\Sigma \mapsto \text{rank}(\Sigma)$  is lower-semicontinuous on  $\mathcal{C}$ , any sequence  $\Sigma_i \in \mathcal{C}_M$  with  $\Sigma_i \rightarrow \Sigma^*$  must obey  $\liminf_i \text{rank}(\Sigma_i) \geq \text{rank}(\Sigma^*) = \dim(S_*)$ , indicating that  $\text{rank}(\Sigma_i) \geq \dim(S_*)$  holds eventually. On the other hand, since we have shown that  $\mathcal{M}_0$  is an identifiable set with respect to  $\tilde{J}$ , this also means that  $\text{rank}(\Sigma_i) \leq \dim(S_*)$  eventually. Combining these, we get  $\text{rank}(\Sigma_i) = \dim(S_*)$  for all large  $i$ . This completes the proof that  $\mathcal{M}$  is an identifiable set with respect to  $\tilde{J}$  when  $\lambda \in (0, \lambda_0]$ .  $\square$

**6.2. Convergence of Minimizers.** Let  $\Sigma_n^*$  and  $\Sigma^*$  denote the sets of minimizers of  $J_n$  and  $J$  respectively, on the compact set  $\mathcal{C}_M$ .

LEMMA 6.2 (Convergence of Minimizers). *Let Assumption 4 hold. As  $n \rightarrow \infty$ ,*

$$(6.6) \quad \text{dist}(\Sigma_n^*, \Sigma^*) \xrightarrow{p} 0 \quad \text{and} \quad \sup\{\text{dist}(0, \partial\tilde{J}(\Sigma_n^*)) | \Sigma_n^* \in \Sigma_n^*\} \xrightarrow{p} 0.$$

PROOF. By Theorem 5.1, there is uniform convergence of objective values  $J_n$  to  $J$  in probability on the compact set  $\mathcal{C}_M$ . This ensures that  $\text{dist}(\Sigma_n^*, \Sigma^*) \xrightarrow{p} 0$ .

By Theorem 5.1, there is also the uniform convergence of gradients  $\nabla J_n$  to  $\nabla J$  in probability on the same set  $\mathcal{C}_M$ . For any minimizer  $\Sigma_n^*$  of  $J_n$  on the convex set  $\mathcal{C}_M$ , the first-order condition must hold:  $0 \in \nabla J_n(\Sigma_n^*) + \mathbf{N}_{\mathcal{C}_M}(\Sigma_n^*)$ . Given that  $|\nabla J_n(\Sigma_n^*) - \nabla J(\Sigma_n^*)| \xrightarrow{p} 0$ , it follows that  $\sup\{\text{dist}(0, \nabla J(\Sigma_n^*) + \mathbf{N}_{\mathcal{C}_M}(\Sigma_n^*)) | \Sigma_n^* \in \Sigma_n^*\} \xrightarrow{p} 0$  as desired.  $\square$

**6.3. Low-rank Set Identifiability: Proof of Theorem 1.2.** We start by considering the case where  $\lambda \in (0, \infty)$ . To see the main idea, assume *temporarily* that there is the *almost sure* convergence:

$$(6.7) \quad \text{dist}(\Sigma_n^*, \Sigma^*) \rightarrow 0 \quad \text{and} \quad \sup\{\text{dist}(0, \partial\tilde{J}(\Sigma_n^*)) | \Sigma_n^* \in \Sigma_n^*\} \rightarrow 0.$$

This assumption is stronger than the convergence in probability stated in Lemma 6.2.

Assuming this almost sure convergence, we show that  $\Sigma_n^* \subseteq \mathcal{M}_0$  holds eventually with probability one (i.e.,  $\exists N_0 < \infty$  such that  $\Sigma_n^* \subseteq \mathcal{M}_0$  for all  $n \geq N_0$ ). To see this, pick  $\Sigma_n^* \in \Sigma_n^*$ . For any subsequence  $\Sigma_{n_i}^*$ , since  $\mathcal{C}_M$  is compact, a subsubsequence  $\Sigma_{n_{i_j}}^*$  exists and converges to some  $\Sigma^* \in \Sigma^*$ . By Theorem 6.1, this subsubsequence  $\Sigma_{n_{i_j}}^*$  must eventually fall within  $\mathcal{M}_0$ . Since this applies to every subsequence  $\Sigma_{n_i}^*$ , Urysohn's subsequence principle implies that the original sequence  $\Sigma_n^*$  must also eventually be in  $\mathcal{M}_0$ . Since this holds for any  $\Sigma_n^* \in \Sigma_n^*$ , it further implies that  $\Sigma_n^* \subseteq \mathcal{M}_0$  eventually.

Thus, under the almost sure convergence (6.7), we have:

$$\mathbb{P}(\exists N_0 < \infty, \text{ such that } \Sigma_n^* \subseteq \mathcal{M}_0 \text{ for all } n \geq N_0) = 1,$$

which implies:

$$(6.8) \quad \lim_{n \rightarrow \infty} \mathbb{P}(\Sigma_n^* \subseteq \mathcal{M}_0) = 1.$$

Now, for the general case where convergence holds in probability (cf. Lemma 6.2),

$$(6.9) \quad \text{dist}(\Sigma_n^*, \Sigma^*) \xrightarrow{p} 0 \quad \text{and} \quad \sup\{\text{dist}(0, \partial\tilde{J}(\Sigma_n^*)) | \Sigma_n^* \in \Sigma_n^*\} \xrightarrow{p} 0.$$

we reduce it to the almost sure case.

Define  $\delta_n = \text{dist}(\Sigma_n^*, \Sigma^*) + \sup\{\text{dist}(0, \partial\tilde{J}(\Sigma_n^*)) | \Sigma_n^* \in \Sigma_n^*\}$ . By Lemma 6.2,  $\delta_n$  converge to zero in probability. Thus any subsequence  $n_j$  has a subsubsequence  $n_{j_k}$  where  $\delta_{n_{j_k}}$  converge to zero *almost surely*. This implies  $\lim \mathbb{P}(\Sigma_{n_{j_k}}^* \subseteq \mathcal{M}_0) = 1$  along  $n_{j_k}$ . Since this holds for every subsequence  $n_j$ , Urysohn's subsequence principle then yields that the convergence  $\lim \mathbb{P}(\Sigma_n^* \subseteq \mathcal{M}_0) = 1$  must hold for the entire sequence.

The proof for the other case  $\lambda \in (0, \lambda_0]$  is similar, with  $\mathcal{M}_0$  replaced by  $\mathcal{M}$ .

**7. Consistent Estimation of the Central Mean Subspace and Its Dimension.** This section proves Theorem 1.3, using Theorem 1.2 and Lemma 6.2. To establish our result, we utilize a matrix perturbation result, which is formally stated in the following lemma:

LEMMA 7.1. *Let  $\Sigma_i$  denote a deterministic sequence such that  $\Sigma_i \rightarrow \Sigma$  as  $i \rightarrow \infty$ . Suppose  $\text{rank}(\Sigma_i) = \text{rank}(\Sigma)$  for all  $i$ . Then, as  $i \rightarrow \infty$ ,*

$$\|\|\Pi_{\text{col}(\Sigma_i)} - \Pi_{\text{col}(\Sigma)}\|\| \rightarrow 0.$$

PROOF. This follows from Davis-Kahan Theorem [81, Section V].  $\square$

We are ready to finish the proof of Theorem 1.3.

PROOF OF THEOREM 1.3. Lemma 6.2 shows the convergence of  $\Sigma_n^*$  to  $\Sigma^*$  in probability. Theorem 1.2 shows that with converging to one probability that  $\text{rank}(\Sigma_n^*) = \text{rank}(\Sigma^*) = \dim(S_*)$  holds for every  $\Sigma_n^* \in \Sigma_n^*$  and  $\Sigma^* \in \Sigma^*$ . Theorem 1.3 then follows from Lemma 7.1.  $\square$

**8. Inner Product Type Kernels Fail.** Various kernels, apart from the rotationally and translation-invariant kernel, have been proposed in the literature. Given the observed phenomenon for kernels  $k_q(w, w') = \phi(\|w - w'\|_2^2)$  (or  $k_\Sigma(x, x') = \phi(\|x - x'\|_\Sigma^2)$ ), it is thereby tempting to ask whether the phenomenon we observe appears with other kernels as well, e.g., kernels of the form  $(w, w') \mapsto \psi(w^T w')$  (or  $(x, x') \mapsto \psi(x^T \Sigma x')$ ).

More precisely, we consider the following alternative objective

$$(8.1) \quad \min_{f, U, \gamma} \frac{1}{2} \mathbb{E}_n[(Y - f(U^T X) - \gamma)^2] + \frac{\lambda}{2} \|f\|_{\mathcal{H}_q}^2.$$

In the above,  $f : \mathbb{R}^q \rightarrow \mathbb{R}$ ,  $\gamma \in \mathbb{R}$  and  $U \in \mathbb{R}^{d \times q}$ . This objective has the exact same mathematical form as our original objective (1.1), but it replaces the definition of  $\mathcal{H}_q$  as the RKHS associated with the kernel  $u_q(w, w') = \psi(w^T w')$ . Here  $\psi$  is a real-valued function that ensures  $u_q$  to be a positive semidefinite kernel for all  $q \in \mathbb{N}$ . Similarly, when  $q \geq d$ , this objective has an equivalent kernel learning formulation:

$$(8.2) \quad \min_{F, \Sigma, \gamma} \frac{1}{2} \mathbb{E}_n[(Y - F(X) - \gamma)^2] + \frac{\lambda}{2} \|F\|_{\mathcal{H}_\Sigma}^2 \quad \text{subject to} \quad \Sigma \succeq 0.$$

In the above,  $\Sigma \in \mathbb{R}^{d \times d}$  is positive semidefinite. This objective has the exact same mathematical form as our original kernel learning formulation (1.2), but it replaces the definition of  $\mathcal{H}_\Sigma$  as the RKHS associated with the inner-product kernel  $u_\Sigma(x, x') = \psi(x^T \Sigma x')$ .

Motivated by Schoenberg’s fundamental result [78], we restrict our attention to analytic  $\psi$  on the real line with  $\psi(t) = \sum_k \xi_k t^k$  where  $\xi_k \geq 0$  for all  $k$ , and  $\sum_k \xi_k > 0$ . These conditions on  $\psi$  guarantee that  $(w, w') \mapsto u_q(w, w')$  (resp.  $(x, x') \mapsto u_\Sigma(x, x')$ ) to be a positive semidefinite kernel for every dimension  $q \in \mathbb{N}$  (resp. for every matrix  $\Sigma \succeq 0$ ).

In Section 9, our extensive numerical experiments suggest that the solution low-rankness phenomenon disappears when we use the kernel  $u_\Sigma$  (or resp.  $u_q$ ) rather than  $k_\Sigma$  (or resp.  $u_\Sigma$ ). This controlled experiment suggests that the phenomenon we observe is specifically tied to the kernel  $k_\Sigma$  (or resp.  $k_q$ ). It helps clarify, as stated in the introduction, that the semidefinite constraint alone can’t take full credit for the phenomenon.

**8.1. Discussion.** In this subsection, we give some basic ideas and results that explain why the kernel learning formulation (8.2) with inner product kernel  $u_\Sigma$  fails to deliver exact low-rank solutions in finite samples. Due to the equivalence, these ideas will apply to the equivalent formulation (8.2) with inner product kernel  $u_q$ . The perspective we take is to illustrate the sharpness property that holds for the learning objective with kernel  $k_\Sigma$  fails to hold when using the inner-product kernel  $u_\Sigma$ . Our derivation below for the kernel  $u_\Sigma$  mimics this paper’s analysis of  $k_\Sigma$ . Note a full-fledged analysis with all the details exceeds the scope of the paper, and may be developed in the authors’ future work.

Let us first introduce the function  $J_u(\Sigma)$  at the population level—the analogue of  $J(\Sigma)$ —which takes partial minimization over  $f, \gamma$ :

$$J_u(\Sigma) = \min_{F, \gamma} \frac{1}{2} \mathbb{E}[(Y - F(X) - \gamma)^2] + \frac{\lambda}{2} \|F\|_{\mathcal{H}_\Sigma}^2.$$

We also use  $F_{\Sigma, \gamma_\Sigma}$  to denote the minimizer of the RHS. Note the definition of  $\mathcal{H}_\Sigma$  is now associated with the inner-product kernel  $u_\Sigma(x, x') = \psi(x^T \Sigma x')$ .

We are now interested in whether the sharpness property holds for  $J_u(\Sigma)$ . To do so, let us first use  $\Sigma^*$  to denote a minimizer of the population objective

$$\text{minimize } J_u(\Sigma) \quad \text{subject to } \Sigma \succeq 0, \quad \|\Sigma\| \leq M.$$

We apply the same idea in Lemma 2.9 to derive the gradient of  $J_u$  (and due to the space constraints, we omit the details of the derivation). Suppose  $\text{supp}(X)$  is compact. Then, for every  $\Sigma \in \mathcal{C}$ :

$$\nabla J_u(\Sigma) = \mathbb{E}[r_\Sigma(X; Y) r_\Sigma(X'; Y') \partial_\Sigma u_\Sigma(X, X')].$$

Here the gradient  $\nabla J_u$  is interpreted in terms of Definition 2.1, and  $r_\Sigma$  is interpreted as the residual  $r_\Sigma(x, y) = y - F_\Sigma(x) - \gamma_\Sigma$ . The gradient formula between  $\nabla J_u$  and  $\nabla J$  is similar.

Let us now suppose that  $\text{col}(\Sigma^*) \subseteq S_*$  (i.e., the analogue of Theorem 1.1 holds for the kernel  $u_\Sigma$ ). Assume  $\Pi_{S_*^\perp} X$  is independent of  $\Pi_{S_*} X$ . Then similar to the proof of Theorem 4.1, we derive

$$\begin{aligned} \Pi_{S_*^\perp} \nabla J_u(\Sigma^*) \Pi_{S_*^\perp} &= \mathbb{E}[r_{\Sigma^*}(X; Y) r_{\Sigma^*}(X'; Y') \psi'(X^T \Sigma^* X') \Pi_{S_*^\perp} X (X')^T \Pi_{S_*^\perp}] \\ &= \mathbb{E}[r_{\Sigma^*}(X; Y) r_{\Sigma^*}(X'; Y') \psi'(X^T \Sigma^* X')] \cdot \Pi_{S_*^\perp} \mathbb{E}[X] \cdot (\Pi_{S_*^\perp} \mathbb{E}[X])^T. \end{aligned}$$

As a result, this shows  $\Pi_{S_*^\perp} \nabla J_u(\Sigma^*) \Pi_{S_*^\perp} = 0$  if  $\mathbb{E}[X] \in S_*^\perp$ .

Note this implies that  $\langle \nabla J_u(\Sigma^*), vv^T \rangle = 0$  holds for any  $v \in S_*^\perp$ . This further implies that if  $\mathbb{E}[X] \in S_*^\perp$ , then we can’t have the analog of sharpness property which holds for  $J_u$ . Indeed,  $\langle \nabla J_u(\Sigma^*), W \rangle = 0$  holds for every  $W \in \mathcal{T}_\mathcal{C}(\Sigma^*)$ , with  $\text{col}(W) \subseteq S_*^\perp$  if  $\mathbb{E}[X] \in S_*^\perp$ . In particular, the sharpness property does not hold when  $\mathbb{E}[X] = 0$ .

In short, for inner-product kernels to possess the sharpness property, our findings indicate that we must make extra distributional assumptions on  $(X, Y)$ .

**9. Synthetic Experiments.** The low-rank structure of the learned bottom-layer weight matrix, as described in the paper, was initially identified through computational experiments rather than derived through mathematical analysis. In this section, we document some observations from our simulation experiments that further characterize the scope of when the phenomenon occurs. In other words, we aim to describe situations when the finite sample solution  $\Sigma_n^*$  of the kernel learning objective (1.2) (or equivalently,  $U_n^*$  of the two-layer objective (1.1)) has rank bounded by the minimum size of projection directions of  $X$  required to achieve full predictive power for the target  $Y$ .

9.1. *Setting and Methodology.* Our experiments are of the following form.

1. We generate  $n$  i.i.d. samples  $(X, Y) \sim \mathbb{P}$  according to

$$Y = f(X) + \epsilon.$$

In the above, the noise term  $\epsilon \sim N(0, \sigma^2)$  is independent from  $X \sim \mathbb{P}_X$ .

2. We then solve the finite sample kernel learning objective

$$(P) \quad \underset{f, \gamma, \Sigma}{\text{minimize}} \quad \frac{1}{2} \mathbb{E}_n[(Y - f(X) - \gamma)]^2 + \frac{\lambda}{2} \|f\|_{\mathcal{H}_\Sigma}^2 \quad \text{subject to} \quad \Sigma \succeq 0.$$

3. We document the column space of our solution  $\Sigma_n^*$  across a grid of choice of  $\lambda$ . We then compare it with  $S_*$  where  $S_*$  is the central mean subspace.

The main purpose of the experiments is to vary the signal form  $f$ , distribution  $\mathbb{P}_X$  and the RKHS  $\mathcal{H}_\Sigma$  to investigate when  $\text{rank}(\Sigma_n^*) \leq \dim(S_*)$  (equivalently,  $\text{rank}(U_n^*) \leq \dim(S_*)$ ) and  $\text{rank}(\Sigma_n^*) = \dim(S_*)$  (equivalently,  $\text{rank}(U_n^*) \leq \dim(S_*)$ ) hold with high probability.

**Function  $f$ .** The function  $f$  takes one of the following forms: (a)  $f(x) = x_1 + x_2 + x_3$  (b)  $f(x) = x_1 x_2$ , (c)  $f(x) = 0.1(x_1 + x_2 + x_3)^3 + \tanh(x_1 + x_3 + x_5)$ , (d)  $f(x) = 2(x_1 + x_2) + (x_2 + x_3)^2 + (x_4 - 0.5)^3$ , (e)  $f(x) = 0$ .

**Algorithm for solving (P).** The objective (P) is non-convex in  $\Sigma$ . However, for a given  $\Sigma$ , partial minimization over  $f$  and  $\gamma$  can be done based on kernel ridge regression. For our experiments, we first derive an explicit formula for  $J_n(\Sigma) = \min_{f, \gamma} \frac{1}{2} \mathbb{E}_n[(Y - f(X) - \gamma)]^2 + \frac{\lambda}{2} \|f\|_{\mathcal{H}_\Sigma}^2$  and evaluate the gradient  $\nabla J_n(\Sigma)$ . To then minimize  $J_n(\Sigma)$  subject to  $\Sigma \succeq 0$ , we perform the very simple gradient descent with projection onto the semidefinite cone  $\mathcal{C} = \{\Sigma : \Sigma \succeq 0\}$  per iteration, using the Armijo rule to search each iteration's stepsize. We terminate gradient descent when the ratio between the difference of consecutive iterates, measured by the Frobenius norm, and the stepsize is below a threshold  $\Delta > 0$ . The algorithm is always initialized at a diagonal matrix with diagonal entry  $1/d$ .

**Size  $n, d, \sigma, \Delta$ .** For all our simulations,  $n = 300$ ,  $d = 50$ ,  $\sigma = 0.1$ ,  $\Delta = 10^{-3}$ .

9.2. *Results.* We first briefly list our claims and then provide the source of evidence that supports our claims.

- (i) The phenomenon  $\text{rank}(\Sigma_n^*) \leq \dim(S_*)$  occurs with high probability under Assumptions 1–4. While this is just the main Theorem 1.2, we further corroborate it with empirical evidence.
- (ii) The phenomenon  $\text{rank}(\Sigma_n^*) \leq \dim(S_*)$  occurs in the solution with high probability for the kernel  $(x, x') \mapsto \phi(\|x - x'\|_\Sigma^2)$  regardless of the independence Assumption 3.
- (iii) The phenomenon  $\text{rank}(\Sigma_n^*) \leq \dim(S_*)$  occurs in the solution with high probability for the kernel  $(x, x') \mapsto \phi(\|x - x'\|_\Sigma^2)$  regardless of whether  $X$  is discrete or continuous.

- (iv) The phenomenon disappears when  $X$  has no predictive power of  $Y$ , i.e.,  $f(x) \equiv 0$ .
- (v) The phenomenon disappears when using the inner product kernel  $(x, x') \mapsto \psi(x^T \Sigma x')$ .

Below we make each claim concrete with evidence.

**Claim (i).** Using  $X \sim \mathcal{N}(0, I)$ , the function  $f$  from Section 9.1 options (a) – (d), and the Gaussian kernel  $k_\Sigma(x, x') = \exp(-\|x - x'\|_\Sigma^2)$ , all Assumptions 1–4 hold. The results are shown in Figure 2.

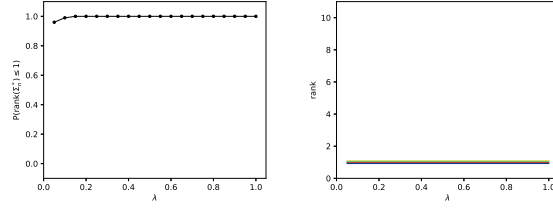
**Claim (ii).** Here  $X \sim \mathcal{N}(0, K)$  where the covariance matrix  $K$  has its  $(i, j)$ -th entry  $K_{i,j} = 0.5^{|i-j|}$ . Thus,  $X$  has correlated covariates. For every regression function  $f$  from Section 9.1 options (a) – (d),  $\Pi_{S_*} X$  is dependent with  $\Pi_{S_*^\perp} X$ , and thus Assumption 3 is violated. The results displayed in Figure 10 (Section B) show that the phenomenon occurs regardless of the independence assumption.

**Claim (iii).** We experiment with two distributions of  $X$ : either  $X$  is discrete with independent coordinates  $X_1, X_2, \dots, X_d$  with  $\mathbb{P}(X_i = 1) = \mathbb{P}(X_i = 0) = 0.5$  or  $X$  is continuous with independent coordinates  $X_1, X_2, \dots, X_d$  with each  $X_i$  uniformly distributed on  $[0, 1]$ . For  $f$  from Section 9.1 options (a) – (d), and the Gaussian kernel  $k_\Sigma(x, x') = \exp(-\|x - x'\|_\Sigma^2)$ , the phenomenon continues to appear in our experiments. See Figure 11, Section B.

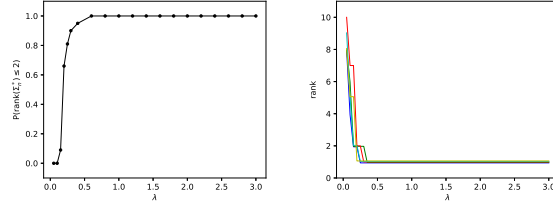
**Claim (iv).** In this experiment,  $X \sim \mathcal{N}(0, I)$ ,  $f(x) \equiv 0$  and  $k_\Sigma(x, x') = \exp(-\|x - x'\|_\Sigma^2)$  is the Gaussian kernel. The solution  $\Sigma_n^*$  is full rank with high probability (in our experiments,  $\Sigma_n^*$  is with probability one full rank over a range of  $\lambda$  values, see Figure 12, Section B).

**Claim (v).** For this experiment, we set  $X \sim \mathcal{N}(0, I)$  and consider two inner product kernels: the linear kernel  $k_\Sigma(x, x') = x^T \Sigma x'$  and the cubic kernel  $k_\Sigma(x, x') = (x^T \Sigma x')^3$ . Given occasional divergence of  $\Sigma_n^*$  in the experiments, we consider  $\min_{f, \gamma, \Sigma} \frac{1}{2} \mathbb{E}_n[(Y - f(X) - \gamma)]^2 + \frac{\lambda}{2} \|f\|_{\mathcal{H}_\Sigma}^2$  subject to  $\Sigma \succeq 0, \|\Sigma\|_{\text{op}} \leq M$ , where  $\|\cdot\|_{\text{op}}$  denotes the operator norm and  $M = 100000$ . We solve the minimization problem in a similar way: first evaluate  $J_n(\Sigma) = \min_{f, \gamma} \frac{1}{2} \mathbb{E}_n[(Y - f(X) - \gamma)]^2 + \frac{\lambda}{2} \|f\|_{\mathcal{H}_\Sigma}^2$  and its gradient  $\nabla J_n(\Sigma)$ , and then perform projected gradient descent onto the bounded constraint set  $\mathcal{C}_M = \{\Sigma : \Sigma \succeq 0, \|\Sigma\|_{\text{op}} \leq M\}$ , using Armijo’s rule to perform stepsize selection. We document the resulting solution  $\Sigma_n^*$ .

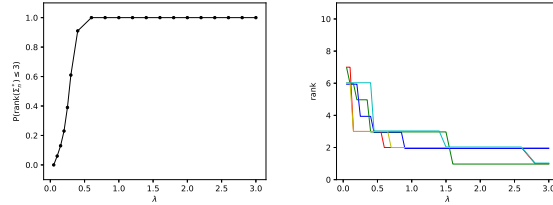
Our findings show that the solution  $\Sigma_n^*$  is with high probability full rank regardless of the choice of the function  $f$  from Section 9.1 options (a)–(d). In fact, in all our experiments,  $\Sigma_n^*$  is with probability one full rank over a range of  $\lambda$  values, see Figure 13 in Section B.



$$(a) f(x) = x_1 + x_2 + x_3.$$



$$(b) f(x) = 0.1(x_1 + x_2 + x_3)^3 + \tanh(x_1 + x_3 + x_5).$$



$$(c) f(x) = 2(x_1 + x_2) + (x_2 + x_3)^2 + (x_4 - 0.5)^3.$$

Fig 2: Plots for Claim (i). For each row, the left panel shows the empirical probability of  $\text{rank}(\Sigma_n^*) \leq \dim(S_*)$  over 100 repeated experiments for different  $\lambda$  values, while the right panel illustrates the rank of  $\Sigma_n^*$  as  $\lambda$  varies, using 5 example pairs of  $(X, y)$ .

**10. Real Data Experiments.** We present two real-world data applications to illustrate the two-layer kernel ridge regression models. Our illustration demonstrates how the model "automatically" regularizes to facilitate dimension reduction for enhanced interpretability and improves prediction accuracy over traditional kernel methods through feature learning.

For transparency and reproducibility, all codes in this section can be found in the website:

<https://github.com/tinachentc/kernel-learning-in-ridge-regression>

**10.1. Illustration I: Car Pricing via Automobile Data.** To demonstrate the practical applicability of our method for dimension reduction, we apply it to the Automobile Data from the UCI Machine Learning Repository [76], with the objective of studying how car price depends on its features. This dataset has been previously analyzed using various dimension reduction techniques, including sliced inverse regression (SIR), sliced average variance estimation (SAVE), and Fourier-based methods [95, Section 6].

We remove one continuous variable (called normalized-losses) containing many missing values. Our final dataset contains  $n = 193$  instances with  $d = 32$  features, including 13 *continuous* features (wheelbase, length, width, height, curb weight, engine size, bore, stroke, compression ratio, horsepower, peak rpm, city mpg, and highway mpg) and 19 *categorical* features, represented as dummy variables (fuel type, aspiration, number of doors, body style, drive wheels, engine location, engine type, and number of cylinders). Following the

literature, we use  $\log(\text{price})$  as the response. Notably, while previous studies often exclude categorical variables, we regress our response  $\log(\text{price})$  against all the available predictors—*continuous* and *categorical*—using our two-layer kernel ridge regression model. Details of the implementation can be found in Appendix C.

Figure 3 displays the 5-fold cross-validation error curve, where each point on the curve represents the averaged error across the folds, alongside the rank of the learned weight matrix  $U$  from our two-layer kernel ridge regression model on the full dataset, evaluated across a range of regularization parameters  $\lambda$ . Notably, Figure 3 demonstrates the *automatic* regularization inherent to our layered model, manifesting as exact low-rank structure in the first-layer weight matrices  $U$ . Notably, for this dataset larger values of  $\lambda$  yield lower ranks of  $U$ , reflecting the model’s increasing preference for parsimonious feature representations.

For model selection, we used the "one-standard-error" rule—choosing the most parsimonious model whose error is within one standard error of the minimum [51, Section 7.10]. This led to selecting  $\lambda = 0.05$ , where the rank of the bottom-layer weight matrix is 4, significantly lower than the ambient feature dimension of 32.

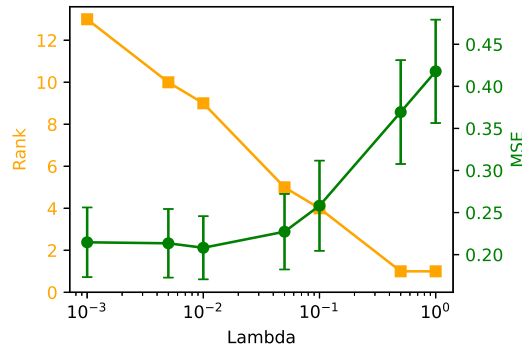


Fig 3: Cross-validation error (green curve) and rank of bottom-layer weight matrix  $U$  (orange curve) versus  $\lambda$ : sequence of  $\lambda$ 's are 0.001, 0.005, 0.01, 0.05, 0.1, 0.5, 1. The plot reveals the emergence of a low-rank phenomenon. Additionally, the standard error of the cross-validation error estimate is shown to facilitate model selection using the "one-standard-error" rule [51, Section 7.10].

Now we provide interpretations of the first two directions identified by our model, which correspond to the first two left singular subspaces of  $U$ . These directions are dominant, as evidenced by the singular values ( $\nu_1 = 0.634$ ,  $\nu_2 = 0.540$ ,  $\nu_3 = 0.086$ ,  $\nu_4 = 0.015$ ). We denote the first two left singular vectors of  $U$  by  $u_1$  and  $u_2$ . Figure 4 provides visualization of  $\log(Y)$  versus the first two singular vector projections. We note that  $\log(\text{price})$  versus  $u_1^T X$  reveals a strong linear relationship, while  $\log(Y)$  versus  $u_2^T X$  is more nonlinear, exhibiting a hyperbolic pattern with two distinct branches.

The first direction, based on the magnitude of components in  $u_1$ , is primarily determined by Horsepower with positive loading (0.563). This indicates that higher horsepower is a key factor in increasing car price.

The second direction is primarily driven by Curb Weight (-0.509), reflecting the vehicle’s overall mass, and significantly influenced by engine type dummy variables, notably OHCV (-0.365). To gain further insights on these dummy variables, we made the following observation: identifying data points associated with luxury manufacturers (Mercedes-Benz, BMW, Jaguar, and Porsche)—information known to us but not to the regression model—revealed

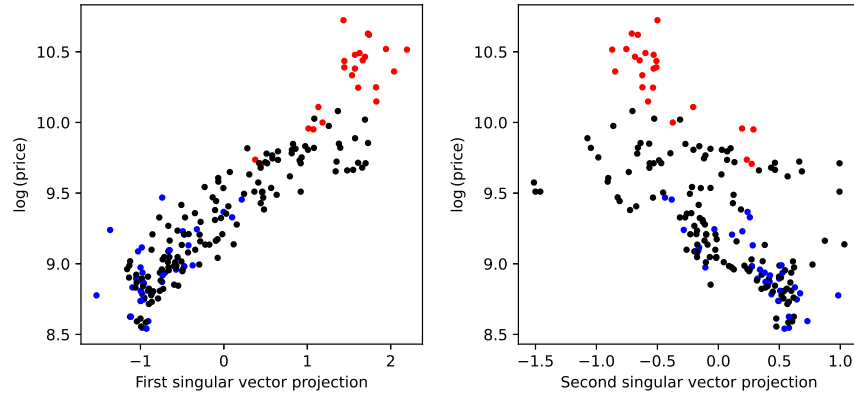


Fig 4: Plot of  $\log(y)$  versus  $x$  projected on top singular vectors of Automobile data. Red points represent luxury manufacturers (Mercedes-Benz, BMW, Jaguar, and Porsche) and blue points represent economy brands (Honda, Chevrolet, Plymouth, and Subaru). Black points are unclassified, as their manufacturer information is unavailable.

interesting patterns. Specifically, car price exhibits a negative association with the second direction  $u_2^T X$  within these luxury cars. A closer examination of the data indicates that OHCV engines appear exclusively in the subset of luxury cars, suggesting that the presence of OHCV engines contributes to higher car prices. Remarkably, this finding further aligns with domain knowledge, as OHCV engines are commonly featured in luxury cars due to their superior performance and smoother operation.

From a statistical perspective, the ability of our layered model to uncover interpretable categorical variables (such as OHCV), in agreement with external domain insights, underscores its capacity to detect interpretable latent structures within the data. Notably, these insights were absent in prior statistical analyses using the SIR, SAVE and Fourier methods [95], where categorical variables were excluded prior to the analysis, likely reflecting the strong reliance of these alternative methods on the continuity of the predictors [30, 22, 95].

**10.2. Illustration II: Digit Classification via SVHN Dataset.** The SVHN (Street View House Numbers) dataset is a real-world image dataset widely used for developing and evaluating machine learning models in digit classification tasks [68]. It consists of roughly 100,000 labeled digits taken from natural scene of house numbers captured by Google Street View. The goal of this classification is to accurately identify the digit located in the middle of each image, which often appears alongside neighboring digits and within complex backgrounds.

We evaluate the performance of various machine learning models—including our two-layer kernel learning model, traditional kernel methods, and two-layer neural network models—on the SVHN dataset, focusing on the binary classification task of distinguishing between closely related digits.

In the main text, we present results for the classification task involving digits 0 and 8 (similar results on classifying digits 5 and 6 are reported in the Appendix C). Example images from the dataset are shown in Figure 5. The training dataset for digits 0 and 8 contains  $n = 9993$  samples, and dimension  $d = 3 \times 1024$ , where 3 stands for the red, green and blue channels, and  $1024 = 32^2$  stands for the size of the image. The test dataset contains  $n_{\text{test}} = 3404$  samples, which are used to evaluate the performance of the models.

Given the objective of this task—extracting the central digit—eliminating irrelevant information aligns naturally with the structure of layered architectures. In the context of two-layer models, this can be achieved by promoting a low-rank weight matrix in the bottom layer,



Fig 5: Sample images of 8 and 0 from SVHN data.

which acts as a filter on the input image, projecting the data onto a lower-dimensional subspace, ideally isolating features concentrated around the mid-region—corresponding to the central digit—while suppressing peripheral background and neighboring digits at the corners. The second layer then leverages this refined representation to make the final prediction.

The primary goal of these experiments is to deepen our understanding and clarify the similarities and fundamental differences in representation and generalization shaped by different machine learning model architectures, including two-layer kernel ridge regression models, traditional kernel methods, and two-layer neural network models.

We wish to make several important remarks on the basis of our numerical findings in this regard. Details of the implementation can be found in Appendix C.

*10.2.1. The importance of feature learning.* We will first demonstrate the importance of feature learning through a comparison between our two-layer kernel ridge regression model and traditional kernel methods in terms of their performance.

For clarity, we recall the two equivalent formulations of our two-layer kernel ridge regression model (recall this equivalence has been established in Proposition 6):

$$\text{Two-Layer Kernel Ridge Regression : } \min_{F, \gamma, \Sigma \succeq 0} \frac{1}{2} \mathbb{E}[(Y - F(X) - \gamma)^2] + \frac{\lambda}{2} \|F\|_{\mathcal{H}_\Sigma}^2$$

$$\text{Two-Layer Kernel Ridge Regression : } \min_{f, \gamma, U} \frac{1}{2} \mathbb{E}[(Y - f(U^T X) - \gamma)^2] + \frac{\lambda}{2} \|F\|_{\mathcal{H}_I}^2$$

These formulations stand in contrast to the standard kernel ridge regression:

$$\text{Standard Kernel Ridge Regression : } \min_{F, \gamma, h \geq 0} \frac{1}{2} \mathbb{E}[(Y - F(X) - \gamma)^2] + \frac{\lambda}{2} \|F\|_{\mathcal{H}_{hI}}^2$$

In our experiments,  $\mathcal{H}_I$ ,  $\mathcal{H}_{hI}$ , and  $\mathcal{H}_\Sigma$  are all Gaussian RKHSs induced by Gaussian kernels. Here, the bandwidth parameter  $h \geq 0$  in  $\mathcal{H}_{hI}$  is also learned in standard kernel ridge regression. The key distinction is that the two-layer kernel ridge regression model learns additional data representations by optimizing the bottom-layer weight matrix  $U$  (or  $\Sigma$  in  $\mathcal{H}_\Sigma$ ), while the standard kernel ridge regression relies on a fixed kernel with only bandwidth selection.

Our empirical results reveal that the two-layer kernel ridge regression formulation achieves significantly improved predictive performance on the SVHN dataset compared to traditional kernel ridge regression. On the full dataset, the test error drops from 12.0% to 7.2%, a remarkable relative reduction of 40% = (12.0% - 7.2%)/12.0% achieved by the two-layer model. Notably, this proportional improvement remains consistent when the training data is subsampled (see Figure 7). For instance, with only 20% of the training dataset, the test error decreases from 20% to 11%, reflecting a similar relative 45% reduction.

This substantial improvement of the two-layer kernel ridge regression model over traditional kernel ridge regression in accuracy can only be attributed to the strength of the layered architecture, which enables the model to adapt effectively to the underlying data structure by *learning the kernel—or equivalently, by learning the data representation*.

To build further intuitions, we visualize the top three singular vectors of the *learned* matrix  $U$ , which correspond to the top three eigenvectors of  $\Sigma$ —the matrix that parameterizes the Gaussian kernel  $\exp(-\|x - x'\|_{\Sigma}^2)$  defining the RKHS  $\mathcal{H}_{\Sigma}$ . This visualization reveals that the learned top singular vectors capture interpretable patterns that highlight structural differences between digits 0 and 8 (see the first row in Figure 6 and caption for details).

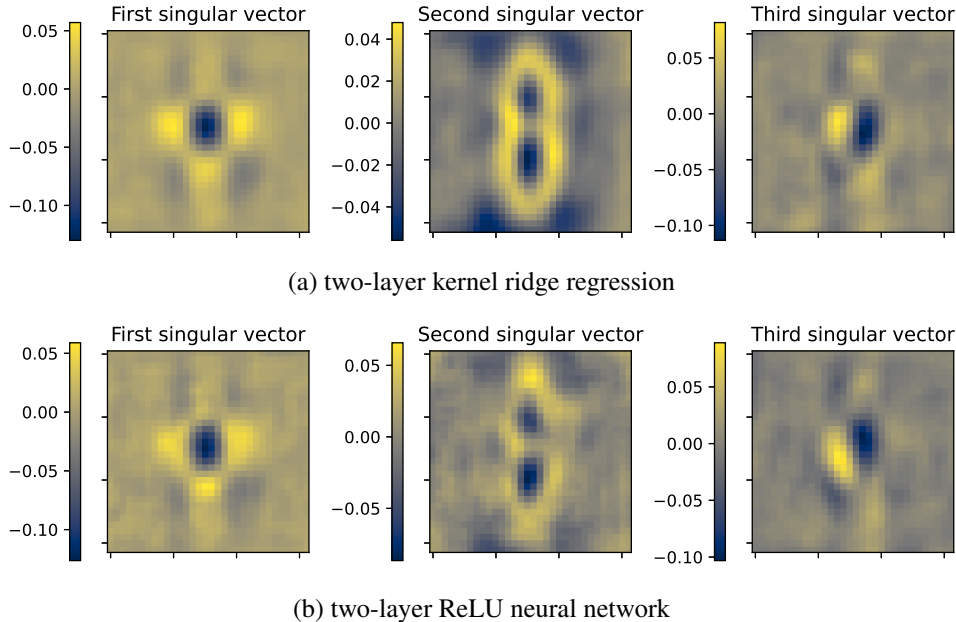


Fig 6: The first row displays the top three left singular vectors of  $U$  (or equivalently, top three eigenvectors of  $\Sigma$ ) of a top-performing two-layer kernel ridge regression model, which achieves a prediction accuracy of 92.83%. The second row shows the top three singular vectors of the bottom layer weight matrix from a top-performing two-layer ReLU neural network on SVHN data, with a prediction accuracy of 90.80%. Each vector technically has a dimension of  $3 \times 1024$  (where 3 stands for the red, green, and blue channels, and 1024 stands for the size of the image); for illustration, we only present the subvector of dimension 1024 that corresponds to the red channel. Both models seem to learn visually interpretable features.

Importantly, these top singular vectors largely influence how the *learned* kernel  $\exp(-\|x - x'\|_{\Sigma}^2)$  measures similarities between two images  $x$  and  $x'$ , highlighting linear combinations of pixels that are effective for distinguishing between digits 0 and 8. This learned representation refines the predictive performance of the kernel ridge regression model in classifications. By contrast, the isotropic Gaussian kernel  $\exp(-h\|x - x'\|_2^2)$ , which treats all pixels uniformly, fails to adapt to the varying importance of different image regions, making the model less effective for distinguishing between similar digits 0 and 8.

**10.2.2. The prevalence of low-rank structure in learned feature matrices.** We demonstrate the prevalence of low-rank structure in the learned feature matrices  $U$  and  $\Sigma$  and provide further empirical evidence that the two-layer kernel ridge regression model inherently favors parsimonious representations of the data.

We examine Figure 8, which plots the prediction accuracy curve against the rank of the learned bottom-layer weight matrix. Notably, the feature matrices  $U$  and  $\Sigma$  from the two-layer kernel ridge regression model consistently exhibits low-rank structures across a broad

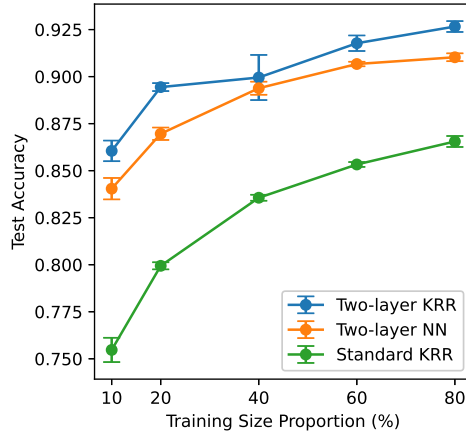


Fig 7: Prediction accuracy for classifying digits 0 and 8, measured on subsamples of the training dataset for Two-layer KRR, Two-layer NN, and Standard KRR. The training datasets are subsampled to different proportions: 10%, 20%, 40%, 60%, and 80%. Each subsampling proportion is repeated 5 times, and the average accuracy is reported with standard error bars.

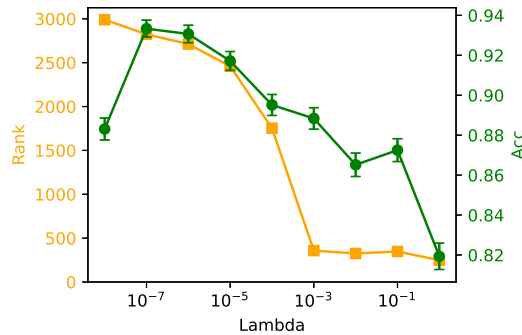


Fig 8: Prediction accuracy (green curve) and rank of bottom-layer weight matrix  $U$  (orange curve) from the two-layer kernel ridge regression model as functions of  $\lambda$ , with  $\lambda$  values taken from the set  $\{10^{-8}, 10^{-7}, 10^{-6}, 10^{-5}, 10^{-4}, 10^{-3}, 10^{-2}, 10^{-1}, 1\}$ .

range of  $\lambda$ . Notably, on this SVHN dataset, the rank of  $U$  and  $\Sigma$  often decrease as  $\lambda$  increases, suggesting the model’s inherent preference for increasingly parsimonious representations. Specifically, for  $\lambda$  values between  $10^{-7}$  to  $10^{-3}$ , the rank of the learned weight matrix drops from approximately 3000 to below 500, while the accuracy remains around 89%, which is above the accuracy by standard kernel ridge regression model.

To delve deeper, we extract the feature matrix  $U$  that attains the highest predictive performance from our model where  $\lambda = 10^{-7}$ , which nominally has a rank of approximately 2700. However, plotting its singular values reveals a very rapid decay in the singular spectrum, indicating that most of the information captured by the model’s feature weight matrix is concentrated in its top singular subspaces. Indeed, when we truncate the learned weight matrix  $U$  to retain only its top 5 singular vectors and then use this reduced-rank approximation of  $U$  as the bottom layer, retraining the second layer preserves over 90% of the original model’s predictive accuracy (Table 9). These results all indicate that the majority of the model’s performance is largely driven by a low-dimensional subspace of the features.

For comparison, we analyze both bottom layer weight matrices from the two-layer kernel ridge regression model and the two-layer ReLU network model that achieve the highest predictive performance. In the later case, the singular value decay is notably slower, leading to a substantially higher effective rank—measured as the ratio of the nuclear norm to the operator norm—than that of our model’s learned matrix  $U$  (see Figure 9 and the accompanying table). Specifically, this ratio (effective rank) is less than 8 for our model, whereas it exceeds 130 in the two-layer neural network. However, truncating the neural network’s bottom layer weight matrix to the top 5 singular vectors also retains over 90% of its predictive power. Importantly, this qualitative observation holds consistently across both top-performing and near-top models, indicating the robustness of our claims.

This suggests that while both layered models rely on low-dimensional subspaces for predictive performance, the two-layer kernel ridge regression model appears to achieve a more compact and efficient representation, as evidenced by the sharper decay of its singular values and lower effective rank.

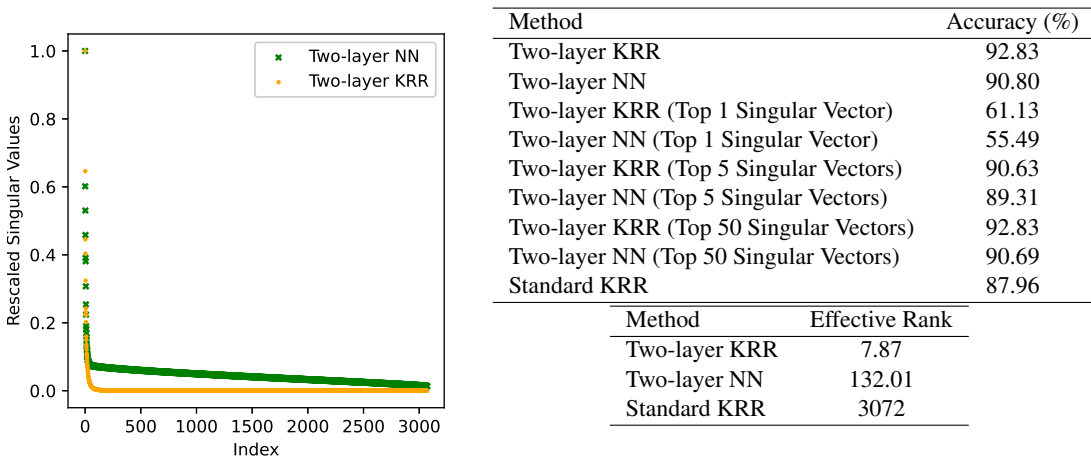


Fig 9: Our two-layer kernel ridge regression model displays similar prediction performance with more compressed feature representations: (a) singular values of the bottom layer weight matrices  $U$ , where orange dots correspond to our model and green crosses correspond to neural network model (b) prediction accuracy for different methods on SVHN dataset (c) effective rank (sum of singular values divided by the maximum singular value) for different methods on SVHN dataset.

Turning our findings into conclusions, results on the SVHN dataset highlight the significance of low-rank structures in feature learning. Our two-layer kernel ridge regression model produces a more compact and efficient representation of the data—evidenced by a much lower effective rank of bottom layer weight matrix  $U$ —than the two-layer ReLU neural network model. All these findings align nicely with the central theme of our paper: two-layer kernel ridge regression models can automatically perform dimension reduction in favorable situations—adapting to the data’s low-dimensional structure by filtering out irrelevant directions, preserving only the most discriminative features without external regularizations.

**11. Discussions.** We would like to close this paper by offering a few comments about the results obtained in this paper and by discussing the possibility of generalizations and extensions.

11.1. *Computations.* In the machine learning literature, training layered models is well-recognized as a computationally and memory-intensive task; this challenge is also evident in the two-layer kernel ridge regression model studied in this paper, where the number of parameters in  $U$  and  $\Sigma$  is at least  $d^2$ . Our main findings on the low-rank nature of the global minimizer suggest that the Burer-Monteiro low-rank matrix factorization technique provides a computationally and memory-efficient solution to this challenge [17], while not sacrificing statistical efficiency. More precisely, this technique can reduce the number of training parameters from  $d^2$  to  $dr$  where  $r = \dim(S_*)$  represents the dimension of the central mean subspace, and our findings show that this approach can provably retain statistical efficiency while having the potential to significantly alleviate computational burdens.

Another promising direction for addressing the computational challenges in our two-layer kernel ridge regression model involves leveraging the random feature model [72]. This approach approximates the kernel function by mapping the input data into a randomized low-dimensional feature space, thereby reducing the computational complexity associated with kernel matrix operations. Specifically, it has the potential to lower the dependence of computational complexity on the sample size from quadratic in  $n$  to linear in  $n$ .

We hope to provide a systematic exploration of these ideas in a follow-up paper.

11.2. *Global Landscape Characterizations.* While the primary objective of this paper is to characterize the statistical properties and low-rank nature of the global minimizer pertaining to the empirical objective  $J_n$ , comprehensive numerical experiments suggest for a wide range of distributions for  $X$ , the application of gradient descent on  $J_n$  frequently results in matrices possessing exactly low rank. Since gradient descent’s convergence to global minimizers is not always guaranteed, our findings suggest that statistical and low-rank properties might extend to local minimizers as well.

That being said, we hope to refine our statistical analysis to gain a deeper understanding of the local minimizers for the kernel learning objective. Achieving this understanding requires characterizations beyond the local landscape around the global minimizers, which could, in turn, lead to rigorous statistical guarantees for gradient-based optimization methods. At a fundamental level, the challenge lies in characterizing the global landscape (including landscape around the local minimum and stationary points) of the population objective, particularly in understanding how the objective depends on the bottom-layer weight matrix.

We have recently made significant progress in this direction and will hopefully present our results in a follow-up paper.

11.3. *Feature Learning in High Dimensional Asymptotics Regime.* This paper initiates the study of feature learning in two-layer kernel ridge regression objectives, presenting basic results that hold at the population level and within an asymptotic framework.

Building on this foundation, an interesting direction for future work is to extend the analysis to high-dimensional asymptotics regime, exploring the statistical properties of the minimizers when both  $n$  and the feature dimensionality  $p$  diverge proportionally. This regime has attracted significant theoretical interest in the two-layer neural network literature, particularly in understanding how gradient steps enhance feature learning and influence the alignment of the bottom-layer weight matrix with the central mean subspace, e.g., [7, 26, 6]. Fully characterizing the statistical properties of minimizers in this regime for the two-layer kernel ridge regression objective appears outstandingly challenging, but analyzing a few gradient descent steps can offer a promising starting point. We anticipate that such an analysis may reveal similar convergence rates to those documented in two-layer neural network literature.

**12. Acknowledgements.** The authors would like to thank X.Y. Han for enriching discussions on the experiments. Feng Ruan would like to thank Lijun Ding for his insightful comments on the initial draft, as well as to Basil Saeed, Lanqiu Yao, and Yuan Yao for their helpful discussions on the presentation.

## APPENDIX A: ADDITIONAL PROOFS

**A.1. Proof of Lemma 3.4.** Recall  $\epsilon_0(S) = \mathbb{E}[\text{Var}(Y|\Pi_S X)] - \mathbb{E}[\text{Var}(Y|X)]$ . Using the bias-variance decomposition, we get

$$\epsilon_0(S) = \mathbb{E}[(\mathbb{E}[Y|\Pi_S X] - \mathbb{E}[Y|X])^2] \geq 0$$

Since by definition  $S_*$  is the *minimal* dimension reduction subspace,  $\epsilon_0(S) > 0$  for every subspace  $S$  with  $\dim(S) < \dim(S_*)$ . To prove Lemma 3.4, we show:

$$(A.1) \quad \inf\{\epsilon_0(S) \mid \dim(S) < \dim(S_*)\} > 0.$$

The proof of (A.1) proceeds by contradiction, using a standard compactness argument.

Assume, for the sake of contradiction, that the infimum in (A.1) is zero. Then there exists a sequence of subspaces  $S_n$  such that  $\epsilon_0(S_n)$  converges to 0 with  $\dim(S_n) < \dim(S_*)$ .

First, the set of orthogonal projection matrices in  $\mathbb{R}^{d \times d}$  with rank bounded by a given  $k \in \mathbb{N}$  is compact. Specifically, the set

$$\left\{ \Pi \in \mathbb{R}^{d \times d} : \Pi = \Pi^T, \Pi^2 = \Pi, \text{tr}(\Pi) \leq k \right\}$$

is compact for every integer  $k \leq d$ . Thus, for the sequence of subspace  $S_n$  with  $\dim(S_n) < \dim(S_*)$ , we can, by taking a subsequence if necessary, assume that  $\Pi_{S_n} \rightarrow \Pi_{S_\infty}$  holds for some subspace  $S_\infty$  where  $\dim(S_\infty) < \dim(S_*)$ .

Next, define for every  $n < \infty$

$$\phi_n(X) = \mathbb{E}[Y|\Pi_{S_n} X] - \mathbb{E}[Y|X].$$

The sequence  $\{\phi_n\}_{n \in \mathbb{N}}$  is uniformly bounded in  $\mathcal{L}_2(\mathbb{P})$ . By the Banach-Alaoglu theorem, the unit ball in  $\mathcal{L}_2(\mathbb{P})$  is weak-\* sequentially compact, so, by taking a subsequence if necessary, we may assume that  $\phi_n$  converges to some  $\phi_\infty$  in  $\mathcal{L}_2(\mathbb{P})$  under the weak-\* topology. This means that  $\lim_n \mathbb{E}[\phi_n(X)h(X)] = \mathbb{E}[\phi_\infty(X)h(X)]$  holds for every  $h \in \mathcal{L}_2(\mathbb{P})$ .

We will show that: (a)  $\phi_\infty(X) = \mathbb{E}[Y|\Pi_{S_\infty} X] - \mathbb{E}[Y|X]$ , and (b)  $\mathbb{E}[\phi_\infty^2(X)] = 0$ .

To prove (a), let's denote  $\gamma_n(X) = \mathbb{E}[Y|\Pi_{S_n} X]$ . For any continuous and uniformly bounded function  $h : \mathbb{R}^d \rightarrow \mathbb{R}$ , we have  $\mathbb{E}[(Y - \gamma_n(X))h(\Pi_{S_n} X)] = 0$ . Let  $\gamma_\infty$  be an accumulation point of  $\gamma_n$  in  $\mathcal{L}_2(\mathbb{P})$  under the weak-\* topology. Since  $\gamma_n$  is uniformly bounded in  $\mathcal{L}_2(\mathbb{P})$ , and  $h(\Pi_{S_n} X)$  converge to  $h(\Pi_{S_\infty} X)$  in  $\mathcal{L}_2(\mathbb{P})$  under the norm topology in  $\mathcal{L}_2(\mathbb{P})$  for every such function  $h$ , we obtain that

$$(A.2) \quad \mathbb{E}[(Y - \gamma_\infty(X))h(\Pi_{S_\infty} X)] = \lim_n \mathbb{E}[(Y - \gamma_n(X))h(\Pi_{S_n} X)] = 0$$

holds for every continuous and uniformly bounded function  $h : \mathbb{R}^d \rightarrow \mathbb{R}$ . This orthogonality to every such function  $h$  implies that  $\gamma_\infty(X) = \mathbb{E}[Y|\Pi_{S_\infty} X]$  in  $\mathcal{L}_2(\mathbb{P})$ . Hence, any accumulation point  $\gamma_\infty$  of  $\gamma_n$  under the weak-\* topology must obey  $\gamma_\infty(X) = \mathbb{E}[Y|\Pi_{S_\infty} X]$ . Claim (a) then follows.

To prove (b), note by our assumption,  $\lim_n \mathbb{E}[\phi_n^2(X)] = \lim_n \epsilon_0(S_n) = 0$ . By Cauchy-Schwartz inequality, we deduce the limit  $\lim_n \mathbb{E}[\phi_n(X)\phi_\infty(X)] = 0$ . This further implies  $\mathbb{E}[\phi_\infty^2(X)] = 0$  since  $\phi_n$  converges to  $\phi_\infty$  under the weak-\* topology in  $\mathcal{L}_2(\mathbb{P})$ .

Now we have shown that  $\epsilon_0(S_\infty) = \mathbb{E}[\phi_\infty(X)^2] = 0$  even though  $\dim(S_\infty) < \dim(S_*)$ . This contradicts the definition of the central mean subspace  $S_*$  being the *minimal* dimension reduction subspace! As a result, the infimum in (A.1) must be thereby strictly positive, and Lemma 3.4 is proved.

**A.2. Proof of Lemma 5.1.** We give details on the proof of the first part of the lemma:

$$\sup_{U \in \mathcal{U}} \|\mathbf{C}_{U; \mathbb{P}_n} - \mathbf{C}_{U; \mathbb{P}}\|_{\text{op}} = o_P(1).$$

Note the second part follows by applying the same argument. We write  $Q_n(U) = \|\mathbf{C}_{U; \mathbb{P}_n} - \mathbf{C}_{U; \mathbb{P}}\|_{\text{op}}$ .

We note uniform convergence in probability holds if (see, e.g., [69, Corollary 2.2])

(i) Pointwise convergence: For each  $U \in \mathcal{U}$ , as  $n \rightarrow \infty$ ,

$$Q_n(U) = \|\mathbf{C}_{U; \mathbb{P}_n} - \mathbf{C}_{U; \mathbb{P}}\|_{\text{op}} = o_P(1).$$

(ii) Uniform Lipschitz condition: There exists a sequence of random variables  $B_n = O_P(1)$  such that for all  $U, U' \in \mathcal{U}$ :

$$|Q_n(U) - Q_n(U')| \leq B_n \times \|U - U'\|_{\text{op}}.$$

The pointwise convergence follows from the literature, e.g., [40, Lemma 5]. Thus, it remains to verify that the random map  $U \mapsto Q_n(U)$  satisfies the uniform Lipschitz condition. Below, we will prove the explicit estimate that holds for all  $U, U'$ :

$$(A.3) \quad |Q_n(U) - Q_n(U')| \leq B_n \times \|U - U'\|_{\text{op}} \\ \text{where } B_n = \sqrt{8\phi(0)|\phi'_+(0)|} \cdot (\sqrt{\mathbb{E}_P[\|X\|_2^2]} + \sqrt{\mathbb{E}_{P_n}[\|X\|_2^2]}).$$

This estimate implies the uniform Lipschitz condition since  $B_n = O_P(1)$  as  $\mathbb{E}_P[\|X\|_2^2] < \infty$ .

To prove the estimate (A.3), we note by the triangle inequality:

$$(A.4) \quad |Q_n(U) - Q_n(U')| \leq \|\mathbf{C}_{U; \mathbb{P}_n} - \mathbf{C}_{U'; \mathbb{P}_n}\|_{\text{op}} + \|\mathbf{C}_{U; \mathbb{P}} - \mathbf{C}_{U'; \mathbb{P}}\|_{\text{op}}$$

Let  $\mathbb{Q}$  be a probability measure (later we will consider  $\mathbb{Q} = \mathbb{P}$  and  $\mathbb{Q} = \mathbb{P}_n$ ). Let  $\mathbb{B}$  denote the unit ball in  $\mathcal{H}_q$ , i.e.,  $\mathbb{B} = \{h : \|h\|_{\mathcal{H}_q} \leq 1\}$ . We note that

$$(A.5) \quad \|\mathbf{C}_{U; \mathbb{Q}} - \mathbf{C}_{U'; \mathbb{Q}}\|_{\text{op}} \\ = \sup_{h_1, h_2 \in \mathbb{B}} |\langle h_1, (\mathbf{C}_{U; \mathbb{Q}} - \mathbf{C}_{U'; \mathbb{Q}})h_2 \rangle| \\ = \sup_{h_1, h_2 \in \mathbb{B}} |\text{Cov}_{\mathbb{Q}}(h_1(U^T X), h_2(U^T X)) - \text{Cov}_{\mathbb{Q}}(h_1((U')^T X), h_2((U')^T X))|$$

The functions  $h$  in  $\mathbb{B}$  are uniformly Lipschitz. To show this, consider any  $h \in \mathbb{B}$ , and  $w_1, w_2 \in \mathbb{R}^q$ . By the reproducing property of the kernel and the Cauchy-Schwarz inequality, we have:

$$|h(w_1) - h(w_2)| = |\langle h, k_q(w_1, \cdot) - k_q(w_2, \cdot) \rangle_{\mathcal{H}_q}| \leq \|h\|_{\mathcal{H}_q} \cdot \|k_q(w_1, \cdot) - k_q(w_2, \cdot)\|_{\mathcal{H}_q}$$

The first term  $\|h\|_{\mathcal{H}_q} \leq 1$  for  $h \in \mathbb{B}$ . The second term obeys

$$\|k_q(w_1, \cdot) - k_q(w_2, \cdot)\|_{\mathcal{H}_q}^2 = 2(\phi(0) - \phi(\|w_1 - w_2\|_2^2)) \leq 2|\phi'_+(0)| \cdot \|w_1 - w_2\|_2^2,$$

by the reproducing property and Taylor's intermediate theorem. Therefore,

$$|h(w_1) - h(w_2)| \leq c_1 \|w_1 - w_2\|, \quad c_1 = \sqrt{2|\phi'_+(0)|}.$$

Additionally, the functions  $h$  in  $\mathbb{B}$  are uniformly bounded in  $L_\infty(\mathbb{R}^q)$  since

$$\|h\|_{L_\infty(\mathbb{R}^q)} = \sup_w |\langle h, k_q(w, \cdot) \rangle| \leq \|h\|_{\mathcal{H}_q} \sup_w \|k_q(w, \cdot)\|_{\mathcal{H}_q} \leq c_2, \quad c_2 = \sqrt{\phi(0)}.$$

We now use the uniform boundedness and Lipschitz property of  $h$  in  $\mathbb{B}$  to upper bound the RHS of (A.5). For every  $h_1, h_2 \in \mathbb{B}$ , we see the decomposition:

$$\begin{aligned} & \text{Cov}_{\mathbb{Q}}(h_1(U^T X), h_2(U^T X)) - \text{Cov}_{\mathbb{Q}}(h_1((U')^T X), h_2((U')^T X)) \\ &= \text{Cov}_{\mathbb{Q}}(h_1(U^T X) - h_1((U')^T X), h_2(U^T X)) + \text{Cov}_{\mathbb{Q}}(h_1((U')^T X), h_2(U^T X) - h_2((U')^T X)) \end{aligned}$$

Given  $h_1, h_2 \in \mathbb{B}$ , the first term on the RHS is bounded by

$$\begin{aligned} \text{Cov}_{\mathbb{Q}}(h_1(U^T X) - h_1((U')^T X), h_2(U^T X)) &\leq \sqrt{\mathbb{E}_{\mathbb{Q}}[(h_1(U^T X) - h_1((U')^T X))^2] \times \mathbb{E}_{\mathbb{Q}}[h_2^2(U^T X)]} \\ &\leq \sqrt{2|\phi'_+(0)|\mathbb{E}_{\mathbb{Q}}[\|U^T X - (U')^T X\|_2^2] \times \phi(0)} \\ &\leq \sqrt{2|\phi'_+(0)|\phi(0)} \cdot \|U - U'\|_{\text{op}} \cdot \sqrt{\mathbb{E}_{\mathbb{Q}}[\|X\|_2^2]}. \end{aligned}$$

Note the same bound holds for the second term. Following (A.5), it leads to the estimate

$$(A.6) \quad \|C_{U;\mathbb{Q}} - C_{U';\mathbb{Q}}\|_{\text{op}} \leq \sqrt{8|\phi'_+(0)|\phi(0)} \cdot \|U - U'\|_{\text{op}} \cdot \sqrt{\mathbb{E}_{\mathbb{Q}}[\|X\|_2^2]}.$$

Applying this to  $\mathbb{Q} = \mathbb{P}$  and  $\mathbb{Q} = \mathbb{P}_n$  yields the desired estimate (A.3), completing the proof.

## APPENDIX B: ADDITIONAL RESULTS ON SYNTHETIC EXPERIMENTS

In this section, we document additional numerical evidence from the synthetic experiments that support the claims (ii)–(v) we made in the main text.

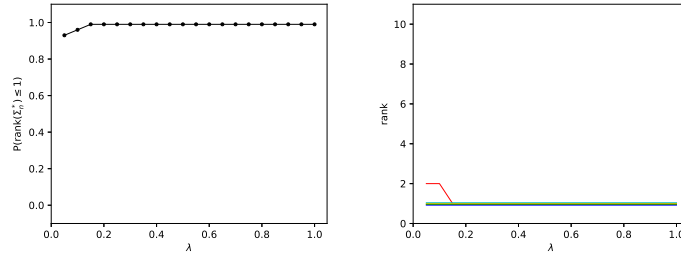
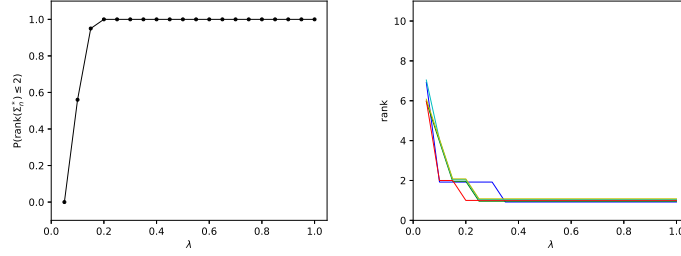
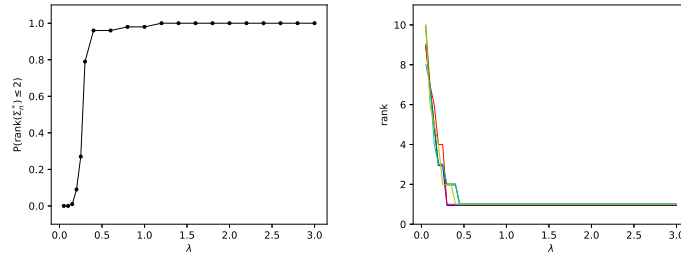
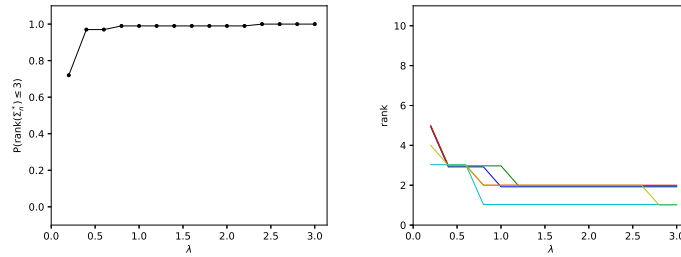
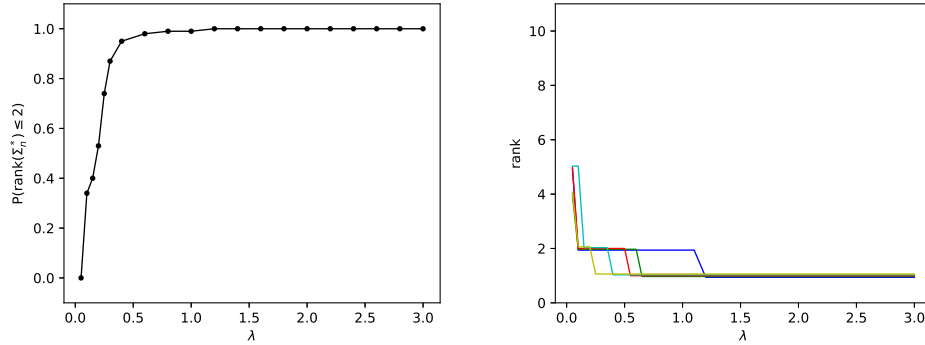
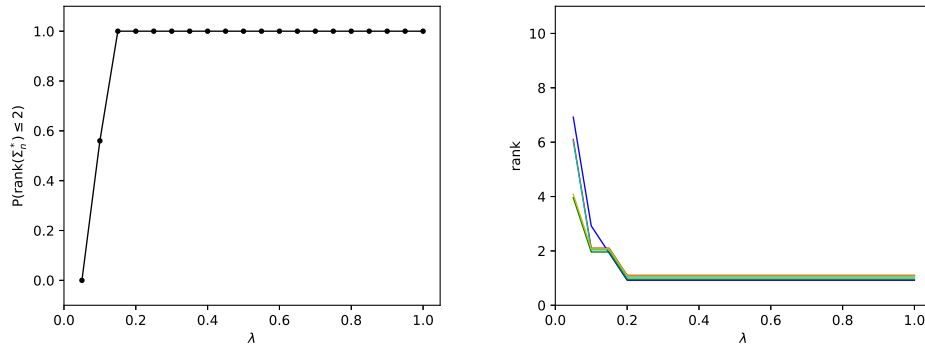
(a)  $f(x) = x_1 + x_2 + x_3$ .(b)  $f(x) = x_1 x_2$ .(c)  $f(x) = 0.1(x_1 + x_2 + x_3)^3 + \tanh(x_1 + x_3 + x_5)$ .(d)  $f(x) = 2(x_1 + x_2) + (x_2 + x_3)^2 + (x_4 - 0.5)^3$ .

Fig 10: Plots for Claim (ii). Here, we use Gaussian kernel  $k_{\Sigma}(x, x') = \exp\{-\|x - x'\|_{\Sigma}^2\}$ . Experimental setting: the covariate  $X \sim \mathcal{N}(0, K)$ , with  $K_{i,j} = 0.5^{|i-j|}$  and the response follows  $Y = f(X) + \mathcal{N}(0, \sigma^2)$  where  $\sigma = 0.1$ . Here, we set  $n = 300$  and  $d = 50$ . For each row, the left panel shows the empirical probability of  $\text{rank}(\Sigma_n^*) \leq \dim(S_*)$  over 100 repeated experiments for different  $\lambda$  values. The right panel displays how the rank of the solution  $\Sigma_n^*$  changes with different  $\lambda$  values, using 5 example pairs of  $(X, y)$ .



(a) Discrete  $X$ ,  $f(x) = 0.1(x_1 + x_2 + x_3)^3 + \tanh(x_1 + x_3 + x_5)$ .



(b) Continuous  $X$ ,  $f(x) = 0.1(x_1 + x_2 + x_3)^3 + \tanh(x_1 + x_3 + x_5)$ .

Fig 11: Plots for Claim (iii). Here, we use Gaussian kernel  $k_{\Sigma}(x, x') = \exp\{-\|x - x'\|_{\Sigma}^2\}$ . Experimental setting: the covariate  $X$  has independent coordinates  $X_i$ , with each  $X_i$  obeying  $\mathbb{P}(X_i = 1) = \mathbb{P}(X_i = 0) = 0.5$  in the discrete setting, and being uniform on  $[0, 1]$  in the continuous setting, and the response follows  $Y = f(X) + \mathcal{N}(0, \sigma^2)$  where  $\sigma = 0.1$ . Here, we set  $n = 300$  and  $d = 50$ .

For each row, the left panel shows the empirical probability of  $\text{rank}(\Sigma_n^*) \leq \dim(S_*)$  over 100 repeated experiments for different  $\lambda$  values. The right panel displays how the rank of the solution  $\Sigma_n^*$  changes with different  $\lambda$  values, using 5 example pairs of  $(X, y)$ .

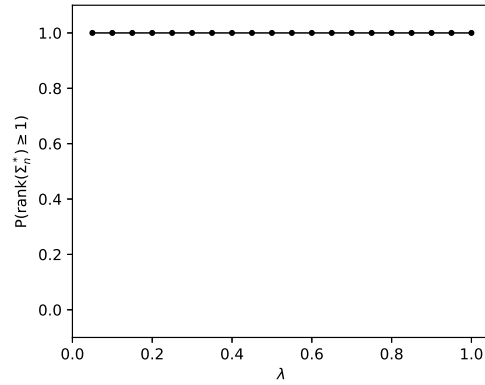


Fig 12: Plot for Claim (iv). Here, we use Gaussian kernel  $k_{\Sigma}(x, x') = \exp\{-\|x - x'\|_{\Sigma}^2\}$ . In this experiment,  $\text{Var}(\mathbb{E}[Y|X]) = 0$  where  $X \sim \mathcal{N}(0, I)$ , and  $Y = \epsilon$ , where  $\epsilon \sim \mathcal{N}(0, \sigma^2)$  is independent of  $X$  with  $\sigma = 0.1$ . Here, we choose  $n = 300$  and  $d = 50$ . The solution is always full rank:  $\text{rank}(\Sigma_n^*) = 50$  for every  $\lambda > 0$  in the 100 repeated experiments.

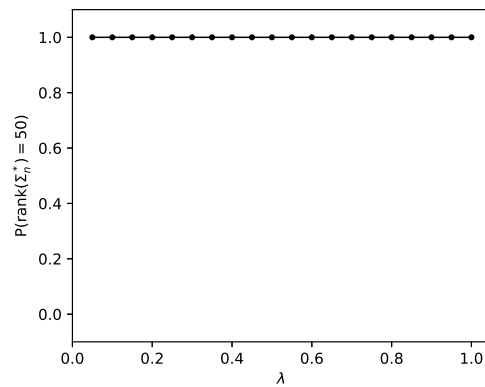


Fig 13: Plot for Claim (v). In this experiment, we use the linear kernel  $k_{\Sigma}(x, x') = x^T \Sigma x'$ . We sample  $X \sim \mathcal{N}(0, I)$  and  $Y = X_1 + X_2 + X_3 + \epsilon$ , where  $\epsilon \sim \mathcal{N}(0, \sigma^2)$  with  $\sigma = 0.1$ . Here, we set  $n = 300$  and  $d = 50$ . The solution is always full rank:  $\text{rank}(\Sigma_n^*) = 50$  for every  $\lambda > 0$  in the 100 repeated experiments.

## APPENDIX C: ADDITIONAL RESULTS FROM REAL DATA EXPERIMENTS

**C.1. Automobile dataset.** We train the two-layer kernel ridge regression model with Gaussian kernel on the Automobile dataset. Our training starts with a 5-fold cross-validation over a range of regularization parameters  $\lambda$ , and we document the mean rank of the solution matrix and cross-validation error with standard error bar in Figure 3. From the same Figure 3, we see that  $\lambda = 0.01$  achieves the smallest cross-validation error.

The tuning parameter  $\lambda$  is subsequently selected using the "one-standard-error" rule. In our case, following Figure 3, we choose  $\lambda = 0.1$  as it yields the most parsimonious model while staying within one standard error of the minimum cross-validation error.

To fix the model, we then train the two-layer KRR with Gaussian kernel using  $\lambda = 0.1$  on the *whole dataset* for full batch projected gradient descent until convergence. The algorithm is initialized as a diagonal matrix with diagonal values  $1/d$ , where  $d = 32$ , while the stepsize for the projected gradient descent is set to be 0.1. This yields a solution matrix  $\Sigma_n^*$  of rank 4.

In Figure 4, we do SVD decomposition of  $\Sigma_n^*$  and project the samples on the singular vectors  $u_1, u_2, u_3, u_4$  corresponding to the 4 non-zero singular values  $\nu_1 = 0.587, \nu_2 = 0.468, \nu_3 = 0.086, \nu_4 = 0.015$ . For documentation, the singular vectors are:

$$\begin{aligned}
u_1 &= 0.236x_1 - 0.281x_2 + 0.280x_3 - 0.060x_4 + 0.150x_5 - 0.181x_6 - 0.003x_7 - 0.275x_8 \\
&\quad + 0.194x_9 + 0.561x_{10} - 0.090x_{11} - 0.240x_{12} + 0.124x_{13} + 0.027x_{14} + 0.019x_{15} + 0.037x_{16} \\
&\quad - 0.097x_{17} - 0.204x_{18} - 0.105x_{19} - 0.075x_{20} - 0.120x_{21} + 0.033x_{22} + 0.040x_{23} - 0.091x_{24} \\
&\quad - 0.051x_{25} - 0.219x_{26} - 0.171x_{27} - 0.014x_{28} - 0.171x_{29} + 0.010x_{30} + 0.038x_{31} - 0.118x_{32} \\
u_2 &= 0.056x_1 - 0.108x_2 + 0.036x_3 - 0.053x_4 - 0.509x_5 + 0.358x_6 - 0.216x_7 - 0.172x_8 \\
&\quad - 0.171x_9 - 0.136x_{10} - 0.036x_{11} - 0.047x_{12} + 0.104x_{13} - 0.155x_{14} + 0.033x_{15} + 0.020x_{16} \\
&\quad + 0.041x_{17} + 0.062x_{18} + 0.129x_{19} + 0.161x_{20} - 0.135x_{21} + 0.071x_{22} - 0.054x_{23} - 0.042x_{24} \\
&\quad - 0.347x_{25} - 0.179x_{26} - 0.365x_{27} - 0.059x_{28} - 0.155x_{29} - 0.172x_{30} - 0.108x_{31} - 0.023x_{32} \\
u_3 &= -0.083x_1 - 0.078x_2 + 0.001x_3 + 0.017x_4 + 0.212x_5 + 0.369x_6 + 0.125x_7 - 0.209x_8 \\
&\quad + 0.354x_9 - 0.418x_{10} + 0.149x_{11} - 0.275x_{12} + 0.187x_{13} + 0.313x_{14} + 0.043x_{15} + 0.022x_{16} \\
&\quad - 0.026x_{17} - 0.029x_{18} + 0.035x_{19} - 0.058x_{20} + 0.042x_{21} - 0.035x_{22} + 0.044x_{23} + 0.149x_{24} \\
&\quad - 0.056x_{25} - 0.212x_{26} + 0.044x_{27} + 0.204x_{28} - 0.125x_{29} + 0.260x_{30} - 0.059x_{31} - 0.038x_{32} \\
u_4 &= 0.053x_1 - 0.055x_2 + 0.097x_3 + 0.060x_4 + 0.391x_5 + 0.126x_6 + 0.023x_7 - 0.063x_8 \\
&\quad - 0.400x_9 - 0.286x_{10} + 0.127x_{11} - 0.098x_{12} + 0.097x_{13} - 0.357x_{14} + 0.000x_{15} + 0.012x_{16} \\
&\quad - 0.060x_{17} - 0.207x_{18} - 0.178x_{19} - 0.238x_{20} + 0.054x_{21} + 0.099x_{22} + 0.089x_{23} + 0.024x_{24} \\
&\quad + 0.239x_{25} + 0.107x_{26} - 0.184x_{27} - 0.158x_{28} - 0.273x_{29} - 0.203x_{30} + 0.015x_{31} + 0.062x_{32}
\end{aligned}$$

where  $x_i$  ( $i = 1, \dots, 32$ ) represents: wheelbase, length, width, height, curb weight, engine size, bore, stroke, compression ratio, horsepower, peak RPM, city MPG, highway MPG, fuel type (gas), aspiration (turbo), number of doors (two), body style (hardtop), body style (hatchback), body style (sedan), body style (wagon), drive wheels (FWD), drive wheels (RWD), engine location (rear), engine type (L), engine type (OHC), engine type (OHCF), engine type (OHCV), number of cylinders (five), number of cylinders (four), number of cylinders (six), number of cylinders (three), number of cylinders (twelve), respectively. And the singular vectors corresponding to top 3 to top 5 singular vectors are shown in Figure 14.

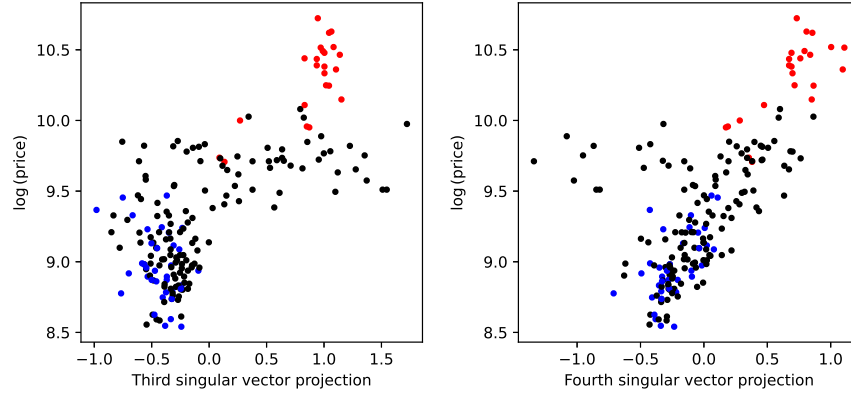


Fig 14: Plot of  $\log(y)$  versus  $x$  projected on top singular vectors of Automobile data. Red points represent luxury manufacturers (Mercedes-Benz, BMW, Jaguar, and Porsche) and blue points represent economy brands (Honda, Chevrolet, Plymouth, and Subaru). Black points are unclassified, as their manufacturer information is unavailable.

## C.2. SVHN dataset.

C.2.1. *Methodology.* We train three different models on digit classifications and use 5-fold cross validation to select the tuning parameters. We then measure the selected model’s performance on the independent test data in the SVHN dataset.

The details of the hyperparameter tuning and training process are documented as follows.

- (Standard Kernel Ridge Regression) We select the Gaussian kernel and tune the kernel bandwidth  $h$  from  $\{2^{-19}\tau, 2^{-18}\tau, \dots, 2^{19}\tau, 2^{20}\tau\}$  where  $\tau$  is defined as the inverse of the square of the median of the  $\ell_2$  distances between the training data points.
- (Two-Layer ReLU Neural Network) We use the ReLU activation function and set the number of neurons to be twice the input dimensionality:  $N_{\text{neurons}} = 6144$ . We tune the regularization parameter  $\lambda$  from  $\{10^{-8}, 10^{-7}, 10^{-6}, 10^{-5}, 10^{-4}, 10^{-3}, 10^{-2}, 10^{-1}, 1\}$ , with the learning rate (stepsize of the gradient method)  $\alpha$  from the set  $\{0.05, 0.1, 0.5, 1\}$ .
- (Two-Layer Kernel Ridge Regression) We select the Gaussian kernel. We tune the regularization parameter  $\lambda$  from  $\{10^{-8}, 10^{-7}, 10^{-6}, 10^{-5}, 10^{-4}, 10^{-3}, 10^{-2}, 10^{-1}, 1\}$ , with the learning rate (stepsize of the projected gradient method)  $\alpha$  from the set  $\{0.05, 0.1, 0.5, 1\}$ .

Notably, we try to keep the hyperparameter tuning for the Two-Layer ReLU Neural Network and the Two-Layer Kernel Ridge Regression fair, as both ridge regularization parameter  $\lambda$  and stepsize  $\alpha$  are selected from the same parameter sets.

C.2.2. *Details of the Main Results in the Main Text.* We document the details behind all the figures shown in the main text.

- In Figure 6, we plot the first three singular vectors of the top-performing models from the trained two-layer kernel ridge regression model and the two-layer neural network model.

Notably, each singular vector technically has a dimension  $3 \times 1024$ . In Figure 6, we plot the subvector of dimension 1024 that corresponds to the red channel. For completeness, Figure 15 presents the results for the green and blue channels. Interestingly, we observe that the subvectors across the three channels are remarkably similar.

- In Figure 7, we subsample our training datasets, and report the prediction accuracies of different methods—two layer kernel ridge regression, standard kernel ridge regression,

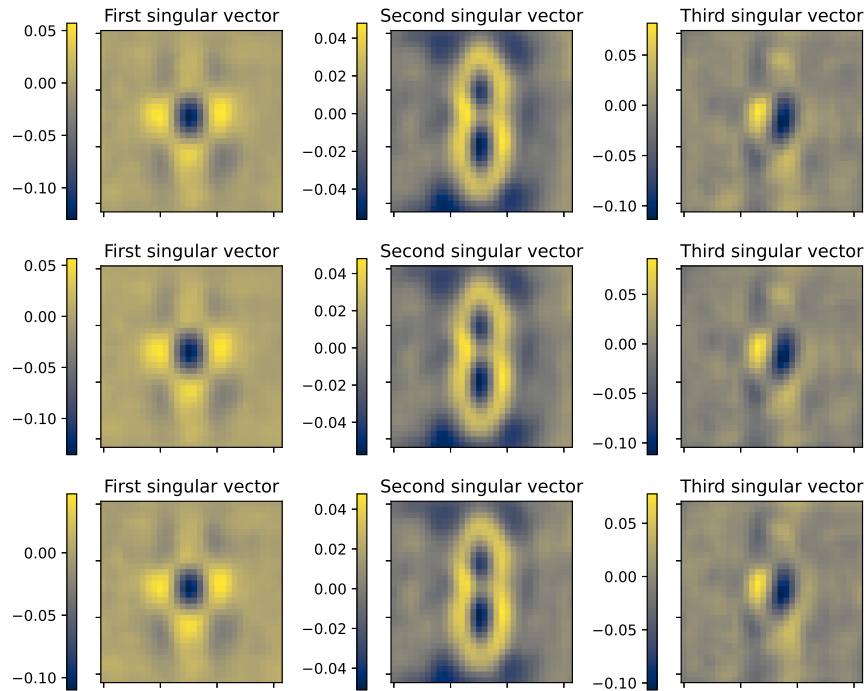
two-layer ReLU Neural Network—on these subsampled datasets. The subsamples take proportions 10%, 20%, 40%, 60%, 80% of the original training datasets. Each subsampling proportion is repeated 5 times, and we report the mean and the standard error of the prediction accuracy on these subsampled datasets.

- In Figure 8, we record the performance of our model over a range of regularization parameter  $\lambda$  from  $\{10^{-8}, 10^{-7}, 10^{-6}, 10^{-5}, 10^{-4}, 10^{-3}, 10^{-2}, 10^{-1}, 1\}$ . For each  $\lambda$ , we tune the stepsize  $\alpha$  from the set  $\{0.05, 0.1, 0.5, 1\}$ , and report the model with the best prediction accuracy. Specifically, for each  $\lambda$ , we document the rank of the bottom layer weight matrix of the selected model, as well as its prediction accuracy, including standard error bars.
- In Figure 9(a), we plot the singular values of the trained two-layer kernel ridge regression model and the two-layer neural network model that achieves the minimum prediction error. We rescale the singular values so that the top singular values are always fixed to be 1. In Figure 9(b), we first document the minimum prediction error achieved by the three different models, namely, two-layer kernel ridge regression models, two-layer ReLU neural networks, and the standard kernel ridge regressions. Additionally, for both the two-layer KRR and two-layer NN models, we truncate the learned bottom-layer weight matrices  $U$  to retain only their top  $k$  singular vectors, where  $k \in \{1, 5, 50\}$ , resulting in  $U_k$ . We then fix  $U_k$  as the bottom layer and retrain the second layer for both two-layer KRR model and NN models and report the prediction accuracies.

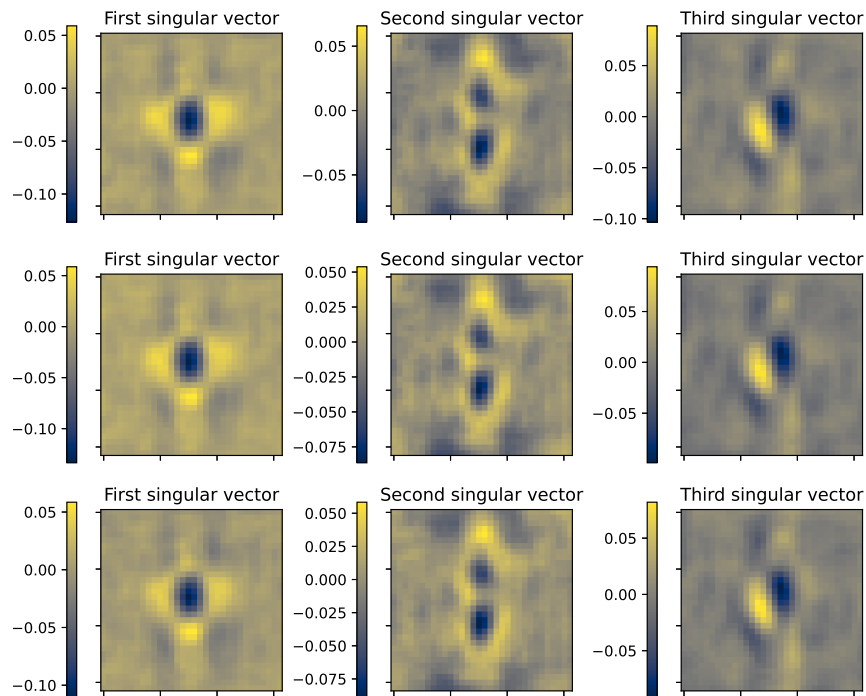
In Figure 9(c), we compute the effective rank of the bottom layer weight matrices from the trained two-layer kernel ridge regression model and the two-layer neural network model that achieves the minimum prediction error. The effective rank for a matrix is defined as the sum of singular values divided by the maximum singular value.

*C.2.3. Results for other Digits Classification.* To further support our claims in the main text, we do parallel experiment results for binary classification of digits 5 and 6 on the SVHN dataset. Parallel Figures 6, 7, 8, 9 on digits 5 and 6 classifications are presented in the following Figures 16, 17, 18, 19. Qualitatively, these results illustrate the same underlying patterns and support the conclusions discussed in the main text.

*C.2.4. Summary.* Our experiments on SVHN provide empirical evidence to support the following claims. (a) Introducing a weight matrix  $U$  in the two-layer kernel ridge regression model can significantly boost prediction accuracies compared to the standard kernel ridge regression model. (b) The two-layer kernel ridge regression model appears to intrinsically promote parsimonious representations of the data. It automatically regularizes the weight matrix  $U$  to low-rankness without external regularizations.

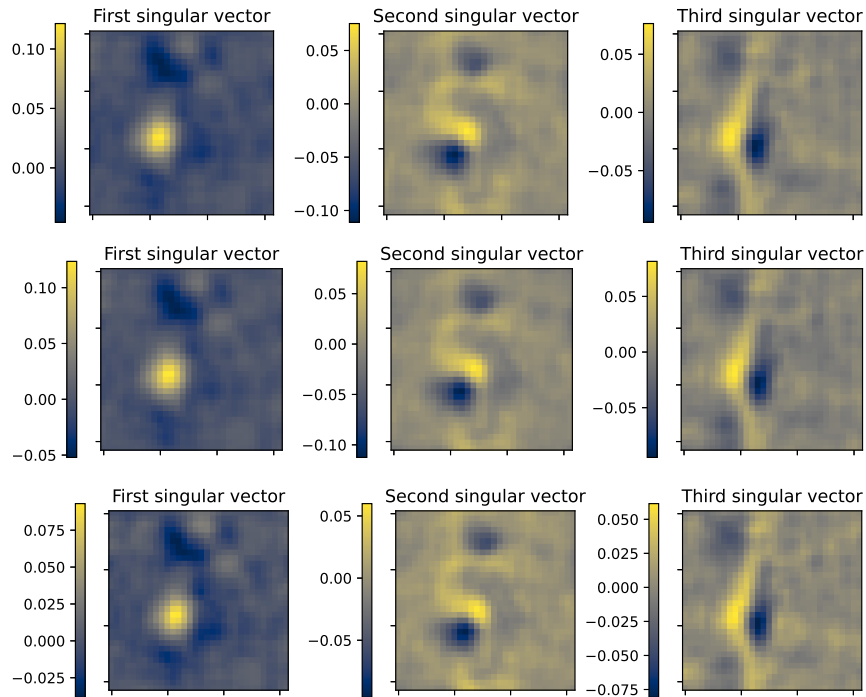


(a) two-layer kernel ridge regression

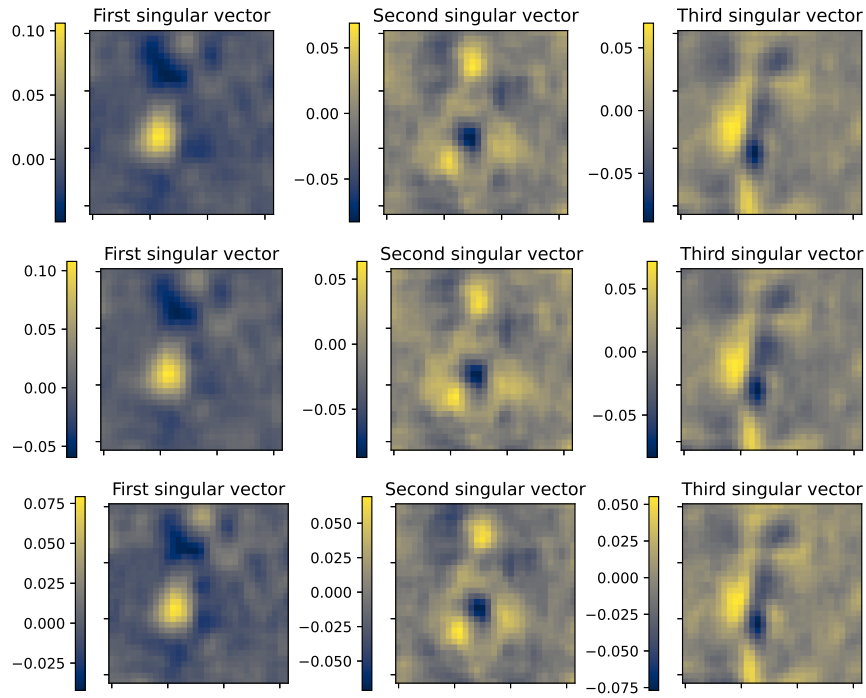


(b) two-layer ReLU neural network

Fig 15: Singular vector plot for classifying digits 0 and 8: The first part corresponds to the top three left singular vectors of  $U$  (or equivalently, top three eigenvectors of  $\Sigma$ ) of our two-layer kernel ridge regression model. The second part corresponds to the top three left singular vectors of the bottom layer weight matrix from a two-layer ReLU neural network on SVHN data. Each method from top to bottom: red, green, blue channels.



(a) two-layer kernel ridge regression



(b) two-layer ReLU neural network

Fig 16: Singular vector plot for classifying digits 5 and 6: The first part corresponds to the top three left singular vectors of  $U$  (or equivalently, top three eigenvectors of  $\Sigma$ ) of our two-layer kernel ridge regression model. The second part corresponds to the top three left singular vectors of the bottom layer weight matrix from a two-layer ReLU neural network on SVHN data. Each method from top to bottom: red, green, blue channels.

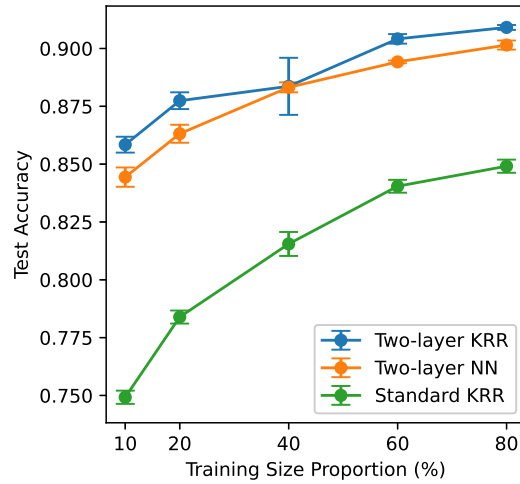


Fig 17: Prediction accuracy for classifying digits 5 and 6, measured on subsamples of the training dataset for Two-layer KRR, Two-layer NN, and Standard KRR. The training datasets are subsampled to different proportions: 10%, 20%, 40%, 60%, and 80%. Each subsampling proportion is repeated 5 times, and the average accuracy is reported with standard error bars.

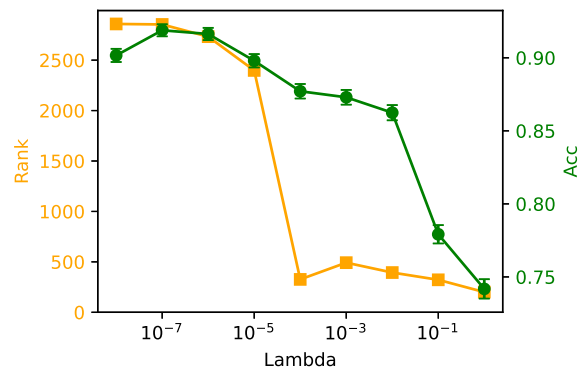
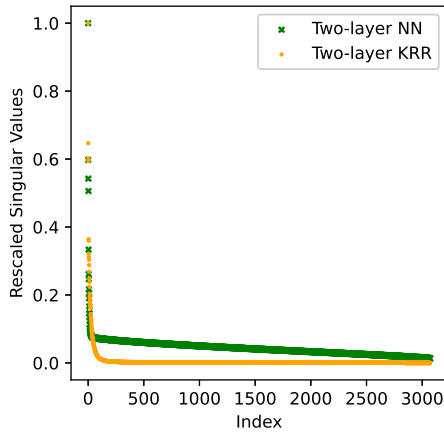


Fig 18: Prediction accuracy (green curve) and rank of bottom-layer weight matrix  $U$  (orange curve) versus  $\lambda$ : sequence of  $\lambda$ 's are  $10^{-8}$ ,  $10^{-7}$ ,  $10^{-6}$ ,  $10^{-5}$ ,  $10^{-4}$ ,  $10^{-3}$ ,  $10^{-2}$ ,  $10^{-1}$ , 1.



Method	Accuracy (%)
Two-layer KRR	91.79
Two-layer NN	90.51
Two-layer KRR (Top 1 Singular Vector)	47.83
Two-layer NN (Top 1 Singular Vector)	57.46
Two-layer KRR (Top 5 Singular Vectors)	88.19
Two-layer NN (Top 5 Singular Vectors)	88.90
Two-layer KRR (Top 50 Singular Vectors)	91.79
Two-layer NN (Top 50 Singular Vectors)	90.42
Standard KRR	86.47

Method	Effective Rank
Two-layer KRR	17.81
Two-layer NN	132.96
Standard KRR	3072

Fig 19: Our two-layer kernel ridge regression model displays similar prediction performance with more compressed feature representations: (a) singular values of the bottom layer weight matrices  $U$ , where orange dots correspond to our model and green crosses correspond to neural network model (b) prediction accuracy for different methods on SVHN dataset (c) effective rank (sum of singular values divided by the maximum singular value) for different methods on SVHN dataset.

## REFERENCES

- [1] ABBE, E., ADSERA, E. B. and MISIAKIEWICZ, T. (2022). The merged-staircase property: a necessary and nearly sufficient condition for sgd learning of sparse functions on two-layer neural networks. In *Conference on Learning Theory* 4782–4887. PMLR.
- [2] ABBE, E., ADSERA, E. B. and MISIAKIEWICZ, T. (2023). Sgd learning on neural networks: leap complexity and saddle-to-saddle dynamics. In *The Thirty Sixth Annual Conference on Learning Theory* 2552–2623. PMLR.
- [3] ALVAREZ, J. M. and SALZMANN, M. (2017). Compression-aware training of deep networks. *Advances in neural information processing systems* **30**.
- [4] ARONSZAJN, N. (1950). Theory of reproducing kernels. *Transactions of the American Mathematical Society* **68** 337–404.
- [5] ARORA, S., COHEN, N., HU, W. and LUO, Y. (2019). Implicit regularization in deep matrix factorization. *Advances in Neural Information Processing Systems* **32**.
- [6] BA, J., ERDOGDU, M. A., SUZUKI, T., WANG, Z. and WU, D. (2024). Learning in the presence of low-dimensional structure: a spiked random matrix perspective. *Advances in Neural Information Processing Systems* **36**.
- [7] BA, J., ERDOGDU, M. A., SUZUKI, T., WANG, Z., WU, D. and YANG, G. (2022). High-dimensional asymptotics of feature learning: How one gradient step improves the representation. *Advances in Neural Information Processing Systems* **35** 37932–37946.
- [8] BAKER, C. R. (1973). Joint measures and cross-covariance operators. *Transactions of the American Mathematical Society* **186** 273–289.
- [9] BARRON, A. R. (1993). Universal approximation bounds for superpositions of a sigmoidal function. *IEEE Transactions on Information theory* **39** 930–945.
- [10] BECKMAN, R. J. and MCKAY, M. D. (1987). Monte Carlo estimation under different distributions using the same simulation. *Technometrics* **29** 153–160.
- [11] BENGIO, Y., COURVILLE, A. and VINCENT, P. (2013). Representation learning: A review and new perspectives. *IEEE transactions on pattern analysis and machine intelligence* **35** 1798–1828.
- [12] BERTHIER, R., MONTANARI, A. and ZHOU, K. (2024). Learning time-scales in two-layers neural networks. *Foundations of Computational Mathematics* 1–84.
- [13] BERTSEKAS, D. P. (1997). Nonlinear programming. *Journal of the Operational Research Society* **48** 334–334.
- [14] BIETTI, A., BRUNA, J. and PILLAUD-VIVIEN, L. (2023). On learning gaussian multi-index models with gradient flow. *arXiv preprint arXiv:2310.19793*.
- [15] BIETTI, A., BRUNA, J., SANFORD, C. and SONG, M. J. (2022). Learning single-index models with shallow neural networks. *Advances in Neural Information Processing Systems* **35** 9768–9783.
- [16] BRUNA, J., PILLAUD-VIVIEN, L. and ZWEIG, A. (2023). On single index models beyond gaussian data. *arXiv preprint arXiv:2307.15804*.
- [17] BURER, S. and MONTEIRO, R. D. (2003). A nonlinear programming algorithm for solving semidefinite programs via low-rank factorization. *Mathematical Programming* **95** 329–357.
- [18] BURKE, J. V. and MORÉ, J. J. (1988). On the identification of active constraints. *SIAM Journal on Numerical Analysis* **25** 1197–1211.
- [19] CANDES, E., FAN, Y., JANSON, L. and LV, J. (2018). Panning for gold: ‘Model-X’ knockoffs for high dimensional controlled variable selection. *Journal of the Royal Statistical Society Series B: Statistical Methodology* **80** 551–577.
- [20] CHAPELLE, O., VAPNIK, V., BOUSQUET, O. and MUKHERJEE, S. (2002). Choosing multiple parameters for support vector machines. *Machine learning* **46** 131–159.
- [21] COOK, R. D. (1998). *Regression graphics*. John Wiley & Sons.
- [22] COOK, R. D. (2004). Testing predictor contributions in sufficient dimension reduction. *The Annals of Statistics* **32** 1062–1092.
- [23] COOK, R. D. and LI, B. (2002). Dimension reduction for conditional mean in regression. *The Annals of Statistics* **30** 455–474.
- [24] COOK, R. D. and NACHTSHEIM, C. J. (1994). Reweighting to achieve elliptically contoured covariates in regression. *Journal of the American Statistical Association* 592–599.
- [25] CUCKER, F. and SMALE, S. (2002). On the mathematical foundations of learning. *Bulletin of the American mathematical society* **39** 1–49.
- [26] CUI, H., PESCE, L., DANDI, Y., KRZAKALA, F., LU, Y. M., ZDEBOROVÁ, L. and LOUREIRO, B. (2024). Asymptotics of feature learning in two-layer networks after one gradient-step. *arXiv preprint arXiv:2402.04980*.

- [27] DAI, Z., KARZAND, M. and SREBRO, N. (2021). Representation costs of linear neural networks: Analysis and design. *Advances in Neural Information Processing Systems* **34** 26884–26896.
- [28] DAMIAN, A., LEE, J. and SOLTANOLKOTABI, M. (2022). Neural networks can learn representations with gradient descent. In *Conference on Learning Theory* 5413–5452. PMLR.
- [29] DANILIDIS, A., DRUSVYATSKIY, D. and LEWIS, A. S. (2014). Orthogonal invariance and identifiability. *SIAM Journal on Matrix Analysis and Applications* **35** 580–598.
- [30] DENNIS COOK, R. (2000). SAVE: a method for dimension reduction and graphics in regression. *Communications in statistics-Theory and methods* **29** 2109–2121.
- [31] DENTON, E. L., ZAREMBA, W., BRUNA, J., LECUN, Y. and FERGUS, R. (2014). Exploiting linear structure within convolutional networks for efficient evaluation. *Advances in neural information processing systems* **27**.
- [32] DEVORE, R. A., HOWARD, R. and MICCHELLI, C. (1989). Optimal nonlinear approximation. *Manuscripta mathematica* **63** 469–478.
- [33] DRUSVYATSKIY, D. (2013). Slope and geometry in variational mathematics.
- [34] DRUSVYATSKIY, D. and LEWIS, A. S. (2014). Optimality, identifiability, and sensitivity. *Mathematical Programming* **147** 467–498.
- [35] DUNN, J. C. (1987). On the convergence of projected gradient processes to singular critical points. *Journal of Optimization Theory and Applications* **55** 203–216.
- [36] FADILI, J., MALICK, J. and PEYRÉ, G. (2018). Sensitivity analysis for mirror-stratifiable convex functions. *SIAM Journal on Optimization* **28** 2975–3000.
- [37] FAN, J. and HUANG, L.-S. (2001). Goodness-of-fit tests for parametric regression models. *Journal of the American Statistical Association* **96** 640–652.
- [38] FOLLAIN, B. and BACH, F. (2023). Nonparametric linear feature learning in regression through regularisation. *arXiv preprint arXiv:2307.12754*.
- [39] FOLLAIN, B. and BACH, F. (2024). Enhanced Feature Learning via Regularisation: Integrating Neural Networks and Kernel Methods. *arXiv preprint arXiv:2407.17280*.
- [40] FUKUMIZU, K., BACH, F. R. and GRETTON, A. (2007). Statistical consistency of kernel canonical correlation analysis. *Journal of Machine Learning Research* **8**.
- [41] FUKUMIZU, K., BACH, F. R. and JORDAN, M. I. (2004). Dimensionality reduction for supervised learning with reproducing kernel Hilbert spaces. *Journal of Machine Learning Research* **5** 73–99.
- [42] FUKUMIZU, K., BACH, F. R. and JORDAN, M. I. (2009). Kernel dimension reduction in regression. *The Annals of Statistics* **37** 1871–1905.
- [43] FUKUMIZU, K., GRETTON, A. and BACH, F. (2005). Statistical convergence of kernel CCA. *Advances in Neural Information Processing Systems* **18**.
- [44] GÖNEN, M. and ALPAYDIN, E. (2011). Multiple kernel learning algorithms. *The Journal of Machine Learning Research* **12** 2211–2268.
- [45] GRETTON, A., BOUSQUET, O., SMOLA, A. and SCHÖLKOPF, B. (2005). Measuring statistical dependence with Hilbert-Schmidt norms. In *International conference on algorithmic learning theory* 63–77. Springer.
- [46] GUNASEKAR, S., WOODWORTH, B. E., BHOJANAPALLI, S., NEYSHABUR, B. and SREBRO, N. (2017). Implicit regularization in matrix factorization. *Advances in neural information processing systems* **30**.
- [47] GUYON, I., WESTON, J., BARNHILL, S. and VAPNIK, V. (2002). Gene selection for cancer classification using support vector machines. *Machine learning* **46** 389–422.
- [48] GYÖRFI, L., KOHLER, M., KRZYŻAK, A. and WALK, H. (2006). *A distribution-free theory of nonparametric regression*. Springer Science & Business Media.
- [49] HARE, W. L. and LEWIS, A. S. (2004). Identifying active constraints via partial smoothness and prox-regularity. *Journal of Convex Analysis* **11** 251–266.
- [50] HARE, W. L. and LEWIS, A. S. (2007). Identifying active manifolds. *Algorithmic Operations Research* **2** 75–82.
- [51] HASTIE, T., TIBSHIRANI, R. and FRIEDMAN, J. H. (2009). *The elements of statistical learning: data mining, inference, and prediction* **2**. Springer.
- [52] HASTIE, T., TIBSHIRANI, R. and WAINWRIGHT, M. (2015). *Statistical learning with sparsity: the lasso and generalizations*. CRC press.
- [53] HIRIART-URRUTY, J.-B. and MALICK, J. (2012). A fresh variational-analysis look at the positive semidefinite matrices world. *Journal of Optimization Theory and Applications* **153** 551–577.
- [54] HRISTACHE, M., JUDITSKY, A., POLZEHL, J. and SPOKOINY, V. (2001). Structure adaptive approach for dimension reduction. *The Annals of Statistics* 1537–1566.
- [55] JACOT, A., GABRIEL, F. and HONGLER, C. (2018). Neural tangent kernel: Convergence and generalization in neural networks. *Advances in neural information processing systems* **31**.

- [56] JI, Z., DUDÍK, M., SCHAPIRE, R. E. and TELGARSKY, M. (2020). Gradient descent follows the regularization path for general losses. In *Conference on Learning Theory* 2109–2136. PMLR.
- [57] JORDAN, M. I., LIU, K. and RUAN, F. (2021). On the self-penalization phenomenon in feature selection. *arXiv preprint arXiv:2110.05852*.
- [58] KIMELDORF, G. and WAHBA, G. (1971). Some results on Tchebycheffian spline functions. *Journal of mathematical analysis and applications* **33** 82–95.
- [59] KOLTCHINSKII, V. and GINÉ, E. (2000). Random matrix approximation of spectra of integral operators. *Bernoulli* 113–167.
- [60] LEWIS, A. S. (2002). Active sets, nonsmoothness, and sensitivity. *SIAM Journal on Optimization* **13** 702–725.
- [61] LI, B., ZHA, H. and CHIAROMONTE, F. (2005). Contour Regression: A General Approach to Dimension Reduction. *The Annals of Statistics* 1580–1616.
- [62] LI, K.-C. (1991). Sliced inverse regression for dimension reduction. *Journal of the American Statistical Association* **86** 316–327.
- [63] LI, Y., MA, T. and ZHANG, H. (2018). Algorithmic regularization in over-parameterized matrix sensing and neural networks with quadratic activations. In *Conference On Learning Theory* 2–47. PMLR.
- [64] LI, Z., LUO, Y. and LYU, K. (2021). Towards resolving the implicit bias of gradient descent for matrix factorization: greedy low-rank learning. In *International Conference on Learning Representations*.
- [65] LIN, Q., ZHAO, Z. and LIU, J. S. (2018). On consistency and sparsity for sliced inverse regression in high dimensions. *The Annals of Statistics* **46** 580–610.
- [66] LUO, W., LI, B. and YIN, X. (2014). On efficient dimension reduction with respect to a statistical functional of interest. *The Annals of Statistics* 382–412.
- [67] MISIAKIEWICZ, T. and MONTANARI, A. (2023). Six lectures on linearized neural networks. *arXiv preprint arXiv:2308.13431*.
- [68] NETZER, Y., WANG, T., COATES, A., BISSACCO, A., WU, B. and NG, A. Y. (2011). Reading digits in natural images with unsupervised feature learning. In *NIPS workshop on deep learning and unsupervised feature learning* **2011** 4. Granada.
- [69] NEWBY, W. K. (1991). Uniform convergence in probability and stochastic equicontinuity. *Econometrica: Journal of the Econometric Society* 1161–1167.
- [70] PARKINSON, S., ONGIE, G. and WILLET, R. (2023). Linear neural network layers promote learning single-and multiple-index models. *arXiv preprint arXiv:2305.15598*.
- [71] RADHAKRISHNAN, A., BEAGLEHOLE, D., PANDIT, P. and BELKIN, M. (2022). Feature learning in neural networks and kernel machines that recursively learn features. *arXiv preprint arXiv:2212.13881*.
- [72] RAHIMI, A. and RECHT, B. (2007). Random features for large-scale kernel machines. *Advances in neural information processing systems* **20**.
- [73] SAMAROV, A. M. (1993). Exploring regression structure using nonparametric functional estimation. *Journal of the American Statistical Association* **88** 836–847.
- [74] SANTNER, T. J., WILLIAMS, B. J., NOTZ, W. I. and WILLIAMS, B. J. (2003). *The design and analysis of computer experiments* **1**. Springer.
- [75] SANZ, H., VALIM, C., VEGAS, E., OLLER, J. M. and REVERTER, F. (2018). SVM-RFE: selection and visualization of the most relevant features through non-linear kernels. *BMC bioinformatics* **19** 1–18.
- [76] SCHLIMMER, J. (1985). Automobile. UCI Machine Learning Repository. DOI: <https://doi.org/10.24432/C5B01C>.
- [77] SCHOENBERG, I. J. (1938). Metric spaces and completely monotone functions. *Annals of Mathematics* 811–841.
- [78] SCHOENBERG, I. J. (1942). Positive definite functions on spheres. *Duke Mathematical Journal*.
- [79] SREBRO, N., RENNIE, J. and JAAKKOLA, T. (2004). Maximum-margin matrix factorization. *Advances in neural information processing systems* **17**.
- [80] SRIPERUMBUDUR, B. K., FUKUMIZU, K. and LANCKRIET, G. R. (2011). Universality, characteristic kernels and RKHS embedding of measures. *Journal of Machine Learning Research* **12**.
- [81] STEWART, G. W. and SUN, J.-G. (1990). Matrix perturbation theory.
- [82] STROMANN, O., NASCETTI, A., YOUSIF, O. and BAN, Y. (2019). Dimensionality reduction and feature selection for object-based land cover classification based on Sentinel-1 and Sentinel-2 time series using Google Earth Engine. *Remote Sensing* **12** 76.
- [83] TAO, T., QIAN, Y. and PAN, S. (2022). Column  $\ell_{2,0}$ -norm regularized factorization model of low-rank matrix recovery and its computation. *SIAM Journal on Optimization* **32** 959–988.
- [84] TIMOR, N., VARDI, G. and SHAMIR, O. (2023). Implicit regularization towards rank minimization in relu networks. In *International Conference on Algorithmic Learning Theory* 1429–1459. PMLR.
- [85] TUKAN, M., MAALOUF, A., WEKSLER, M. and FELDMAN, D. (2021). No fine-tuning, no cry: Robust svd for compressing deep networks. *Sensors* **21** 5599.

- [86] VAN DER VAART, A. W. (2000). *Asymptotic statistics* **3**. Cambridge university press.
- [87] WAHBA, G. (1990). *Spline models for observational data*. SIAM.
- [88] WAINWRIGHT, M. J. (2019). *High-Dimensional Statistics: A Non-Asymptotic Viewpoint* **48**. Cambridge University Press.
- [89] WESTON, J., MUKHERJEE, S., CHAPELLE, O., PONTIL, M., POGGIO, T. and VAPNIK, V. (2000). Feature selection for SVMs. *Advances in neural information processing systems* **13**.
- [90] WRIGHT, S. J. (1993). Identifiable surfaces in constrained optimization. *SIAM Journal on Control and Optimization* **31** 1063–1079.
- [91] XIA, Y., TONG, H., LI, W. K. and ZHU, L.-X. (2002). An adaptive estimation of dimension reduction space. *Journal of the Royal Statistical Society Series B: Statistical Methodology* **64** 363–410.
- [92] YIN, X. and LI, B. (2011). Sufficient dimension reduction based on an ensemble of minimum average variance estimators. *The Annals of Statistics* 3392–3416.
- [93] YU, Z., DONG, Y. and SHAO, J. (2016). On marginal sliced regression for ultrahigh dimensional model-free feature selection. *The Annals of Statistics* **44** 2594–2623.
- [94] ZENG, P. (2008). Determining the dimension of the central subspace and central mean subspace. *Biometrika* **95** 469–479.
- [95] ZHU, Y. and ZENG, P. (2006). Fourier methods for estimating the central subspace and the central mean subspace in regression. *Journal of the American Statistical Association* **101** 1638–1651.